AD_____

Award Number: W81XWH-07-1-0065

TITLE: Effects of Radiation on Proteasome Function in Prostate Cancer Cells

PRINCIPAL INVESTIGATOR: Frank Pajonk, M.D., Ph.D.

CONTRACTING ORGANIZATION: University of California
Los Angeles, CA 90024

REPORT DATE: February 2012

TYPE OF REPORT: Annual Summary

PREPARED FOR: U.S. Army Medical Research and Materiel Command
Fort Detrick, Maryland 21702-5012

REPORT DOCUMENTATION PAGE

Form Approved
OMB No. 0704-0188

1. REPORT DATE	2. REPORT TYPE	3. DATES COVERED
February 2012	Annual Summary	15 January 2007 – 14 January 2012

4. TITLE AND SUBTITLE

Effects of Radiation on Proteasome Function in Prostate Cancer Cells

5a. CONTRACT NUMBER

5b. GRANT NUMBER
W81XWH-07-1-0065

5c. PROGRAM ELEMENT NUMBER

6. AUTHOR(S)

Frank Pajonk

E-Mail: Fpajonk@mednet.ucla.edu

5d. PROJECT NUMBER

5e. TASK NUMBER

5f. WORK UNIT NUMBER

7. PERFORMING ORGANIZATION NAME(S) AND ADDRESS(ES)

University of California
Los Angeles, CA 90024

8. PERFORMING ORGANIZATION REPORT NUMBER

9. SPONSORING / MONITORING AGENCY NAME(S) AND ADDRESS(ES)
U.S. Army Medical Research and Materiel Command
Fort Detrick, Maryland 21702-5012

10. SPONSOR/MONITOR'S ACRONYM(S)

11. SPONSOR/MONITOR'S REPORT NUMBER(S)

12. DISTRIBUTION / AVAILABILITY STATEMENT
Approved for Public Release; Distribution Unlimited

13. SUPPLEMENTARY NOTES

14. ABSTRACT

None provided.

15. SUBJECT TERMS
None provided.

16. SECURITY CLASSIFICATION OF:			17. LIMITATION OF ABSTRACT	18. NUMBER OF PAGES	19a. NAME OF RESPONSIBLE PERSON
a. REPORT	b. ABSTRACT	c. THIS PAGE			USAMRMC
U	U	U	UU	61	19b. TELEPHONE NUMBER *(include area code)*

Table of Contents

Introduction

The proteasome is involved in the progression of the cell cycle and its degrading activity controls the lifetime of most cellular proteins, including many regulatory proteins. This multicatalytic complex is also the main target of many cancer therapies, including radiation, and our lab has already extensively shown data on radiation-induced proteasome inhibition. Based on the observation that radiation causes chemical modifications to many proteins and/or enzymes present in a cell through free radicals production, we hypothesized that irradiation induces structural, other than functional changes within the 26S subunits and proteins interacting with it. These conformational changes are the ones that eventually affect its activity, thus its capacity of degrading proteins.

As a cell progresses through the cell cycle-specific proteins need to be degraded in order for the cell to proceed to the next phase. So far, the activity of the 26S proteasome was thought to be constant throughout the different phases of the cell cycle, and that the degradation of specific proteins was only dependent on their ubiquitination and not by the activity levels of the proteasome itself. Our hypothesis is that there is another level of regulation that happens as the cell progresses through the cell cycle. This level is mediated by regulating the degradation efficiency of the proteasome itself. If this were in fact true, than cells would dynamically change the state of the proteasome through the cell cycle, which could explain why radiation can only partially inhibit proteasome function if the susceptibility of the proteasome to radiation changes with its regulation.

Body

The main purpose of this study was to understand how proteasomes are affected by ionizing radiation and how activity of this protease alters radiation responses of prostate cancer cells.

During year one and two of the proposal we established a system that allowed for immune-precipitation of complete 26S proteasomes from PC-3 prostate cancer cells. The system relies on overexpression of a Rpn11 subunit that carries a biotin tag. Purifying proteasomes using the tagged subunit had substantial advantages of the more laborious technique that utilizes glycerol gradients. Using mass spectrometry we identified proteasome subunits that were phosphorylated in response to irradiation (year 1). However, we failed confirming these posttranslational modifications using 2D gels and phospho-specific antibodies. Nevertheless, we identified a large number of proteasome interacting proteins (PIPs) and the composition of this group of protein differed substantially between irradiated and non-irradiated proteasome and was dependent on the availability of ATP (year 2).

During our irradiation experiments we experienced fluctuations in the effect of radiation on the function of the proteasome; depending on the culture conditions the inhibitory effect of radiation varied between 0 and 40%, suggesting that proteasomes are far more dynamic than we initially thought. A major discovery in year 2 and 3 was the observation that the overall activity of the proteasome changes during the progression of a cell through the cell cycle. During the G1-phase of the cell cycle, the activity of this protease was low but increased when cells progressed into S- and G2/M-phase of the cell cycle (see year 3). 2D experiments followed by mass spectrometry identified the proteasome alpha 3 subunit to be phosphorylated at a tyrosine site in cycling cells and that this phosphorylation was replaced with a serine phosphorylation in cells arrested at the G1/boundary. Future research will aim on identifying the kinases and phosphatases involved in this process. So far, we have not been able to show differential radiation sensitivity for prostate cancer cells during the different phases of the cell cycle and thus cannot correlate it to changes in proteasome activity (year 5, Figure 1 & 2).

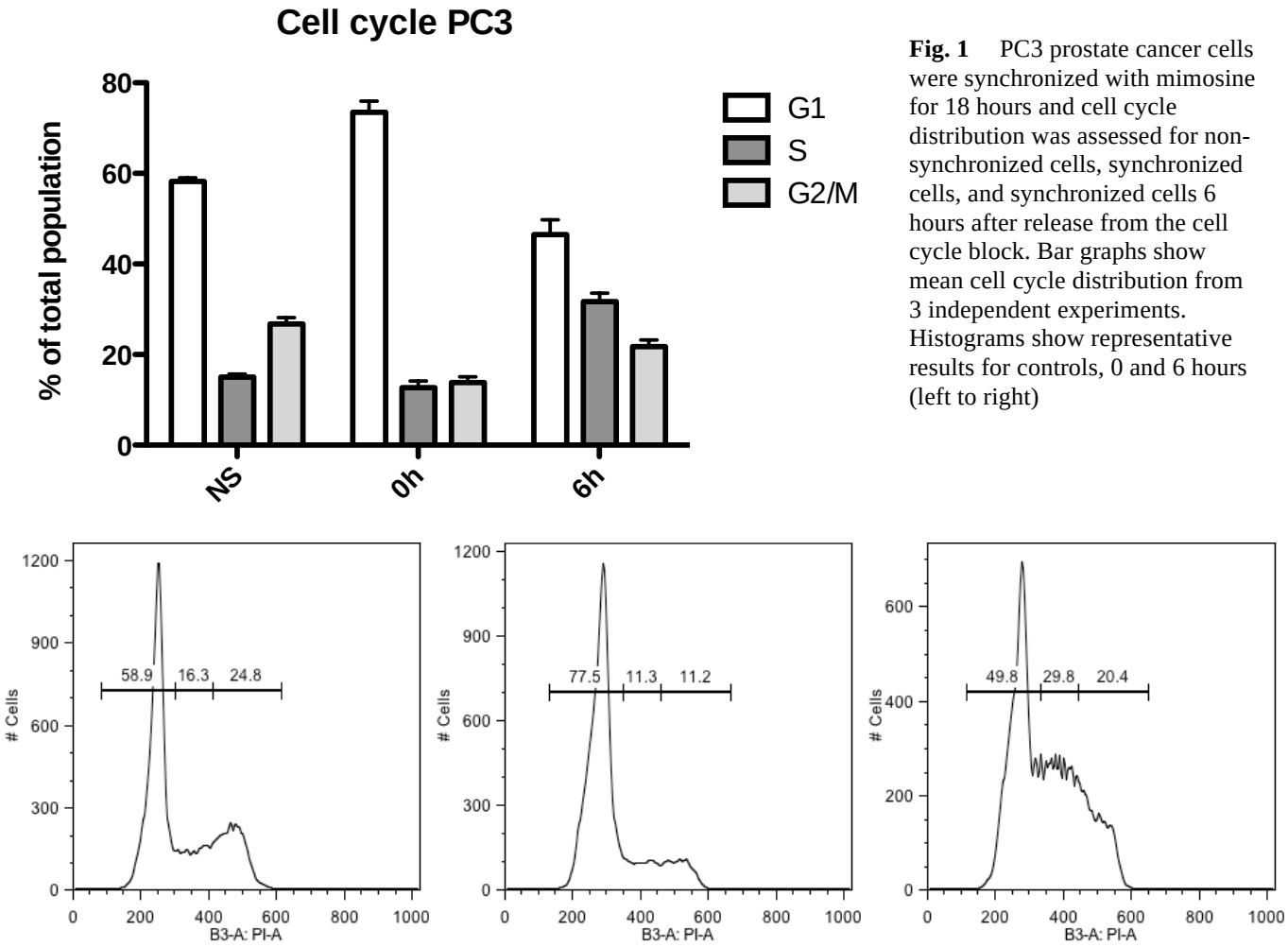

Fig. 1 PC3 prostate cancer cells were synchronized with mimosine for 18 hours and cell cycle distribution was assessed for non-synchronized cells, synchronized cells, and synchronized cells 6 hours after release from the cell cycle block. Bar graphs show mean cell cycle distribution from 3 independent experiments. Histograms show representative results for controls, 0 and 6 hours (left to right)

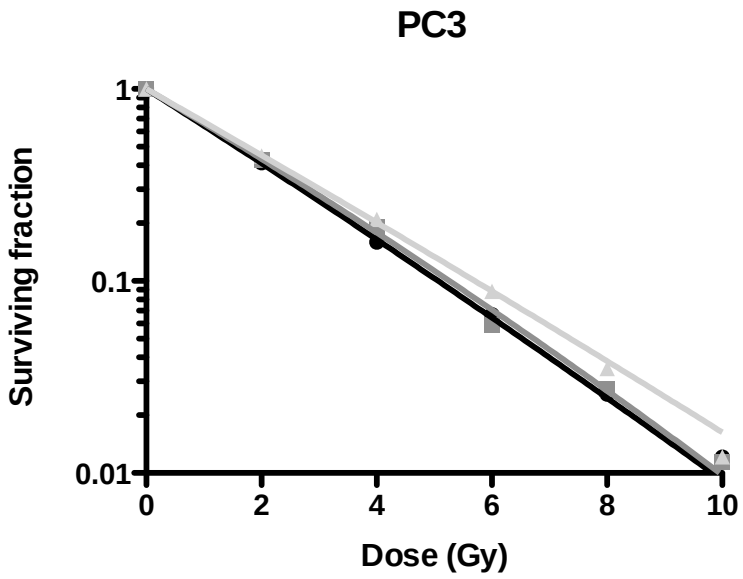

Figure 2
Clonogenic survival assay for PC3 cells. Normally cycling cells, synchronized cells, and cells 6 hours after being released from the cell cycle block were compared. No significant cell cycle-dependent differences in radiation sensitivity were observerd.

An additional major discovery was the observation that prostate cancers, like breast cancer and glioma, are heterogeneous with regard to their ability to form tumors and their response to radiation. Like in breast cancer and glioma, radiation-resistant prostate cancer cells could be prospectively identified based on their intrinsically low proteasome activity (year 4). Future research will investigate if patients with prostate cancers containing large numbers of cells with low proteasome activity have a poor prognosis.

KEY RESEARCH ACCOMPLISHMENTS:

- identification of novel proteasome interacting proteins in response to irradiation
- discovery of proteasome activity fluctuations during the cell cycle
- identification of proteasome alpha 3 subunit to be differentially phosphorylated during different phases of the cell cycle.
- Identification of intrinsically low proteasome activity as a general marker for cancer stem cells and for prospective identification of a radioresistant subpopulation of prostate cancer cells.

Reportable outcomes:

Posters

Poster presentation, William H. McBride, James Brush, Keisuke Iwamoto, Kwanghee Kim, Frank Pajonk, Milena Pervan. *Irradiation alters protein expression through direct effects on the 26S proteasome*, AACR, Los Angeles, 2007

Poster presentation, William H. McBride, Frank Pajonk, Kei Iwamoto, James Brush, Kwanghee Kim, *Radiation modifies cell signalling through altering proteasome structure and function*, International Wolfsberg Meeting, 2007

Oral and *poster* presentation at the Radiation Research Society (RRS) 54th Annual Meeting, 21-24 September, Boston: Lorenza Della Donna, Chann Lagadec, Erina Vlashi, Kwanghee Kim, Tyson McDonald, Julian Whitelegge, William H. McBride and Frank Pajonk *Radiation-induced posttranslational modification and expression of proteasome subunits, 2008*

Poster presentation at the AACR 10th Annual Meeting (Denver, CO) Lorenza Della Donna, Erina Vlashi, Chann Lagadec, Julian Whitelegge, Puneet Souda, Polin Nikolay, Malcom Mattes, William McBride and Frank Pajonk. *Quantitative proteomic analysis of radiation induced posttranslational modifications of the 26S proteasome, 2009*

Lorenza Della Donna, Chann Lagadec, Erina Vlashi, Carmen Dekmezian, Puneet Souda, Julian Whitelegge, and Frank Pajonk. Regulation of 26S proteasome activity by radiation during the different phases of the cell cycle. 56th annual Meeting of the Radiation Research Society, Grand Wailea Resort Hotel and Spa, Maui, September 25-29.

Lorenza Della Donna, Chann Lagadec, Erina Vlashi, Carmen Dekmezian, Julian Whitelegge, Puneet Souda and Frank Pajonk. The Activity of the 26S Proteasome is Modulated during the Different Phases of the Cell Cycle. 1st PPDUP (Proteomics of Protein Degradation & Ubiquitin Pathways) Conference, June 6th-8th, 2010, Vancouver, British Columbia, Canada (*Excellent Poster Presentation Award*).

Invited Lectures

Therapeutic Resistance of Cancer Stem Cells, World Stem Cell Summit, Pasadena, October 2011

Radiation Resistance of Cancer Stem Cells, International Wolfsberg Meeting, Switzerland, 2011

The Metabolic State Of Cancer Stem Cells And Cancer Stem Cell Plasticity, Keynote Presentation, Western Radiobiology Review Course, Edmonton, Canada, 2011

Cancer Stem Cells, SIT Workshop, Annual Meeting of the Radiation Research Society, Maui, September, 2010

Cancer Stem Cells – Lesson learned from the needle in the haystack, Annual Meeting of the Radiation Research Society, Maui, September, 2010

Radiation-induced Cancer Stem Cell Plasticity, NIH/NCI, Bethesda, September, 2010

Illuminating the Seed Instead of the Soil: Imaging of Cancer Stem Cells, Novel targeting drugs and Radiotherapy - from the bench to the clinic, Toulouse (France), June, 2010

Cancer Stem Cell Imaging, Avison Biomedical Symposium 2010, Seoul (South Korea), February, 2010

Radiation Resistance of Cancer Stem Cells – Mechanisms and Implications, Gordon Research Conference on Radiation Oncology, Galveston, January, 2010

Radiation Responses of Cancer Stem Cells, ASTRO, Chicago, November, 2009

Imaging, Tracking, and Targeting of Cancer Stem Cells, University of California Irvine, Mai, 2009

Heterogeneity Within and Between Cancers: The Stem Cell Problem in Radiotherapy, ASTRO, Boston, September 24, 2008

Treatment responses of cancer stem cells, The Inaugural Alberta Cancer Research Institute Research Meeting, Banff, Canada, November, 8th, 2007

Heterogeneity Within and Between Cancers: The Stem Cell Problem in Radiotherapy, ASTRO, Los Angeles, October 28, 2007

Proteasomes, Cancer Stem Cells, and Radiation, UCLA Center for Biological Radioprotectors, Los Angeles, September 2007

Breast Cancer Stem Cells and Radiation, International Congress of Radiation Research (ICRR), San Francisco, 2007

The Proteasome - Mediator of Effects and Side Effects in Cancer Therapy, Department of Cardiology, UCLA, 2007

Breast Cancer Stem Cell Response to Cancer Treatment, JCCC, UCLA, 2007

Awards

SIT Travel Award to Lorenza Della Donna from the Radiation Research Society (RRS), 54th Annual Meeting, 21-24 September, Boston, 2008

Lorenza Della Donna, Chann Lagadec, Erina Vlashi, Carmen Dekmezian, Julian Whitelegge, Puneet Souda and Frank Pajonk. The Activity of the 26S Proteasome is Modulated during the Different Phases of the Cell Cycle. 1st PPDUP (Proteomics of Protein Degradation & Ubiquitin Pathways) Conference, June 6th-8th, 2010, Vancouver, British Columbia, Canada (*Excellent Poster Presentation Award*).

Manuscripts

Vlashi E, Kim K, Dealla Donna L, Lagadec C, McDonald T, Eghbali M, Sayre J, Stefani E, McBride W, Pajonk F: *In-vivo imaging, tracking, and targeting of cancer stem cells.* J Natl Cancer Inst 2009, 101:350-359.

Pajonk F, Vlashi E, McBride WH: *Radiation Resistance of Cancer Stem Cells - The 4R's of Radiobiology Revisited. Stem Cells* 2010. Apr;28(4):639-48.

Vlashi E, McBride WH, Pajonk F: *Radiation responses of cancer stem cells.* J Cell Biochem 2009, 108:339-342.

Donna LD, Lagadec C, Pajonk F., *Radioresistance of prostate cancer cells with low proteasome activity*. Prostate. 2011 Sep 19. Epub ahead of print

Lagadec C, Vlashi E, Della Donna L, Dekmezian C, Pajonk F, *Radiation-induced Reprograming of Breast Cancer Cells, Stem Cells, 2012,* Epub ahead of print

Development of cell lines

PC3-ZsGreen-cODC, cells report for proteasome activity
DU145-ZsGreen-cODC, cells report for proteasome activity
LNCap-ZsGreen-cODC, cells report for proteasome activity

PC3-Rpn11-ZsGreen-cODC, cells report for proteasome activity and allow immune-precipitation of intact 26S proteasomes.
DU145-Rpn11-ZsGreen-cODC, cells report for proteasome activity and allow immune-precipitation of intact 26S proteasomes.

Funding applied for

15NB-0153 (Pajonk, F.) 07/01/09-30/06/11
California Breast Cancer Research Program
Innovative Development and Exploratory Award (IDEA) Competitive Renewal
Modulation of breast cancer stem cell response to radiation.

This project investigates how the response of breast cancer stem cells to radiation can be modulated targeting the developmental Notch signaling pathway.
Role: PI

RO1 1R01CA137110-01 (Pajonk, F.) 12/01/09-06/30/2014
National Cancer Institute
The 26S Proteasome in Cancer Stem Cells
This project investigates the role of the proteasome for the maintenance of the cancer stem cell phenotype**.**
Role: PI

RO1 1R01CA161294-01 (Pajonk, F.) pending
National Cancer Institute
Erythropoietin and Breast Cancer Stem Cells
This project studies the effect of Epo and radiation on cancer stem cells
Role: PI

S10 1S10OD010789-01 (Pajonk, F.) pending
A Small Animal Radiation Research Platform
National Cancer Institute
Role: PI

Employment or research opportunities applied for and/or received

Pajonk, F., Tenure track faculty position, Department of Radiation Oncology, University of California, Los Angeles, 2007

Pajonk, F., Tenure, Department of Radiation Oncology, University of California, Los Angeles, 2009

Lagadec, C., Assistant Research Biologist, Department of Radiation Oncology, University of California, Los Angeles, 2011

Personnel supported by this award
Pajonk, Frank MD/PhD; Lagadec, Chann PhD

Conclusions
Within this proposal we established intrinsically low proteasome activity as a marker for radioresistant subpopulations of prostate cancer cells with increased tumorigenicity. We conclude that proteasomes differentially associate with PIPs after exposure to ionizing radiation and that proteasome activity is subject to regulation through posttranslational modification during the progression of a cell through the cell cycle.

Radioresistance of Prostate Cancer Cells With Low Proteasome Activity

Lorenza Della Donna,[1] Chann Lagadec,[1] and Frank Pajonk[1,2]*

[1]Department of Radiation Oncology, David Geffen School of Medicine at UCLA, Los Angeles, California
[2]Jonsson Comprehensive Cancer Center at UCLA, Los Angeles, California

BACKGROUND. Prostate cancer is frequently treated with radiotherapy. While treatment results are in general excellent, some patients relapse and current systemic therapies are not curative, thus, underlining the need for novel targeted therapies. Proteasome inhibitors have been suggested as promising new agents against solid tumors including prostate cancer but initial results from clinical trials are disappointing.

METHODS. In this study we tested if prostate cancer cells are heterogeneous with regard to their intrinsic 26S proteasome activity, which could explain the lack of clinical responses to bortezomib. PC-3 and DU145 prostate cancer cells and an imaging system for proteasome activity were used to identify individual cells with low proteasome activity. Clonogenic survival assays, a sphere-forming assay and an in vivo limiting dilution assay were used to characterize radiation sensitivity, self-renewal capacity, and tumorigenicity of the different subsets of cells.

RESULTS. We identified a small population of cells with intrinsically low 26S proteasome activity. Fractionated radiation enriched for these cells and clonogenic survival assays and sphere-forming assays revealed a radioresistant phenotype and increased self-renewal capacity.

CONCLUSIONS. We conclude that low 26S proteasome activity identifies a radioresistant prostate cancer cell population. This population of cells could be responsible for the clinical resistance of advanced prostate cancer to proteasome inhibitors and radiation.

KEY WORDS: **proteasome; radioresistance; self-renewal; tumorigenicity**

INTRODUCTION

Cancer of the prostate continues to be a leading cause for cancer deaths in men [1] and is usually treated with radiotherapy alone or in combination with surgery [2]. Treatment results are in general excellent [3]. However, some patients relapse locally and/or systemically, indicating that a resistant population of cancer cells may have survived the radiation treatment. When prostate cancers progress and metastasize, the tumors frequently become hormone-refractory and classical chemotherapy regimens do not offer a curative approach. Thus, there is a need for novel targeted therapies in advanced prostate cancer [4].

The ubiquitin-proteasome system is the major non-lysosomal system for degradation of intracellular proteins [5]. Its activity is fundamental for many cellular processes, such as cell-cycle regulation, gene expression, cell differentiation, and immune response [6]. Experimental data suggested, that the proteasome could be a novel target in prostate cancer

Grant sponsor: Department of Defense; Grant number: W81XWH-07-1-0065; Grant sponsor: National Cancer Institute; Grant number: RO1 CA137110.

Lorenza Della Donna and Chann Lagadec contributed equally to this work.

*Correspondence to: Prof. Frank Pajonk, Department of Radiation Oncology, David Geffen School of Medicine at UCLA, 10833 Le Conte Ave., Los Angeles, CA 90095-1714.
E-mail: fpajonk@mednet.ucla.edu
Received 4 August 2011; Accepted 25 August 2011
DOI 10.1002/pros.21489
Published online in Wiley Online Library (wileyonlinelibrary.com).

[7,8]. However, in first clinical trials the FDA-approved proteasome inhibitor bortezomib had only little anti-tumor activity against prostate cancer [9–13].

We previously reported that low intrinsic proteasome activity in glioma and breast cancer cells correlated with resistance to proteasome inhibitors and radiation [14,15]. We hypothesized that the malignant cells in prostate cancer are heterogeneous and that a radioresistant cell population with intrinsically low 26S proteasome activity can also be found in prostate cancer. To address this hypothesis we assessed proteasome activity in cells from two commonly used prostate cancer lines and characterized their radiation response and tumorigenicity.

MATERIALS AND METHODS

Cell Culture, Reagents, and Antibodies

Human PC-3 and DU145 cell lines were purchased from ATCC (Manassas, VA) and cultured under standard conditions as monolayers in DMEM media supplemented with 5% antibiotics (Invitrogen, Carlsbad, CA) and 10% heat-inactivated fetal bovine serum (FBS, Sigma, St. Louis, MO) or as prostate spheres in phenol-red-free DMEM/F12 media, 0.4% BSA (Sigma), B27 (Invitrogen), 5 μg/ml bovine insulin (Sigma), 4 μg/ml heparin (Sigma), 20 ng/ml fibroblast growth factor 2 (Sigma), and 20 ng/ml epidermal growth factor (Sigma). Prostate spheres were initiated from single cells seeded at a density of 10,000 cells/ml. DMEM media, antibiotics, and trypsin were purchased from Invitrogen.

PC-3 and DU145 cell lines were transduced with the ZsGreen-cODC proteasome function reporter system as described previously [16]. Briefly, the viral expression vector in which the C-terminal degron of the murine ornithine decarboxylase (cODC) was fused to ZsGreen were constructed as follows: The degron coded by the carboxyl-terminal 37 amino acids of ODC fused to ZsGreen (ZsGreen-cODC) was digested with *Bgl*II and *Not*I from pZsProsensor-1 (BD Biosciences, San Jose, CA) and cloned into the *Bam*HI and *Eco*RI sites of the retroviral vector pQCXIN (BD Biosciences) using the *Not*I–*Eco*RI DNA oligonucleotide adaptor (EZCLONE Systems, New Orleans, LA). pQCXIN/ZsGreen-cODC was transfected into GP2-293 pantropic retroviral packaging cells (BD Biosciences). The retrovirus collected from the supernatant of the packaging cells was used to infect the different cell lines. Stable transfectants were selected with G418 (Invitrogen).

To determine that the cells not accumulating the ZsGreen-cODC protein in untreated cell cultures still contained the expression vector, the cells were incubated with 0.5 μM of the proteasome inhibitor MG-132 (Calbiochem, San Diego, CA) overnight and the accumulation of the ZsGreen-cODC protein due to proteasome inhibition was analyzed by flow cytometry.

In all other experiments, accumulation of ZsGreen-cODC protein was analyzed by fluorescence microscopy (Olympus IX71 inverted fluorescent microscope) or flow cytometry (MACSquant analyzer, Miltenyi Biotec GmbH, Auburn, CA). In flow cytometry experiments cells were defined as ''ZsGreen-cODC-positive'' if the fluorescence in the FL-2 channel (FITC) exceeded the fluorescence of non-transfected control by at least two orders of magnitude.

Determining Radiosensitivity of Cells With Low and High Proteasome Activity

Monolayer and prostate sphere cultures were plated at a density of 400,000 cells/well or 10,000 cells/ml, respectively, in six-well plates. Twenty-four hours after plating, cells were irradiated once a day for 5 days with 0, 1, 2, 3, 4, or 5 Gy using an experimental 200KV X-Ray irradiator (Gulmay Medical Ltd, Camberley, England). For each fraction size (5×1, 5×2, 5×3, 5×4, 5×5 Gy) the total number of ZsGreen-cODC-negative and -positive cells was determined by flow cytometry 24, 48, and 72 hr after the last irradiation dose. Control cells were sham-irradiated.

Clonogenic Survival Assay and Sphere-Forming Assays

For clonogenic survival assays, cells derived from monolayers were irradiated as single cell suspensions. After irradiation, an appropriate number of cells was plated into 10 cm Petri dishes into DMEM media, supplemented with 10% FBS. Three weeks later, cells were fixed with methanol, stained with crystal violet and colonies cells were counted. In order to assess sphere formation, cells derived from spheres were irradiated as single cell suspensions, and plated into ultra-low adhesion 96-well plates at clonogenic densities from 1 to 256 cells/well in 100 μl of sphere media. Three weeks later, the number of spheres per well was counted. Data points were fitted using a linear-quadratic model.

Primary and Secondary Sphere Formation Assay

PC-3 and DU145 cells expressing ZsGreen-cODC were grown in sphere media as sphere cultures (primary spheres) and sorted into ZsGreen-cODC-negative and -positive cell populations by FACS into ultra low adhesion 96-well plate at a density of one

cell per well in DMEM/F12 supplemented with 0.4% BSA (Sigma), 10 ml/500 ml B27 (Invitrogen), 5 μg/ml bovine insulin (Sigma), 4 μg/ml heparin (Sigma), 20 ng/ml fibroblast growth factor 2 (bFGF, Sigma), and 20 ng/ml epidermal growth factor (EGF, Sigma). After 3 weeks, the number of spheres formed per plate were counted and expressed as a percentage of the initial number of cells plated. Cells were also plated in sphere media into 100 mm suspension dishes at 10,000 cells/ml, and allowed to form spheres for 15 days, these cells were used for secondary sphere forming experiments.

For both primary and secondary sphere formation, three independent experiments were performed.

Tumorigenicity and In Vivo Imaging

Six- to 8-week-old male nude (nu/nu) mice originally from The Jackson Laboratories (Bar Harbor, ME) were re-derived, bred, and maintained in a defined flora environment in the animal facilities of the Department of Radiation Oncology, University of California, Los Angeles (Los Angeles, CA) in accordance with all local and national guidelines for the care of animals.

PC-3-ZsGreen-cODC cells were sorted by FACS into ZsGreen-cODC-negative and -positive cells. 10^6, 10^5, 10^4, 10^3, 10^2, 10 ZsGreen-cODC-negative cells or -positive cells per inoculum were injected in Matrigel (BD Bioscience) into the thighs. Mice injected with ZsGreen-cODC-negative and -positive cells were imaged for the presence of ZsGreen-cODC-positive cells with the Maestro In Vivo Imaging System (Cambridge Research & Instrumentation, Woburn, MA) before being sacrificed. Tumor growth was monitored on a daily basis and mice were sacrificed when tumor diameters reached the criteria for euthanasia.

Statistical Methods

All data are represented as means ± standard error means (SEMs). In general, a P-value of ≤ 0.05 in a paired two-sided Student's t-test was used to test for statistically significant differences.

RESULTS

Radiation Response of Prostate Cancer Cells With High or Low Proteasome Activity

Two commonly used prostate cancer cell lines, PC-3 and DU145, were stably infected with an expression vector for a fusion protein between the green fluorescent protein, ZsGreen, and the C-terminal degron of murine ornithine decarboxylase (cODC). This sequence targets the fusion protein for ubiquitin-independent degradation by the proteasome [14]. Cells with low proteasome activity accumulate the fluorescent fusion protein and can be detected by fluorescent microscopy or flow cytometry.

In both cell lines, a small population of cells (PC-3: 2.5 ± 1.3%; DU-145: 2.3 ± 0.6%) accumulated the reporter protein ZsGreen-cODC, indicating low proteasome function (Fig. 1A,B). However, when cells were incubated with the proteasome inhibitor MG-132 (0.5 μM over night), all cells accumulated the fusion protein thus, indicating stable expression of the construct in all cells (Fig. 1C/D).

Next we tested if cells accumulating the ZsGreen-cODC reporter (low proteasome activity) could be enriched by irradiation. PC-3 cells were irradiated with 5 × 1, 5 × 2, 5 × 3, 5 × 4, or 5 × 5 Gy and the number of ZsGreen-cODC-negative and positive cells was assessed 24, 48, and 72 hr after the last radiation dose (Fig. 2A–C). Fractionated irradiation increased the absolute and relative number of ZsGreen-cODC-positive cells (low proteasome activity) significantly (5 × 2 Gy: 3-fold ± 0.12, n = 4, $P < 0.001$, paired two-sided Student's t-test), while the number of ZsGreen-cODC-negative cells declined (5 × 2 Gy: 0.45-fold ± 0.03, n.s., paired two-sided Student's t-test), indicating differential radiation sensitivity of both cell populations. The increase persisted when cells were analyzed at 48 and 72 hr after the last fraction, supporting preferential killing of cells with high 26S proteasome activity by ionizing radiation (Fig. 2E).

To compare the radiation sensitivity of clonogenic cells from monolayer cultures with that of sphere-forming cells we performed clonogenic survival assays and sphere forming capacity assays with cells irradiated with 0, 2, 4, 6, or 8 Gy (Fig. 2F). The radiation sensitivity of cells cultured as monolayers was comparable between DU-145 and PC-3 cells. However, cells able to initiate prostate spheres exhibited a highly radioresistant phenotype.

Self-Renewal Capacity and Tumorigenicity of Prostate Cancer Cell Subpopulations

To further investigate differences between prostate cancer cells with high and low proteasome activity we studied their self-renewal capacity and tumorigenicity using an in vitro sphere-forming assay and an in vivo limiting dilution assay.

Sphere forming capacity assays were performed by growing PC-3-ZsGreen-cODC cells in monolayer cultures and sorting them in ZsGreen-cODC-negative or -positive cells by fluorescence-activated cell sorting (FACS) at a density of 1 cell/well into 96-well ultra-low adhesion plates. After 3 weeks, the number of

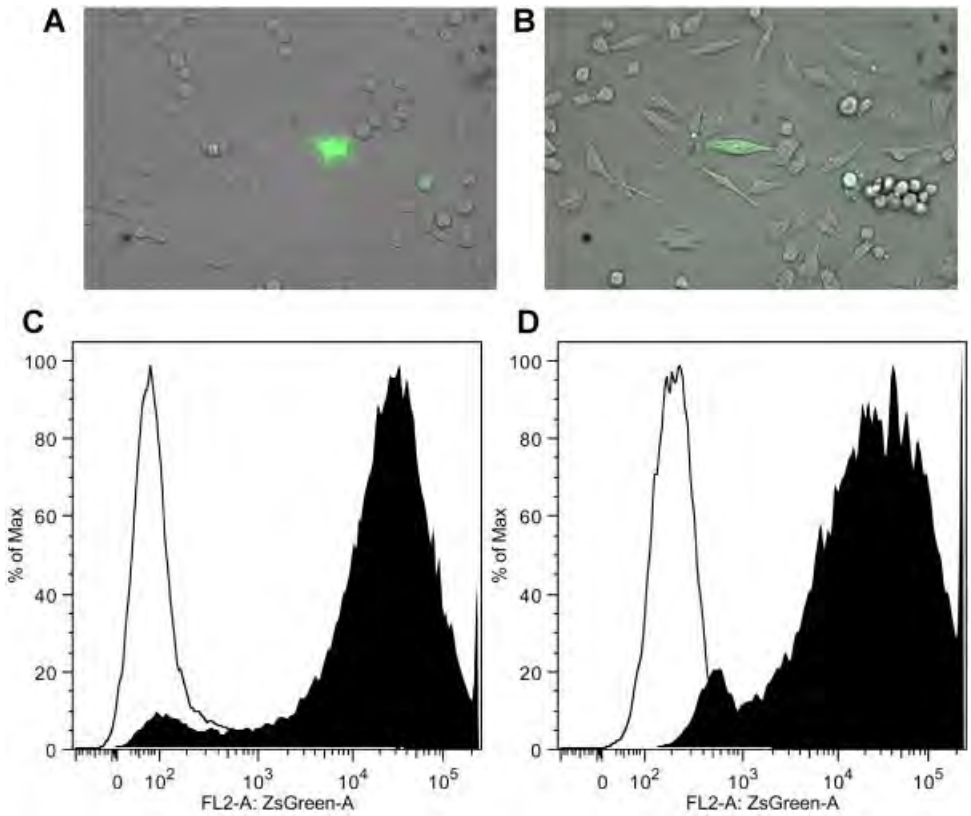

Fig. 1. PC-3 (**A**) and DUI45 (**B**) prostate cancer lines contain a small population of cells with intrinsically low proteasome activity. Composite images (phase contrast and green fluorescence) of cells with stably trasfected with am expression vector coding for a fusion protein between the green fluorescent protein ZsGreen and the C-terminal degron of murine ornithine decarboxylase (cODC). Accumulation of the fusion protein indicates lack of 26S protesome function. When PC-3-ZsGreen-cODC (**C**) and DUI45-ZsGreen-cODC (**D**) cells were incubated with the proteasome inhibitor MG-I32 (0.5 μM) over night, all cells accumulated the fusion protein.

prostate spheres formed per plate was counted and expressed as a percentage of the initial number of cells plated. Three independent experiments were undertaken, twelve 96-well plates were used per each experiment. ZsGreen-cODC-positive cells had statistically significant higher sphere forming capacity than ZsGreen-cODC-negative cells. In PC-3, 15% of the ZsGreen-cODC-positive cells and only of the 5% ZsGreen-cODC-negative formed primary spheres ($P = 0.04$). In DU145, 8% of the ZsGreen-cODC-positive population and only 4% of the ZsGreen-cODC-negative ($P = 0.02$) formed primary spheres (Fig. 2).

The secondary sphere formation assays performed in PC-3 or DU145 showed a higher secondary sphere-forming capacity for cells with low proteasome activity compared to the ZsGreen-cODC-negative population (Fig. 3).

In order to investigate the tumorigenicity of these two subpopulations, PC-3-ZsGreen-cODC cells were sorted by FACS into ZsGreen-cODC-negative and -positive cells and injected subcutaneously into the thighs of 6- to 8-week-old male Nu/Nu mice. When TD_{50} values (the number of cells required to form a tumor in 50% of the animals) were calculated, ZsGreen-cODC-positive showed 1 log lower TD_{50} values than ZsGreen-cODC-negative cells (8.6×10^2 vs. 9.7×10^3). However, this difference was statistically not significant (paired two-sided Student's *t*-test). In vivo imaging of the tumors revealed that cells with low proteasome activity were unevenly distributed throughout the tumor and that ZsGreen-cODC-positive cells redistributed into cells with high and cells with low proteasome activity. In contrary, cells with low proteasome activity did not produce progeny with low proteasome activity (Fig. 3).

DISCUSSION

In our previous work we reported excellent anti-tumor activity of proteasome inhibitors against a variety of solid tumors including prostate cancer [8]. However, when proteasome inhibitors were used against solid cancers in clinical trials, clinical

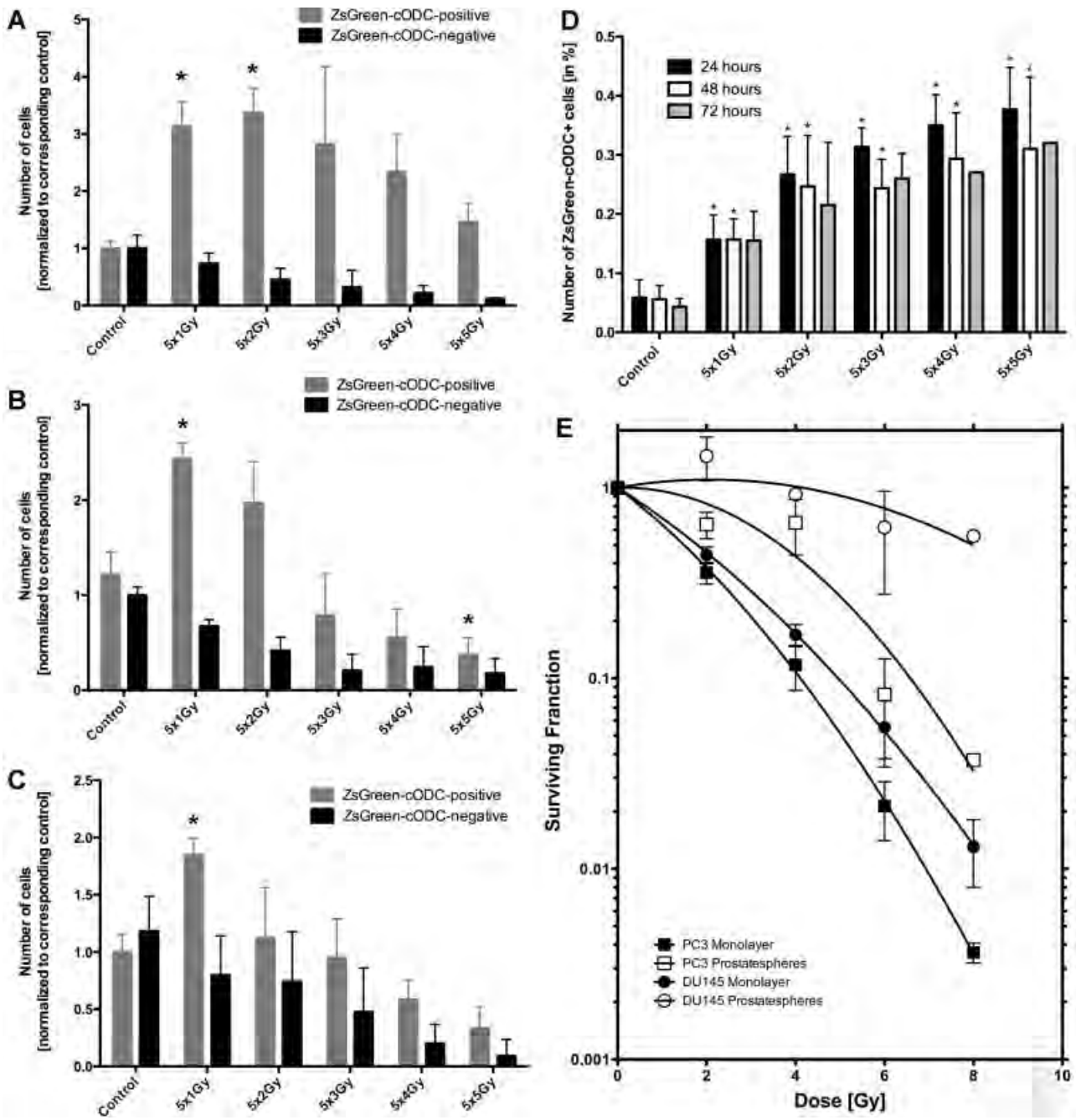

Fig. 2. Number of ZsGreen-cODC-negative and ZsGreen-cODC-positive cells, 24 hr (**A**), 48 hr (**B**), and 72 hr (**C**) after five daily fractions of radiation. Clinically used fractions of 2 Gy cause a significant increase in the number of cells with low proteasome activity (ZsGreen-cODC-positive) while the number of cells with high proteasome activity declines ($^*P < 0.05$, Student's *t*-test). **D**: Percentage of ZsGreen-cODC-positive cells at 24, 48, and 72 hr after tha last fraction of radiation. **E**: Clonogenic survival and survival of sphere-forming cells after singles doses of radiation. Sphere-forming cells have a radioresistant phenotype.

responses were rather disappointing [9–13]. The reasons for this failure are unknown. In the present study we tested the hypothesis that prostate cancer cells are heterogeneous with regard to the activity of the 26S proteasome, the target of proteasome inhibitors. We used two established prostate cancer cell lines and an imaging system for proteasome activity to test this hypothesis and to characterize these cells (Fig. 4).

We found that a small population of prostate cancer cells accumulated the ZsGreen-cODC reporter

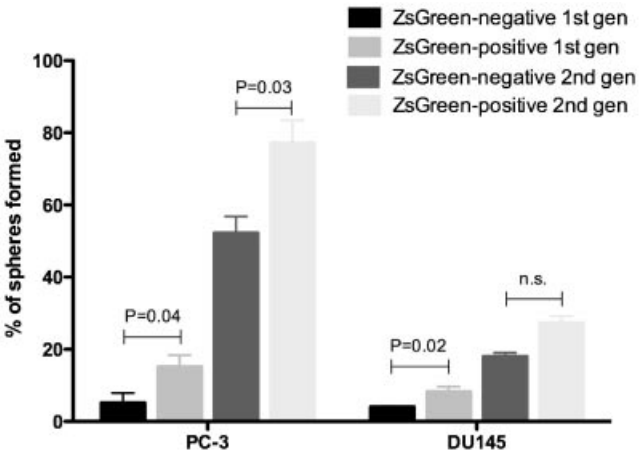

Fig. 3. Primary and secondary sphere formation from sorted ZsGreen-cODC-negative and -positive cells. In both PC-3 and DUI45, ZsGreen-cODC-positive cells showed increased sphere-formation.

protein in the absence of any treatment indicating intrinsically low proteasome function. Similar results were previously reported for glioma, breast, and lung cancer cells [14,15,17]. Like breast cancer and glioma cells with low proteasome activity [14,15], those prostate cancer cells were more radioresistant than the bulk tumor cell population and fractionated radiation enriched for these cells. A radioresistant phenotype has bee recently reported for breast cancer cells with low proteasome subunit expression [18]. This suggested that if this population of cells also existed in clinical samples it could drive recurrences after radiation treatment. Consistent with this hypothesis, cells with low proteasome activity showed increased self-renewal capacity in vitro. However, tumorigenicity measured by TD_{50} values of cells with low proteasome activity, did not significantly exceed that of cells with high proteasome activity, indicating that prostate cancer cells with low proteasome activity were not enriched for tumor-initiating cells. However, xenografts could be generated from as few as 100 ZsGreen-cODC-positive and 1,000 ZsGreen-cODC-negative cells, respectively, indicating a high frequency of tumor-initiating cells in established prostate cancer cell lines.

CONCLUSIONS

We conclude that established prostate cancer cell lines are heterogeneous with regard to their intrinsic proteasome activity and that they contain a radioresistant subpopulation of cells that can be identified by low proteasome activity. The existence of this subpopulation of cells in clinical samples needs to be established in future studies. If it exists it may explain the lack of clinical responses when bortezomib is used against advanced hormone-refractory prostate cancer.

ACKNOWLEDGMENTS

F.P. was supported by grants of the Department of Defense (W81XWH-07-1-0065) and the National Cancer Institute (CA137110-01).

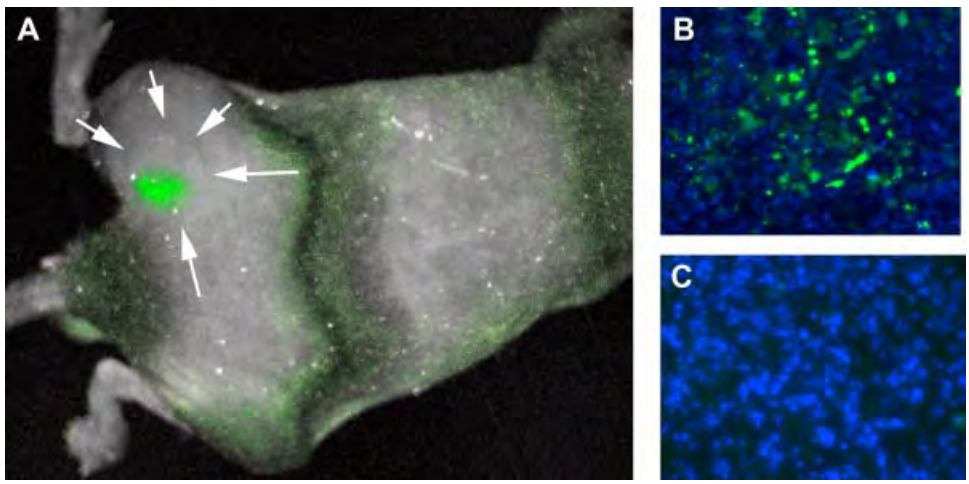

Fig. 4. **A**: In vivo imaging of a PC-3 xenograft formed by sorted ZsGreen-cODC-positive cells (white arrows). ZsGreen-cODC-positive cells are not uniformly distributed throughout the tumor but cluster in groups. Sections of tumors formed by ZsGreen-cODC-positive (**B**) and -negative (**C**) cells. ZsGreen-cODC-positive cells redistribute into ZsGreen-cODC positive and negative cells while progeny of ZsGreen-negative cells all have high proteasome activity (ZsGreen-cODC-negative).

REFERENCES

1. Jemal A, Siegel R, Xu J, Ward E. Cancer statistics, 2010. CA Cancer J Clin 2010;60(5):277–300.
2. Freedland SJ. Screening, risk assessment, and the approach to therapy in patients with prostate cancer. Cancer 2011;117(6): 1123–1135.
3. Alicikus ZA, Yamada Y, Zhang Z, Pei X, Hunt M, Kollmeier M, Cox B, Zelefsky MJ. Ten-year outcomes of high-dose, intensity-modulated radiotherapy for localized prostate cancer. Cancer 2011;117(7):1429–1437.
4. Stavridi F, Karapanagiotou EM, Syrigos KN. Targeted therapeutic approaches for hormone-refractory prostate cancer. Cancer Treat Rev 2010;36(2):122–130.
5. Pajonk F, McBride WH. The proteasome in cancer biology and treatment. Radiat Res 2001;156(5):447–459.
6. Coux O. The 26S proteasome. Prog Mol Subcell Biol 2002;29: 85–107.
7. Pajonk F, Himmelsbach J, Riess K, Sommer A, McBride WH. The human immunodeficiency virus (HIV)-1 protease inhibitor saquinavir inhibits proteasome function and causes apoptosis and radiosensitization in non-HIV-associated human cancer cells. Cancer Res 2002;62(18):5230–5235.
8. Pajonk F, van Ophoven A, Weissenberger C, McBride WH. The proteasome inhibitor MG-132 sensitizes PC-3 prostate cancer cells to ionizing radiation by a DNA-PK-independent mechanism. BMC Cancer 2005;5(1):76.
9. Morris MJ, Kelly WK, Slovin S, Ryan C, Eicher C, Heller G, Scher HI. A phase II trial of bortezomib and prednisone for castration resistant metastatic prostate cancer. J Urol 2007; 178(6):2378–2383; discussion 2383–2384.
10. LoConte NK, Thomas JP, Alberti D, Heideman J, Binger K, Marnocha R, Utecht K, Geiger P, Eickhoff J, Wilding G, Kolesar J. A phase I pharmacodynamic trial of bortezomib in combination with doxorubicin in patients with advanced cancer. Cancer Chemother Pharmacol 2008;63(1):109–115.
11. Hainsworth JD, Meluch AA, Spigel DR, Barton J Jr, Simons L, Meng C, Gould B, Greco FA. Weekly docetaxel and bortezomib as first-line treatment for patients with hormone-refractory prostate cancer: A Minnie Pearl Cancer Research Network phase II trial. Clin Genitourin Cancer 2007;5(4):278–283.
12. Dreicer R, Petrylak D, Agus D, Webb I, Roth B. Phase I/II study of bortezomib plus docetaxel in patients with advanced androgen-independent prostate cancer. Clin Cancer Res 2007; 13(4):1208–1215.
13. Papandreou CN, Daliani DD, Nix D, Yang H, Madden T, Wang X, Pien CS, Millikan RE, Tu SM, Pagliaro L, Kim J, Adams J, Elliott P, Esseltine D, Petrusich A, Dieringer P, Perez C, Logothetis CJ. Phase I trial of the proteasome inhibitor bortezomib in patients with advanced solid tumors with observations in androgen-independent prostate cancer. J Clin Oncol 2004;22(11):2108–2121.
14. Vlashi E, Kim K, Dealla Donna L, Lagadec C, McDonald T, Eghbali M, Sayre J, Stefani E, McBride W, Pajonk F. In-vivo imaging, tracking, and targeting of cancer stem cells. J Natl Cancer Inst 2009;101(5):350–359.
15. Lagadec C, Vlashi E, Della Donna L, Meng Y, Dekmezian C, Kim K, Pajonk F. Survival and self-renewing capacity of breast cancer initiating cells during fractionated radiation treatment. Breast Cancer Res 2010;12(1):R13.
16. Vlashi E, Kim K, Lagadec C, Donna LD, McDonald JT, Eghbali M, Sayre JW, Stefani E, McBride W, Pajonk F. In vivo imaging, tracking, and targeting of cancer stem cells. J Natl Cancer Inst 2009;101(5):350–359.
17. Pan J, Zhang Q, Wang Y, You M. 26S proteasome activity is down-regulated in lung cancer stem-like cells propagated in vitro. PLoS ONE 2010;5(10):e13298.
18. Smith L, Qutob O, Watson MB, Beavis AW, Potts D, Welham KJ, Garimella V, Lind MJ, Drew PJ, Cawkwell L. Proteomic identification of putative biomarkers of radiotherapy resistance: A possible role for the 26S proteasome? Neoplasia 2009; 11(11):1194–1207.

In Vivo Imaging, Tracking, and Targeting of Cancer Stem Cells

Erina Vlashi, Kwanghee Kim, Chann Lagadec, Lorenza Della Donna, John Tyson McDonald, Mansoureh Eghbali, James W. Sayre, Encrico Stefani, William McBride, Frank Pajonk

Background There is increasing evidence that solid cancers contain cancer-initiating cells (CICs) that are capable of regenerating a tumor that has been surgically removed and/or treated with chemotherapy and/or radiation therapy. Currently, cell surface markers, like CD133 or CD44, are used to identify CICs in vitro; however, these markers cannot be used to identify and track CICs in vivo. The 26S proteasome is the main regulator of many processes within a proliferating cell, and its activity may be altered depending on the phenotype of a cell.

Methods Human glioma and breast cancer cells were engineered to stably express ZsGreen fused to the carboxyl-terminal degron of ornithine decarboxylase, resulting in a fluorescent fusion protein that accumulates in cells in the absence of 26S proteasome activity; activities of individual proteases were monitored in a plate reader by detecting the cleavage of fluorogenic peptide substrates. Proteasome subunit expression in cells expressing the fusion protein was assessed by quantitative reverse transcription—polymerase chain reaction, and the stem cell phenotype of CICs was assessed by a sphere formation assay, by immunohistochemical staining for known stem cell markers in vitro, and by analyzing their tumorigenicity in vivo. CICs were tracked by in vivo fluorescence imaging after radiation treatment of tumor-bearing mice and targeted specifically via a thymidine kinase–degron fusion construct. All *P* values were derived from two-sided tests.

Results Cancer cells grown as sphere cultures in conditions, which enrich for cancer stem cells (CSCs), had decreased proteasome activity relative to the respective monolayers (percent decrease in chymotryptic-like activity of sphere cultures relative to monolayers—U87MG: 26.64%, 95% confidence interval [CI] = 10.19 to 43.10, GL261, 52.91%, 95% CI = 28.38 to 77.43). The cancer cells with low proteasome activity can thus be monitored in vitro and in vivo by the accumulation of a fluorescent protein (ZsGreen) fused to a degron that targets it for 26S proteasome degradation. In vitro, ZsGreen-positive cells had increased sphere-forming capacity, expressed CSC markers, and lacked differentiation markers compared with ZsGreen-negative cells. In vivo, ZsGreen-positive cells were approximately 100-fold more tumorigenic than ZsGreen-negative cells when injected into nude mice (ZsGreen positive, 30 mice per group; ZsGreen negative, 31 mice per group), and the number of CICs in tumors increased after 72 hours post radiation treatment. CICs were selectively targeted via a proteasome-dependent suicide gene, and their elimination in vivo led to tumor regression.

Conclusion Our results demonstrate that reduced 26S proteasome activity is a general feature of CICs that can easily be exploited to identify, track, and target them in vitro and in vivo.

J Natl Cancer Inst 2009;101:350–359

Cancer cell propagation in vivo has been explained by the "stochastic model" (1,2), which claims that every cancer cell in a tumor can ultimately acquire a capacity for self-renewal and multilineage potency so that it can repopulate an entire tumor. The stochastic model of cancer has long been regarded as the only working model of cancer organization, largely because until recently it has not

Affiliations of authors: Division of Molecular and Cellular Oncology, Department of Radiation Oncology (EV, KK, CL, LDD, JTM, WM, FP), Department of Anesthesiology (ME, ES), David Geffen School of Medicine at University of California, Los Angeles, Biostatistics and Radiological Sciences, School of Public Health (JWS), University of California, Los Angeles, Jonsson Comprehensive Cancer Center (WM, FP), University of California, Los Angeles.

Correspondence to: Frank Pajonk, MD, PhD, Division of Molecular and Cellular Oncology, Department of Radiation Oncology, David Geffen School of Medicine at University of California, Los Angeles, 10833 Le Conte Ave, Los Angeles, CA 90095-1714 (e-mail: fpajonk@mednet.ucla.edu).

See "Funding" and "Notes" following "References."

DOI: 10.1093/jnci/djn509

been possible to prospectively isolate the very small population of cancer stem cells (CSCs) from the bulk of an unselected tumor cell population for characterization. In addition, working with unselected cell populations is inexpensive and experimental responses of the bulk of these cells can be easily used as a rationale for pharmaceutical approaches against cancer. Unfortunately, and despite an enormous effort, these approaches based on the behavior of unselected cell populations, even those termed targeted cancer therapies, have not yet resulted in cancer cures.

An alternative view of cancer cell propagation that is now supported by an increasing body of experimental evidence is the hierarchical model (3). It assumes that most, if not all, solid cancers are characterized by a hierarchical organization in which there are small populations of cancer stem cells (CSCs) or cancer-initiating cells (CICs) that are capable of repopulating an entire tumor, but whose progeny lacks this ability (1). Although this model has long been postulated, it has only recently become possible to provide supporting experimental evidence because of technological advances, such as the availability of sophisticated fluorescence-activated cells sorting (FACS) instruments, which are capable of efficiently isolating viable populations of rare cells from the bulk of tumor cells based on their expression of several cell surface markers. An increasing number of cell surface markers have been used to distinguish CSCs and CICs from the bulk of the tumor cells and to demonstrate their self-renewal capacity, multilineage potency, lack of expression of differentiation markers, and increased tumorigenicity when injected into immune-deficient mice (4–10). CSCs/CICs identified in this way have been shown to be relatively resistant to conventional anticancer therapies, such as chemotherapy and/or radiation therapy (11–13), and there is now strong evidence to suggest that a successful cancer treatment strategy will have to be based on the elimination of this cell population via novel therapeutic approaches. Thus, although it is becoming increasingly important to identify, track, and target CSCs/CICs in vivo, available markers are not very suitable for the purpose. A reliable system that would allow identification and tracking of CSCs/CICs would be an invaluable tool to study the effects of established and novel therapies on CSCs/CICs, but one that requires identification of cellular factors specific to this population.

The 26S proteasome is a multicatalytic protease complex with at least three distinct kinds of proteolytic activities—chymotrypsin like, trypsin like, and caspase like. It accounts for almost 1% of total protein expressed in eukaryotic cells and is a key regulator of many cellular functions, including cell cycle control, DNA repair, cell death, and survival (14). Its inhibition causes apoptosis and sensitization of cells to chemotherapeutic agents (15) and ionizing radiation (16,17). Furthermore, conventional anticancer therapies, for example, ionizing radiation (18), chemotherapeutic drugs (19,20), and hyperthermia (21), inhibit the proteasome, suggesting that their anticancer activity may be mediated by effects on this protein complex.

A proteasome inhibitor, bortezomib, is in clinical use for patients suffering from multiple myeloma or mantle cell lymphoma (22). However, despite its excellent preclinical efficacy in animal models of other cancers, bortezomib failed to demonstrate antitumor activity as a single agent in patients with solid cancers in clinical trials, suggesting that CICs might not be affected by proteasome inhibition (23–27). The results of these clinical studies prompted us to investigate proteasome activity and subunit expression in CICs of solid cancers relative to that in monolayer cultures and to examine whether proteasome activity is a useful marker for CICs. To monitor proteasome activity in living cells, we generated cancer cell lines that stably expressed a fusion protein consisting of a fluorescent protein fused to a degron, a sequence that targets the fusion protein for destruction by the proteasome. We also generated cancer cell lines expressing the degron fused to the suicide gene thymidine kinase (TK) to specifically investigate the effect of eliminating cells with low proteasome activity on sphere-forming capacity and self-renewal in vitro and tumor growth in vivo.

CONTEXT AND CAVEATS

Prior knowledge

It had become evident that in many solid cancers there are small subpopulations of cells with stem cell–like properties known as cancer initiating cells (CICs) (or cancer stem cells [CSCs]) that are relatively resistant to conventional cancer therapies. Methods to identify and track these cells in vivo were lacking.

Study design

Cancer cells were engineered to express a fluorescent protein that is a target of the 26S protesome, a multiprotein complex which appeared to have reduced proteolytic activity in CICs. The correlation of various CIC/CSC phenotypes in the engineered cells with fluorescence, and thus 26S proteosome activity, was assessed.

Contribution

This study found that reduced 26S proteosome activity was closely correlated with CIC phenotypes in glioma and breast cancer cells. Thus, engineering cells to express a substrate of the protease is a viable method to identify and track these cell populations in vivo.

Implications

The ability to identify and track CICs in animal models of cancer may allow better assessment of therapeutic approaches compared to conventional methods such as measuring tumor response.

Limitations

The CICs with low protease activity may themselves be a heterogenous population of cells that needs to be further defined.

From the Editors

Materials and Methods

Cell Culture

Human U87MG glioma cell line was a kind gift from Dr P. Michel (Department of Pathology, University of California, Los Angeles, Los Angeles, CA). Murine GL261 glioma and 67NR breast cancer cell lines were a kind gift from Dr Sandra DeMaria (Department of Pathology, New York University School of Medicine, New York, NY). Human U343 and MCF-7 breast cancer cell lines were purchased from American Type Culture Collection (Manassas, VA). All cells were cultured in log-growth phase in Dulbecco's Modified

Eagle Medium (DMEM) (Invitrogen, Carlsbad, CA) (supplemented with 10% fetal bovine serum [Sigma, St Louis, MO] and penicillin and streptomycin cocktail [Sigma]) and were grown in a humidified incubator at 37°C at 5% CO_2. To obtain CICs, MCF-7, 67NR, U87MG, U343, and GL261 cells were seeded into selection media (DMEM/F12, 0.4% bovine serum albumin (BSA) [Sigma], 10 mL per 500 mL B27 [Invitrogen], 5 μg/mL bovine insulin [Sigma], 4 μg/mL heparin [Sigma], 20 ng/mL fibroblast growth factor 2 [bFGF, Sigma], and 20 ng/mL epidermal growth factor [EGF, Sigma]) at a density of 1000 cells per mL. Under these conditions, only CICs and early progenitor cells survive and proliferate, whereas differentiated cells die (28).

Generation of Stable Cell Lines Expressing ZsGreen-cODC and TK-ZsGreen-cODC Fusion Proteins Using Retroviral Transduction

Proteasomal degradation of most proteins depends on their ubiquitination. However, a small number of proteins such as ornithine decarboxylase (ODC) contain amino acid sequences that are directly recognized by the proteasome, which leads to the immediate destruction of the proteins that contain them. Viral expression vectors in which the carboxyl terminus of the murine ornithine decarboxylase (cODC) degron was fused to reporter proteins were constructed as follows. ZsGreen-cODC: The degron from the carboxyl-terminal 37 amino acids of ODC fused to ZsGreen (ZsGreen-cODC) was digested with *Bgl*II and *Not*I from pZsProsensor-1 (BD Biosciences, San Jose, CA) and cloned into the *Bam*HI and *Eco*RI sites of the retroviral vector pQCXIN (BD Biosciences) using the *Not*I-*Eco*RI DNA oligonucleotide adaptor (EZCLONE Systems, New Orleans, LA). TK-ZsGreen-cODC: ZsGreen-cODC was amplified from pZsProsensor-1 and cloned into the *Bam*HI and *Eco*RI sites of pQCXIN vector (pQCXIN-*Bam*H1-ZsGreen-ODC). The sequence of TK was amplified from pORF-HSVtk expression vector (InvivoGen, San Diego, CA) and cloned into pQCXINBamH1-ZsGreen-cODC using the *Not*I and *Bam*HI sites (pQCXIN/TK-ZsGreen-ODC). pQCXIN/ZsGreen-cODC or pQCXIN/TK-ZsGreen-cODC was transfected into GP2-293 pantropic retroviral packaging cells (BD Biosciences). The retrovirus collected from the supernatant of the packaging cells was used to infect the different cell lines. Stable transfectants were selected with G418 (Invitrogen). The accumulation of ZsGreen-cODC protein was monitored by flow cytometry (FL-1 channel). To determine that the cells not accumulating the ZsGreen-cODC protein still contained the expression vector, the cells were incubated with 50 μM of the proteasome inhibitor MG-132 (Calbiochem, San Diego, CA) for 4 hours and the accumulation of the ZsGreen-cODC protein due to proteasome inhibition was analyzed by flow cytometry.

Primary Sphere Formation Assay

ZsGreen-cODC–expressing U87MG cells were grown in selection media as sphere cultures (primary spheres) and were sorted into ZsGreen-negative and -positive populations by FACS. Cells were defined as "ZsGreen positive" if the fluorescence in the FL-1 channel exceeded the fluorescence of nontransfected control cells by at least three orders of magnitude. The two cell populations were plated in selection media into 96-well plates, ranging from 1 to 100 cells per well. Growth factors, EGF and bFGF, were added every 3 days, and the cells were allowed to form spheres (secondary spheres) for 7–10 days. The number of spheres formed per well was then counted and expressed as a percentage of the initial number of cells plated. Four independent experiments were performed.

Proteasome Function Assays

Chymotryptic, tryptic, and caspase proteasome activities were measured as described previously (29) with a few minor modifications. MCF-7, 67NR, U87MG, U343, and GL261 cells were washed with phosphate buffered saline (PBS) and pelleted by centrifugation. Glass beads and homogenization buffer (25 mM Tris [pH 7.5], 100 mM NaCl, 5 mM ATP, 0.2% [vol/vol] Nonidet P-40 and 20% glycerol) were added to the cells, and the mixtures were vortexed for 1 minute. Beads and cell debris were removed by centrifugation at 4°C. Protein concentration in the resulting crude cellular extracts was determined by the Micro (bicinchoninic acid) protocol (Pierce, Rockford, IL) with BSA (Sigma) as standard. To measure 26S proteasome activity, 100 μg of protein from crude cellular extracts of each sample was diluted with buffer I (50 mM Tris [pH 7.4], 2 mM dithiothreitol, 5 mM $MgCl_2$, 2 mM ATP) to a final volume of 1 mL (assayed in quadruplicate). The fluorogenic proteasome substrates Suc-LLVY-AMC (chymotryptic substrate; Biomol International, Plymouth Meeting, PA), Z-ARR-AMC (tryptic substrate; Calbiochem), and Z-LLE-AMC (caspase-like substrate; Biomol International) were dissolved in dimethyl sulfoxide DMSO and added to a final concentration of 80 μM in 1% DMSO. Proteolytic activities were continuously monitored by measuring the release of the fluorescent group, 7-amido-4-methylcoumarin (AMC), with the use of a fluorescence plate reader (Spectramax M5, Molecular Devices, Sunnyvale, CA) at 37°C, at excitation and emission wavelengths of 380 and 460 nm, respectively.

Luminescence ATP Detection Assay

Single-cell suspensions derived from U87MG-ZsGreen-cODC monolayer cultures (1000 cells) or 3-day-old primary sphere cultures were plated into 96-well plates of DMEM or DMEM/F12 selection medium (100 μL per well). The proteasome inhibitor PS341 (kind gift of Julian Adams, Millennium Pharmaceuticals, Cambridge, MA) was added at the indicated concentrations. After 5 days of incubation, 40 μL of ATP-lite substrate (Perkin-Elmer, Waltham, MA) was added to each well and luminescence was measured immediately using a fluorescence plate reader (Spectramax M5).

Quantitative Reverse Transcription–Polymerase Chain Reaction

Total RNA was isolated from U87MG monolayer cells and from sorted ZsGreen-cODC–positive and –negative cells using TRIZOL Reagent (Invitrogen). Complementary DNA (cDNA) synthesis was carried out using TaqMan Reverse Transcription Reagents (Applied Biosystems, Foster City, CA). Quantitative polymerase chain reaction (PCR) of proteasome subunit cDNAs was performed in an iQ5 Real-Time PCR Detection System (Bio-Rad, Hercules, CA) using the 2× iQ SYBR Green Supermix (Bio-Rad). C_t for each gene was determined after normalization to GAPDH,

and $\Delta\Delta C_t$ was calculated relative to the designated reference sample. Gene expression values were then set equal to $2^{-\Delta\Delta Ct}$ as described by the iQ5 Optical System Software (Bio-Rad). All PCR primers were synthesized by Invitrogen and designed to amplify human *GAPDH* and the human proteasome subunits *Lmp2*, *Y*, *Mecl1*, *Z*, *Lmp7*, *X*, *11S PA28alpha*, *11S PA28beta*, *19S ATPase PSMC1*, and *19S non-ATPase PSMD4* (all primer sequences are provided in the Supplementary Methods, available online).

Mice

Nude (nu/nu), 6- to 8-week-old female mice originally from The Jackson Laboratories (Bar Harbor, ME) were rederived, bred, and maintained in a Defined Flora environment in the Association for the Assessment and Accreditation of Laboratory Animal Care International–accredited animal facilities of the Department of Radiation Oncology, University of California, Los Angeles (Los Angeles, CA) in accordance with all local and national guidelines for the care of animals. We used 74 mice for the in vivo experiments: 61 mice were used for the tumorgenicity experiments, 10 mice were implanted with U87-TK-ZsGreen-ODC tumors, and three mice were used to analyze the effect of fractionated radiation on U87MG-ZsGreen-ODC tumors.

Tumor Xenotransplantation and Tumorigenicity

U87MG-ZsGreen–high or U87MG-ZsGreen–negative cells derived from 5- to 6-day-old spheres and sorted by FACS were injected subcutaneously into both thighs of nude mice (10^6, 10^5, 10^4, 10^3, or 10^2 cells per inoculum), and each tumor was considered as the unit of analysis. The number of tumors used for each group is summarized in Table 1. Tumor growth was monitored on a weekly basis, and the mice were killed by CO_2 asphyxiation when the tumor size reached the protocol guidelines requiring euthanasia (1.3 cm in diameter).

Fractionated Radiation

Subcutaneous tumors (average diameter of 1 cm) generated from implanting 1×10^6 cells derived from unselected U87MG-ZsGreen-cODC monolayers into the thighs of nude mice were irradiated with 3 Gy for 5 consecutive days, using a cobalt-60 source (dose rate 0.6 Gy/min). The thighs of anesthetized mice bearing the tumor were placed in a 5 × 5-cm radiation field of the cobalt-60 source, whereas the rest of the body was shielded. The mice were anesthetized at different time points after irradiation and imaged for the macroscopic presence of ZsGreen-positive cells in the tumors using the Maestro In-Vivo Imaging System (Cambridge Research & Instrumentation, Woburn, MA).

Immunocytochemistry

Spheres from U87MG-ZsGreen-cODC cells that were 5–6 days old were transferred onto glass slides by cytocentrifugation (Cytospin; Shandon Elliot, London, UK) and fixed with 4% formaldehyde. The cells were incubated in permeabilization buffer (10% saponin, 0.5% BSA, in PBS) for 10 minutes, followed by incubation with the following primary antibodies for 30 minutes at room temperature: rabbit anti-human nestin (1:500) (Abcam, Cambridge, MA), rabbit anti-human glial fibrillary acidic protein (GFAP) (1:1000) (Abcam), mouse anti-human TUJ-1 (1:1000) (Abcam), mouse anti-human Sox2 (10 μg/mL) (R&D Systems, Minneapolis, MN), or mouse anti-human Musashi-1 (10 μg/mL) (R&D Systems). For staining with the mouse anti-human 19S regulator non-ATPase subunit Rpn2 (1:200) (Biomol International), the slides were first incubated with 5% goat serum in PBS and Triton to block nonspecific antibody binding, and then with the primary antibody overnight at 4°C. The secondary antibodies tetramethyl rhodamine isothiocynate (TRITC)-conjugated goat anti-rabbit IgG [1:200], and TRITC-conjugated goat anti-mouse Fab [1:80], both from Sigma) were diluted in PBS and 1% BSA/0.5% saponin and incubated with the cells for 1 hour. Hoechst 33342 (5 μg/mL; Invitrogen) solution was added for nuclear staining. The slides were visualized with an Olympus IX71 inverted fluorescent microscope.

Immunohistochemistry

Tumors were removed from sacrificed mice and fixed in buffered formalin. The tissue was then embedded in paraffin and cut into 4-μm sections. The tissue sections were deparaffinized in xylene (2 × 5 minutes) and rehydrated in a graded series of ethanol solutions (100%, 90%, 75%, 50%, and 25%) for 5 minutes each, followed by a final rinse in PBS. Antigen retrieval was performed by incubating the sections with CAREZYME I-Trypsin solution (BioCare Medical, Concord, CA). The sections were incubated with 10% goat serum in PBS to block nonspecific binding. The primary antibodies, rabbit anti-human Ki67 (1:100) (Abcam), and mouse anti-human CD31 (10 μg/mL) (Abcam) were diluted in 1% BSA and PBS and incubated with the sections overnight at 4°C. TRITC-conjugated secondary antibodies (TRITC-conjugated goat anti-rabbit IgG [1:80], and TRITC-conjugated goat anti-mouse Fab [1:400], both from Sigma) diluted in 1% BSA and PBS were added for 1 hour. Hoechst 33342 was added for 10 minutes at room temperature. The sections were visualized using an Olympus IX71 inverted fluorescent microscope.

Statistical Analysis

All results are expressed as mean values with 95% confidence intervals. For the proteasome activity assays, normal distributions of the data were confirmed using a Kolmogorov–Smirnov test. All statistical

Table 1. Enhanced tumor formation by cells with low levels of 26S proteasome*

	Fraction (%) of injected mice that developed tumors		
No. of cells injected	Injected with ZsGreen-high cells	Injected with ZsGreen-negative cells	Injected with ZsGreen-negative cells, and excluding ZsGreen-positive tumors†
10^2	1/4 (25%)	0/3	0/3
10^3	8/11 (73%)	1/4 (25%)	0/3
10^4	10/11 (91%)	5/9 (56%)	2/6 (33%)
10^5	4/4 (100%)	7/10 (70%)	4/7 (57%)
10^6	—	4/5 (80%)	2/3 (67%)

* The ZsGreen protein was fused to the murine ornithine decarboxylase degron and its accumulation was thus an indicator of low proteasome activity.

† When the tumors that arose from injections with ZsGreen-negative cells resulted in macroscopically green tumors, they were excluded from the total number of tumors formed from the ZsGreen-negative population.

comparisons used a two-sided paired Student's *t*-test. The test was applied to normalized data to compensate for the variance of measurements between biologically independent replicates of the same experiments. Statistical significance was defined as $P \leq .05$.

Results

Proteasome Activities of CICs in Breast Cancer and Glioma

We recently reported that sublethal doses of ionizing radiation increased the number of CICs in breast cancer (13) and sought to prevent this increase by blocking cell cycle progression using proteasome inhibitors. The approach was ineffective because CICs derived from mammospheres (data not shown) or glioma neurospheres were very resistant to proteasome inhibition (Supplementary Figure 1, A and B, available online). To monitor 26S proteasome activity in living cells, we stably transduced murine and human glioma and breast cancer cells lines with a fusion of a fluorescent protein, ZsGreen, and the degron from the cODC using retroviral vectors. The cODC is recognized by the 26S proteasome in an ubiquitin-independent manner (30), thus leading to immediate degradation of the ZsGreen fluorescent protein. Untreated monolayer cultures of U87MG exhibited low background fluorescence in more than 94% of the cells, but very few cells (<4%) displayed high levels of ZsGreen expression (Figure 1, A). Treatment of cultures with proteasome inhibitors, such as MG-132, caused 100% of cells to express ZsGreen (data not shown). Interestingly, primary spheres that are derived from U87MG cells under serum-free conditions and which are highly enriched for CICs (31,32) were greatly enriched for ZsGreen-positive cells (Figure 1, B), indicating that CICs may have low 26S proteasome activity.

To validate this observation, we performed fluorogenic proteasome function assays using monolayer and primary sphere cultures from U87MG human glioma and GL261 murine glioma cells (29). Chymotrypsin-like activity, the predominant activity of the 26S proteasome, as well as caspase-like activity were reduced in the sphere cultures, whereas the trypsin-like activity of U87MG cells was increased (percent decrease in proteasome activities of sphere cultures relative to monolayer cultures, mean of difference: chymotryptic-like activity, 26.64%, 95% CI = 10.19 to 43.10, $P = .02$, n = 3; trypsin-like activity, −39.46%, 95% CI = −88.18 to 9.266, $P = .08$, n = 4; caspase-like activity, 38.74%, 95% CI = 15.29 to 62.20, $P = .01$, n = 4; GL261: chymotryptic-like activity, 52.91%, 95% CI = 28.38 to 77.43, $P = .006$, n = 4; trypsin-like activity, 65.23%, 95% CI = 49.03 to 81.43, $P = .001$, n = 4; caspase-like activity, 52.88%, 95% CI = −18.22 to 124, $P = .09$, n = 3; Figure 1, C and D). Using the same fluorogenic peptide assays, reduced proteasome activity was further confirmed in U343 human glioma cells (proteasome activities of sphere cultures relative to the monolayer, mean of difference: chymotryptic-like activity, 37.74%, $P = .01$; trypsin-like activity, 26.25%, $P = .03$; caspase-like activity, 35.34%, $P = .04$; Supplementary Figure 1, C, available online), as well as in human and murine breast cancer cells, MCF-7 and 67NR (proteasome activities of sphere cultures

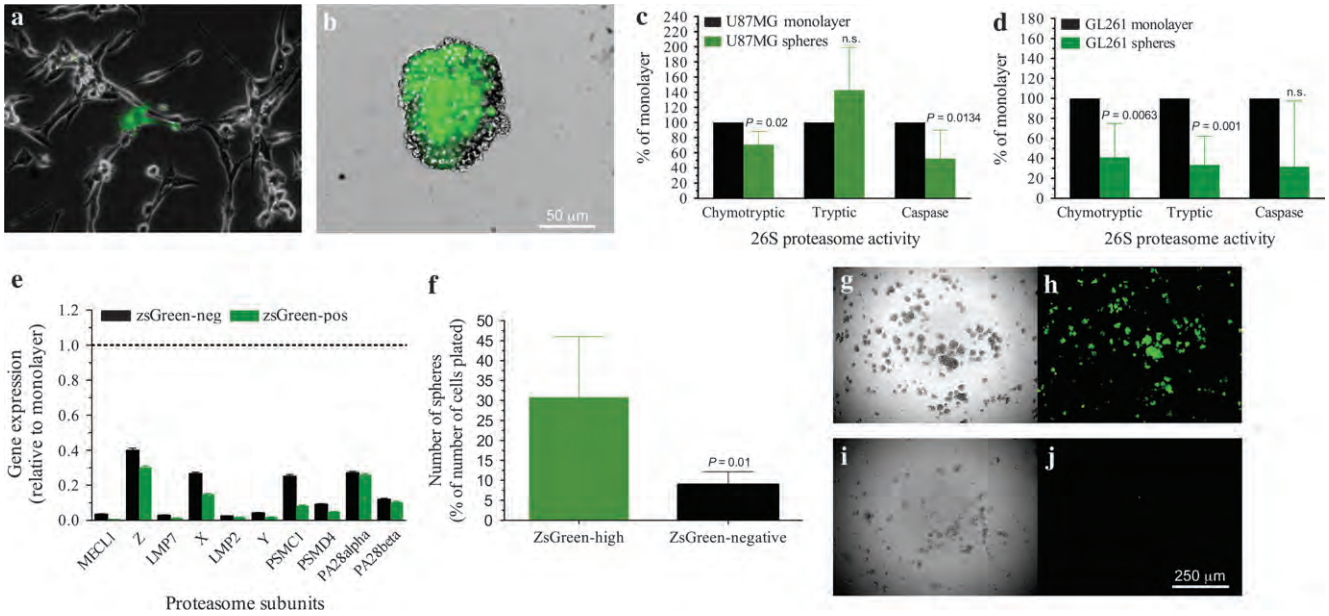

Figure 1. Characterization of cancer-initiating cells based on their proteasome activity. **A, B**) Frequency of cells in U87MG monolayer cultures (A) and U87MG-derived primary spheres (B) with accumulation of ZsGreen-cODC, and thus low proteasome activity. **C, D**) Proteasome activities of the 26S proteasome in U87MG (C) and GL261 (D) monolayer and sphere cultures. Means ± 95% confidence intervals (CIs) derived from three to four independent experiments (four replicates per experiment). The Kolmogorov–Smirnov test was used to confirm the normal distribution of the data, and the Student's paired, two-tailed *t*-test were performed. **E**) Reverse transcription—polymerase chain reaction analysis of expression of mRNAs encoding proteasome components in ZsGreen-positive and ZsGreen-negative cells derived from spheres relative to expression in unselected monolayers (**dotted line**), three independent experiments. **F**) Number of spheres formed from the ZsGreen-high population vs the ZsGreen-negative population after sorting with flow cytometry into 96-well plates. Means ± 95% CIs from four independent experiments are shown. **G, H**) Secondary spheres derived from fluorescence-activated cells–sorted ZsGreen-high (G and H) and ZsGreen-negative cells (**I, J**). An image of bright field (**left**) and ZsGreen fluorescence (**right**) is shown for both populations.

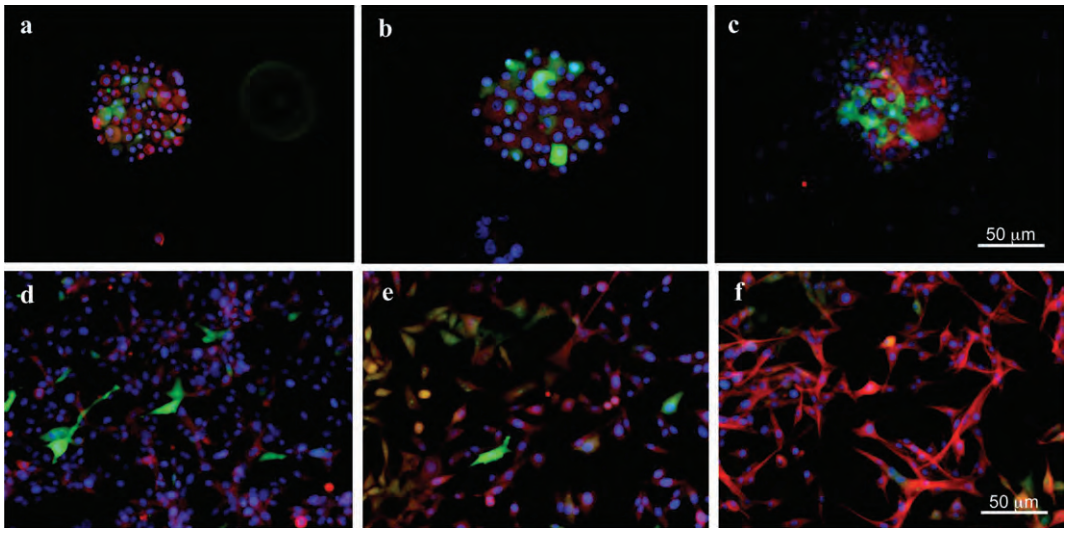

Figure 2. Cancer stem cell phenotype of cancer cells with low proteasome activity. **A–C**) Cytospins of U87MG-ZsGreen-cODC–derived neurospheres. ZsGreen-positive cells are positive for the stem cell marker nestin (**red**, A) but negative for the differentiation markers glial fibrillary acide protein (red, B) and TUJ-1 staining of neuron-specific class III β-tubulin (red, C). **D–F**) U87MG-ZsGreen-cODC–derived neurospheres differentiated in the presence of fetal bavine serum. Cells lost expression of ZsGreen and nestin (red, D) but expressed the differentiation markers GFAP (red, E) and exhibited TUJ-1 staining of neuron-specific class III β-tubulin (red, F). Counterstaining was performed with 4′,6-diamidino-2-phenylindole (**blue**).

relative to the monolayer, mean of difference—MCF-7: chymotryptic-like activity, 56.62%, P = .1; trypsin-like activity, 56.51%, P = .02; caspase-like activity, 36.92%, P = .041; 67NR: chymotryptic-like activity, 46.4%, P = .004; trypsin-like activity, 15.87%, P = .008; caspase-like activity, 55.45%, P = .055; Supplementary Figure 1, D and E, available online), indicating that reduced proteasome activity in CICs is a feature found across tumor entities of different species. Furthermore, quantitative reverse transcription—polymerase chain reaction revealed that several proteasome subunit mRNAs were decreased more than 100-fold in sphere cultures of CICs compared with cells in monolayer cultures (Figure 1, E). Confocal microscopy imaging for the Rpn2 subunit of the regulatory 19S cap of the 26S proteasome revealed a marked decrease in its expression in cells positive for ZsGreen (low proteasome activity), whereas cells lacking ZsGreen (high proteasome activity) expressed substantial levels of Rpn2 (Supplementary Figure 2, A–D, available online). Interestingly, a low 20S proteasome function has previously been reported for embryonic stem cells (33).

CICs, Proteasome Activity, and the CSC Phenotype

ZsGreen-high cells had a statistically significantly higher secondary sphere-forming capacity compared with the ZsGreen-negative population (average number of spheres formed, expressed as a percentage of the number of cells plated: ZsGreen-high cells versus ZsGreen-negative cells = 31% vs 9%; difference = 22%, 95% CI = 9.5% to 34.5%, P = .01, n = 4; Figure 1, F). The ZsGreen-high cells redistributed into ZsGreen-positive and -negative cells. By contrast, ZsGreen-negative cells formed only a few small spheres, which did not contain any ZsGreen-positive cells when analyzed by fluorescent microscopy (Figure 1, G–J).

Further immunohistochemical characterization of the ZsGreen-positive cells derived from U87MG-ZsGreen-cODC spheres revealed that they were positive for the stem cell marker nestin (Figure 2, A, and Supplementary Figure 2, E, available online), which is a substrate of the 26S proteasome (34), and negative for the differentiation markers GFAP and neuron-specific class III β-tubulin (Figure 2, B and C). When U87MG-ZsGreen-cODC spheres were allowed to attach to the surface of the culture dishes and were exposed to serum-containing standard growth media (differentiating conditions), the number of ZsGreen-positive cells declined, and the attached cells became positive for GFAP and neuron-specific class III β-tubulin, indicating that they had undergone differentiation (Figure 2, D–F). Similarly, spheres derived from the U343 human glioma cells stably expressing the ZsGreen-cODC reporter also expressed stem cell markers, such as Musashi-1 and Sox2 (Supplementary Figure 2, F and G, available online), in the ZsGreen-positive cells, whereas the ZsGreen-negative cells expressed the differentiation markers GFAP and TUJ-1 (Supplementary Figure 2, H and I, available online).

An important test for validating the identity of a CIC population is the demonstration of increased tumorigenicity in vivo. Therefore, the tumorigenicity of U87MG-ZsGreen-cODC cells was tested by first sorting them into ZsGreen-high and -negative populations using FACS. Different cell numbers from each population were injected subcutaneously into nude mice in numbers ranging from 10^2 to 10^6 cells per injection. Analysis of the sorted populations immediately after sorting revealed that 99.75% of ZsGreen-negative population were in fact negative for the fluorescent protein; thus, we estimated that one in 400 ZsGreen-negative cells injected was ZsGreen positive. Given that as few as 100 ZsGreen-positive cells could form a tumor (Table 1), we expected that some tumors would form in mice injected with at least 10^3 ZsGreen-negative cells and that those tumors would contain ZsGreen-positive cells. This was confirmed by in vivo fluorescent imaging, which demonstrated that some of the tumors arising from inoculation of sorted ZsGreen-negative cells contained ZsGreen-positive cells (Figure 3, C and D). Also, as mentioned above (Figure 1, G–J), ZsGreen-negative cells never repopulated into ZsGreen-positive cells in vitro; therefore, we concluded that formation of a

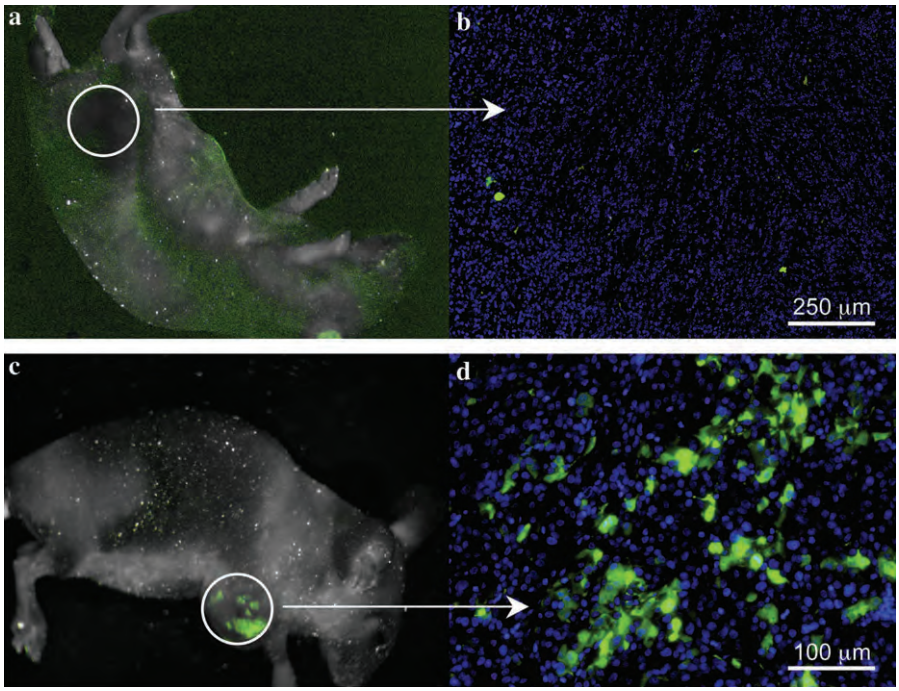

Figure 3. Tumorigenicity of cancer cells with low proteasome activity. **A, B**) ZsGreen-negative tumors derived from the ZsGreen-negative fraction of sorted sphere cells, viewed macroscopically or at high magnification. **C, D**) ZsGreen-positive tumors due to the contaminating presence of ZsGreen-positive cells in the negative fraction.

ZsGreen-positive tumor in vivo from the injection of ZsGreen-negative cells was due to the less than 100% purity of this population after sorting. Mice were inspected for tumor formation on a daily basis, and the presence of ZsGreen-positive cells was monitored by in vivo imaging for all macroscopic tumors. When we excluded tumors deriving from ZsGreen-negative cells contaminated with ZsGreen-positive cells (visible in macroscopic imaging, Figure 3, C and D) from the total number of tumors formed, we found that the ZsGreen-positive cells exhibited approximately 100-fold increased tumorigenicity compared with the ZsGreen-negative cells, suggesting that glioma cells with reduced proteasome activity are highly enriched for CICs (Table 1).

To examine if the ZsGreen-cODC reporter could be used to identify CICs in tumors, we stained sections of tumors derived from monolayer cultures of U87MG-ZsGreen-cODC cells with antibodies against the endothelial marker CD31 to identify vasculature. ZsGreen-positive cells were mainly found in perivascular regions and were absent in necrotic or avascular areas of the tumor (Supplementary Figure 3, A–C, available online). This observation was consistent with a previous report by Calabrese et al. (35), showing brain tumor stem cells to reside in a perivascular niche. In this context, it is important to note that the percentage of ZsGreen-positive cells in U87MG-ZsGreen-cODC tumors greatly exceeded the low percentage of ZsGreen-positive cells seen in vitro, which is consistent with earlier reports showing higher numbers of CICs in vivo than might be expected from in vitro observations (31).

Tracking and Targeting of CICs In Vivo Based on Proteasome Activity

These findings motivated us to test if this reporter could be used to track CICs by in vivo imaging. We recently showed that daily local fractionated irradiation (5 × 3 Gy) causes an increase in CICs numbers in vitro (13) and hypothesized that this increase was the mechanism for accelerated repopulation (36). Therefore, we mimicked this schedule in vivo. Imaging of U87MG-ZsGreen-cODC tumor-bearing mice revealed a steady increase in the fluorescent signal, which was consistent with an increase in the ZsGreen-positive cell population (Figure 4, A–D). The fact that the increase in ZsGreen fluorescence was seen 72 hours after the last fraction of radiotherapy reflects changes only in ZsGreen-positive cell numbers and not general proteasome inhibition by the radiation (18). Furthermore, the location of the positive cells near blood vessels indicated that hypoxia-induced proteasome inhibition was not a factor in the increase in ZsGreen-positive cells. These experiments demonstrate that CICs in a tumor can be imaged macroscopically in vivo and that their response to radiation therapy can be followed temporally.

The localization of ZsGreen-positive cells adjacent to blood vessels, which is traditionally thought of as a proliferative zone (37), prompted us to test if these cells were indeed proliferating, using Ki67 staining as a marker. Only a minority of ZsGreen-positive cells was also Ki67 positive (Figure 4, E). However, after sublethal fractionated irradiation (5 × 3 Gy) of tumor-bearing mice, the number of ZsGreen-positive cells in tumors increased (Figure 4, F and G) and the number of double-positive (ZsGreen-positive and Ki67-positive) cells tripled (n = 2) (Figure 4, H), suggesting that accelerated tumor repopulation may derive from the ZsGreen-positive cell compartment.

To explore if constitutive reduction of proteasome activity in CICs could be exploited therapeutically, we expressed a fusion protein consisting of TK, ZsGreen, and the cODC degron in U87MG cells. These cells were tested for sphere-forming capacity

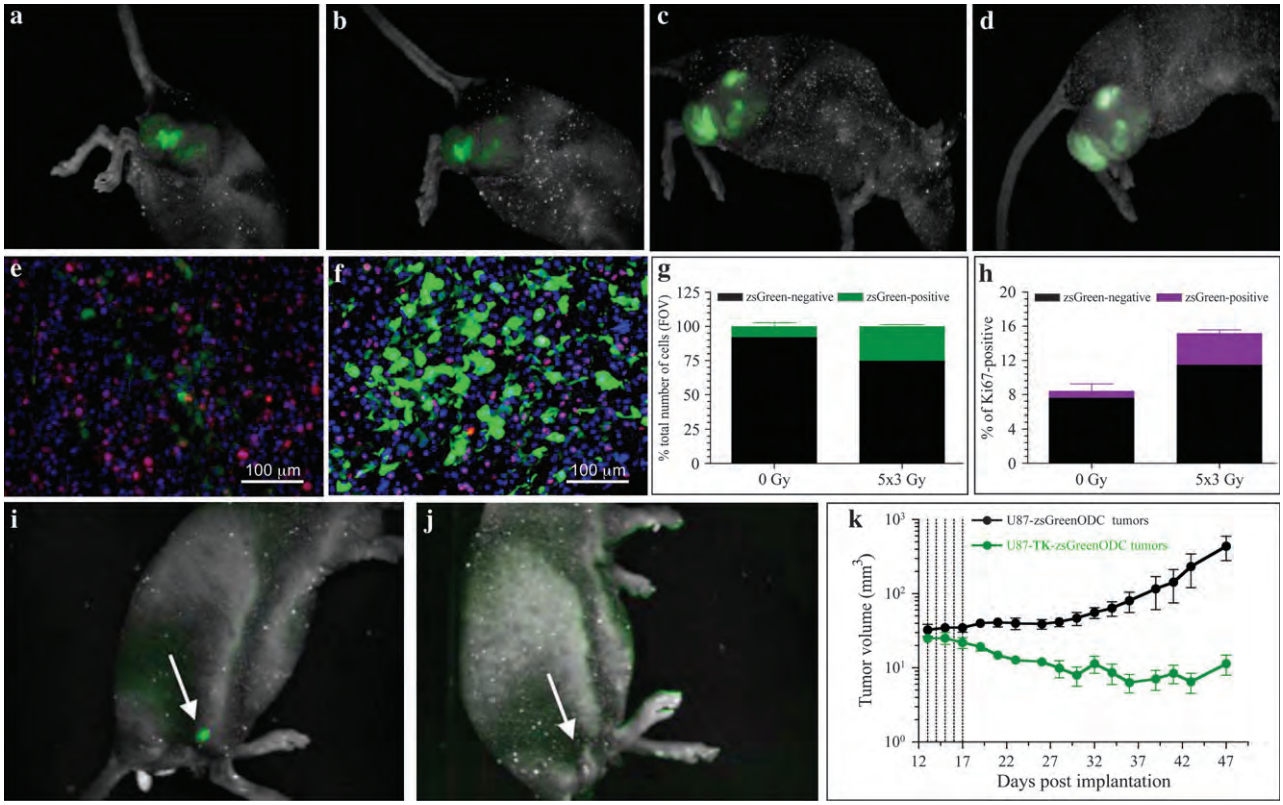

Figure 4. The effect of fractionated radiation on cancer-initiating cells in vivo. **A–D**) U87MG-ZsGreen-cODC–expressing tumors subjected to fractionated radiation and imaged before treatment (A), after a 3-Gy radiation exposure (B), after 5- × 3-Gy radiation exposures (C), or 72 hours after the last fraction (D). **E, F**) High-magnification views of untreated tumors (E), in which the proliferating, Ki67-positive population of cells displays high proteasome activity with only a few low proteasome activity (ZsGreen-positive) cells, and tumors treated with daily fractions of 3 Gy (F), in which the number of ZsGreen-positive cells increased substantially (**G**) as did the percentage of cells that were positive for Ki67 (**H**). Counterstaining with 4′,6-diamidino-2-phenylindole (**blue**). Mean values and 95% confidence intervals (CIs) are shown for two independent experiments. **I–K**) Mice with tumors derived from U87MG cells expressing a fusion protein of thymidine kinase, ZsGreen and the carboxyl terminus of the murine ornithine decarboxylase degron, treated with ganciclovir (5 intraperitoneal injections of 50 mg/kg starting on day 12 after implantation [**I**] and 18 days after initiation of treatment [**J**]). **K**) Growth of the tumors in the mice treated with ganciclovir. Tumor volume (mm^3) was assessed with calipers and are shown as means ± 95% CIs (n = 5 mice per group).

(self-renewal) in vitro and tumor formation in vivo in the presence or absence of the TK substrate ganciclovir, which would be expected to eliminate ZsGreen-positive cells accumulating the ZsGreen-TK-cODC fusion protein. Treatment with ganciclovir selectively killed ZsGreen-positive cells, thus abrogating the sphere-forming capacity in vitro (Supplementary Figure 4, A–E, available online), and caused tumor regression in vivo (mean tumor volumes on day 48 post tumor implantation: ZsGreen-ODC tumors = 612.2 mm^3, n = 5, TK-ZsGreen-ODC tumors = 9.495 mm^3, n = 6; difference = 602.7 mm^3, 95% CI = 164.3 to 1041 mm^3, $P = .0125$, Student's *t*-test) (Figure 4, I–K).

Discussion

Here, we provide evidence that constitutively reduced 26S proteasome activity is a general feature of CICs in glioma and breast cancer cells. Consistent with this finding, Rpn2, which is thought to feed substrates into the 20S core particle (38), was nearly absent in CICs. Like normal stem cells, CICs are usually considered quiescent (39,40) with low protein turnover and reduced metabolism and thus they may not need an ATP-dependent protein degradation machinery (41).

Using a reporter construct for 26S proteasome activity, we were able to identify CICs in cell populations in vitro and in vivo. In vivo, these cells localized around blood vessels (Supplementary Figure 3, available online) consistent with a recent report by Calabrese et al. (35) showing that brain tumor stem cells reside in a perivascular niche.

Reduced proteasome activity coincided with the expression of stem cell markers and a lack of differentiation markers (Supplementary Figure 2, available online). Cells with low proteasome activity also showed increased self-renewal capacity and could form tumors in immunologically incompetent mice from as few as 100 cells (Figure 1 and Table 1). Taken together, our results indicate that the population of cells identified by reduced proteasome activity was identical or overlapped with CICs and that reduced 26S proteasome activity is a property of CICs that can cross species barriers.

Our study has several limitations. First, the fusion protein–negative cell populations in our study were not 100% pure, and purging of the remaining contaminating ZsGreen-positive cells via specific targeting with ganciclovir would have caused considerable toxicity. However, given this impurity, our study likely underestimates the difference in tumorgenicity between ZsGreen-positive

and ZsGreen-negative cells. Second, we cannot rule out the possibility that ZsGreen-negative cells can eventually become ZsGreen-positive cells. Long-term experiments that follow single cells will be necessary to address this question. Finally, like all other investigators to our knowledge, we have required approximately 100 ZsGreen-positive cells to form tumors in vivo. Therefore, it is possible that ZsGreen-positive cells need to be further purified to obtain a pure CSC population.

Although the cell population with reduced proteasome activity was noncycling in vivo, it responded to fractionated doses of ionizing radiation by rapidly undergoing proliferation. This observation suggests that regulation of proteasome function in CICs can be turned on temporarily to allow progression through the cell cycle (a gain of proteasome function would not necessarily be detected by ZsGreen-cODC which has a half-life of >3.5 hours in cells). This switch in function may be highly dependent on developmental pathways as suggested by the fact that Notch signaling–dependent increases in stem cell numbers occur after sublethal doses of fractionated radiation in breast cancer (13) and may be an indicator of accelerated repopulation observed clinically in radiation therapy (an increased tumor growth rate during gaps in radiation treatment has been described in the context of clinical radiation therapy) (36). Because accelerated repopulation of tumors is a major cause of treatment failure, tracking of CICs in vivo may facilitate the search for novel therapeutic approaches that improve radiation therapy outcome. One possible application of being able to track CICs is the use of fusion of fluorescent proteins, suicide genes, and the cODC degron in gene therapy. Similar to our experiments with cells expressing the TK-ZsGreen-ODC fusion protein, the suicide gene can be substituted for the gene of interest, whereas the fluorescent component of the reporter will allow for the tracking of the cells accumulating the suicide protein, as well as their subsequent elimination. Using a TK-ZsGreen-cODC vector, we demonstrated that CICs could be targeted specifically which led to tumor control (Figure 4).

Our observations also offer a simple explanation for the high expression levels of known stem cell markers like BMI-1 and nestin in CICs that are both substrates of the proteasome (34,42). Furthermore, because the proteasome is also responsible for the generation of peptides presented to the immune system on Major histocompatibility complex -I molecules, our data suggest that CSCs may be immunologically silent or express antigens that may not be targeted by many current immunotherapy approaches. Finally, this system allows for screening of novel compounds that might modulate 26S proteasome function specifically in CICs, which could lead to novel targeted therapies against this therapeutically important cancer cell subpopulation.

References

1. Reya T, Morrison SJ, Clarke MF, Weissman IL. Stem cells, cancer, and cancer stem cells. *Nature.* 2001;414(6859):105–111.
2. Lagasse E. Cancer stem cells with genetic instability: the best vehicle with the best engine for cancer. *Gene Ther.* 2008;15(2):136–142.
3. Park CY, Tseng D, Weissman IL. Cancer stem cell-directed therapies: recent data from the laboratory and clinic. *Mol Ther.* 2008.
4. Al-Hajj M, Wicha MS, Benito-Hernandez A, Morrison SJ, Clarke MF. Prospective identification of tumorigenic breast cancer cells. *Proc Natl Acad Sci USA.* 2003;100(7):3983–3988.
5. Singh SK, Hawkins C, Clarke ID, et al. Identification of human brain tumour initiating cells. *Nature.* 2004;432(7015):396–401.
6. Fang D, Nguyen TK, Leishear K, et al. A tumorigenic subpopulation with stem cell properties in melanomas. *Cancer Res.* 2005;65(20):9328–9337.
7. Collins AT, Berry PA, Hyde C, Stower MJ, Maitland NJ. Prospective identification of tumorigenic prostate cancer stem cells. *Cancer Res.* 2005;65(23):10946–10951.
8. Ricci-Vitiani L, Lombardi DG, Pilozzi E, et al. Identification and expansion of human colon-cancer-initiating cells. *Nature.* 2007;445(7123):111–115.
9. Prince ME, Sivanandan R, Kaczorowski A, et al. Identification of a subpopulation of cells with cancer stem cell properties in head and neck squamous cell carcinoma. *Proc Natl Acad Sci USA.* 2007;104(3):973–978.
10. Li C, Heidt DG, Dalerba P, et al. Identification of pancreatic cancer stem cells. *Cancer Res.* 2007;67(3):1030–1037.
11. Eramo A, Ricci-Vitiani L, Zeuner A, et al. Chemotherapy resistance of glioblastoma stem cells. *Cell Death Differ.* 2006;13(7):1238–1241.
12. Bao S, Wu Q, McLendon RE, et al. Glioma stem cells promote radioresistance by preferential activation of the DNA damage response. *Nature.* 2006;444(7120):756–760.
13. Phillips TM, McBride WH, Pajonk F. The response of CD24(−/low)/CD44+ breast cancer-initiating cells to radiation. *J Natl Cancer Inst.* 2006;98(24):1777–1785.
14. Pajonk F, McBride WH. The proteasome in cancer biology and treatment. *Radiat Res.* 2001;156(5):447–459.
15. Cusack JC Jr, Liu R, Houston M, et al. Enhanced chemosensitivity to CPT-11 with proteasome inhibitor PS-341: implications for systemic nuclear factor-kappaB inhibition. *Cancer Res.* 2001;61(9):3535–3540.
16. Pajonk F, Pajonk K, McBride WH. Apoptosis and radiosensitization of Hodgkin cells by proteasome inhibition. *Int J Radiat Oncol Biol Phys.* 2000;47(4):1025–1032.
17. Pajonk F, van Ophoven A, Weissenberger C, McBride WH. The proteasome inhibitor MG-132 sensitizes PC-3 prostate cancer cells to ionizing radiation by a DNA-PK-independent mechanism. *BMC Cancer.* 2005;5(1):76.
18. Pajonk F, McBride WH. Ionizing radiation affects 26s proteasome function and associated molecular responses, even at low doses. *Radiother Oncol.* 2001;59(2):203–212.
19. Fekete MR, McBride WH, Pajonk F. Anthracyclines, proteasome activity and multi-drug-resistance. *BMC Cancer.* 2005;5(1):114.
20. Piccinini M, Tazartes O, Mezzatesta C, et al. Proteasomes are a target of the anti-tumor drug vinblastine. Online Epub ahead of print *Biochem J.* 2001;356(pt 3):835–841.
21. Pajonk F, van Ophoven A, McBride WH. Hyperthermia-induced proteasome inhibition and loss of androgen receptor expression in human prostate cancer cells. *Cancer Res.* 2005;65(11):4836–4843.
22. Kane RC, Bross PF, Farrell AT, Pazdur R. Velcade: U.S. FDA approval for the treatment of multiple myeloma progressing on prior therapy. *Oncologist.* 2003;8(6):508–513.
23. Blaney SM, Bernstein M, Neville K, et al. Phase I study of the proteasome inhibitor bortezomib in pediatric patients with refractory solid tumors: a Children's Oncology Group study (ADVL0015). *J Clin Oncol.* 2004;22(23):4752–4757.
24. Davis NB, Taber DA, Ansari RH, et al. Phase II trial of PS-341 in patients with renal cell cancer: a University of Chicago phase II consortium study. *J Clin Oncol.* 2004;22(1):115–119.
25. Gomez-Abuin G, Winquist E, Stadler WM, et al. A phase II study of PS-341 (Bortezomib) in advanced or metastatic urothelial cancer. A trial of the Princess Margaret Hospital and University of Chicago phase II consortia. *Invest New Drugs.* 2007;25(2):181–185.
26. Kondagunta GV, Drucker B, Schwartz L, et al. Phase II trial of bortezomib for patients with advanced renal cell carcinoma. *J Clin Oncol.* 2004;22(18):3720–3725.
27. Shah MH, Young D, Kindler HL, et al. Phase II study of the proteasome inhibitor bortezomib (PS-341) in patients with metastatic neuroendocrine tumors. *Clin Cancer Res.* 2004;10(18 pt 1):6111–6118.
28. Reynolds BA, Tetzlaff W, Weiss S. A multipotent EGF-responsive striatal embryonic progenitor cell produces neurons and astrocytes. *J Neurosci.* 1992;12(11):4565–4574.

29. Glas R, Bogyo M, McMaster JS, Gaczynska M, Ploegh HL. A proteolytic system that compensates for loss of proteasome function. *Nature.* 1998; 392(6676):618–622.
30. Matsuzawa S, Cuddy M, Fukushima T, Reed JC. Method for targeting protein destruction by using a ubiquitin-independent, proteasome-mediated degradation pathway. *Proc Natl Acad Sci USA.* 2005;102(42): 14982–14987.
31. Hemmati HD, Nakano I, Lazareff JA, et al. Cancerous stem cells can arise from pediatric brain tumors. *Proc Natl Acad Sci USA.* 2003;100(25): 15178–15183.
32. Ponti D, Costa A, Zaffaroni N, et al. Isolation and in vitro propagation of tumorigenic breast cancer cells with stem/progenitor cell properties. *Cancer Res.* 2005;65(13):5506–5511.
33. Hernebring M, Brolen G, Aguilaniu H, Semb H, Nystrom T. Elimination of damaged proteins during differentiation of embryonic stem cells. *Proc Natl Acad Sci USA.* 2006;103(20):7700–7705.
34. Mellodew K, Suhr R, Uwanogho DA, et al. Nestin expression is lost in a neural stem cell line through a mechanism involving the proteasome and Notch signalling. *Brain Res Dev Brain Res.* 2004;151(1–2):13–23.
35. Calabrese C, Poppleton H, Kocak M, et al. A perivascular niche for brain tumor stem cells. *Cancer Cell.* 2007;11(1):69–82.
36. Withers HR, Maciejewski B, Taylor JM, Hliniak A. Accelerated repopulation in head and neck cancer. *Front Radiat Ther Oncol.* 1988;22:105–110.
37. Tannock IF. Population kinetics of carcinoma cells, capillary endothelial cells, and fibroblasts in a transplanted mouse mammary tumor. *Cancer Res.* 1970;30(10):2470–2476.
38. Rosenzweig R, Osmulski PA, Gaczynska M, Glickman MH. The central unit within the 19S regulatory particle of the proteasome. *Nat Struct Mol Biol.* 2008;15(6):573–580.
39. Holtz MS, Forman SJ, Bhatia R. Nonproliferating CML CD34+ progenitors are resistant to apoptosis induced by a wide range of proapoptotic stimuli. *Leukemia.* 2005;19(6):1034–1041.
40. Holtz M, Forman SJ, Bhatia R. Growth factor stimulation reduces residual quiescent chronic myelogenous leukemia progenitors remaining after imatinib treatment. *Cancer Res.* 2007;67(3):1113–1120.
41. Babbitt SE, Kiss A, Deffenbaugh AE, et al. ATP hydrolysis-dependent disassembly of the 26S proteasome is part of the catalytic cycle. *Cell.* 2005;121(4):553–565.
42. Ben-Saadon R, Zaaroor D, Ziv T, Ciechanover A. The polycomb protein Ring1B generates self atypical mixed ubiquitin chains required for its in vitro histone H2A ligase activity. *Mol Cell.* 2006;24(5):701–711.

Funding

E. Vlashi was supported by a training grant from the National Institute of Biomedical Imaging and BioEngineering (2 T32 EB002101-31). This work was supported by a grant from the Department of Defense (PC060599), by a grant of the California Breast Cancer Research Program (BC060077), and by a developmental grant from the In Vivo Cellular and Molecular Imaging Centre at University of California, Los Angeles (PI: H. Herschman, NIH P50CA08630608) to F. Pajonk.

Notes

The authors are grateful for the excellent technical support provided by the staff of the Defined Flora animal facility of the Department of Radiation Oncology at the University of California, Los Angeles. The authors take full responsibility for the study design; collection, analysis, and interpretation of the data; the decision to submit the manuscript for publication; and the writing of the manuscript.

Manuscript received July 3, 2008; revised November 24, 2008; accepted December 31, 2008.

STEM CELLS®

CANCER STEM CELLS

Radiation-induced Reprograming of Breast Cancer Cells

Chann Lagadec[1], Erina Vlashi[1], Lorenza Della Donna[1], Carmen Dekmezian[1], and Frank Pajonk[1,2*]

[1]Department of Radiation Oncology, David Geffen School of Medicine at UCLA; [2]Jonsson Comprehensive Cancer Center at UCLA

Key words. Breast cancer stem cells • radiation • Notch • proteasome • dedifferentiation

ABSTRACT

Breast cancers are thought to be organized hierarchically with a small number of breast cancer stem cells (BCSCs) able to re-grow a tumor while their progeny lack this ability. Recently, several groups reported enrichment for BCSCs when breast cancers were subjected to classical anticancer treatment. However, the underlying mechanisms leading to this enrichment are incompletely understood.

Using non-BCSCs sorted from patient samples, we found that ionizing radiation reprogrammed differentiated breast cancer cells into induced BCSCs (iBCSCs). iBCSCs showed increased mammosphere formation, increased tumorigenicity and expressed the same stemness-related genes as BCSCs from non-irradiated samples. Reprogramming occurred in a polyploid subpopulation of cells, coincided with re-expression of the transcription factors Oct4, Sox-2, Nanog, and Klf4, and could be partially prevented by Notch inhibition.

We conclude that radiation may induce a BCSC phenotype in differentiated breast cancer cells and that this mechanism contributes to increased BCSC numbers seen after classical anti-cancer treatment.

INTRODUCTION

Recent clinical and preclinical data support the view that many solid cancers, including breast cancers, are organized hierarchically with a small number of cancer stem cells (CSCs) able to re-grow a tumor while their progeny lack this feature [1, 2]. Clinically, CSCs have been associated with higher rates of recurrence and metastasis [3, 4]. Importantly, CSCs in breast cancer and glioma have been found to be relatively resistant to radiation and chemotherapy compared to their non-tumorigenic progeny [5-7]. Consistent with these reports, several groups reported enrichment for CSCs when solid cancers were subjected to classical anti-cancer treatments [5, 6, 8].

Using an *in vitro* system we quantified the number of breast CSCs (BCSCs) surviving after radiation treatment in patient samples as well as in several breast cancer lines. When we compared the absolute number of breast CSCs (BCSCs) that survived radiation treatment to the number of BCSCs expected to survive we found a profound enrichment in BCSCs after exposure to ionizing radiation, and such a drastic increase in numbers could not easily be explained by differences in radiation sensitivity and/or by active repopulation. Here we report that ionizing

Author contributions: C.L.: Conception and design, Collection and assembly of data, Data analysis and interpretation, Manuscript writing; E.V.: Conception and design, Data analysis and interpretation; L.D.D.: Conception and design; C.D.: Collection and assembly of data; F.P.: Conception and design, Data analysis and interpretation, Manuscript writing, Final approval of manuscript, Financial support

*Correspondence address: Frank Pajonk, MD, PhD, Department of Radiation Oncology, David Geffen School of Medicine at UCLA, 10833 Le Conte Ave, Los Angeles, CA 90095-1714, Phone: +1 310 206 8733, Fax: +1 310 206 1260, email: fpajonk@mednet.ucla.edu; Grant Support: FP was supported by grants from the *California Breast Cancer Research Program* (15NB-0153) the *Department of Defense* (W81XWH-07-1-0065) and the *National Cancer Institute* (5RO1CA137110). CL was supported by an award from the Ward Family Foundation.; Received August 04, 2011; accepted for publication January 29, 2012. 1066-5099/2012/$30.00/0 doi: 10.1002/stem.1058

radiation induced a BCSC phenotype in previously non-tumorigenic cells. This transition was Notch-dependent and coincided with up-regulation of transcription factors used to generate induced pluripotent cells from differentiated normal cells.

METHODS

Cell culture

Human SUM159PT breast cancer cell lines were purchased from Asterand (Asterand, Inc., MI). Human MCF-7 and T47D breast cancer cell lines were purchased from American Type Culture Collection (Manassas, VA). SUM159PT-ZsGreen-cODC, MCF-7-ZsGreen-cODC, T47D-ZsGreen-cODC, were obtained as described in Vlashi et al. [9]. SUM159PT cells were cultured in log-growth phase in F12 Medium (Invitrogen, Carlsbad, CA) supplemented with 5% fetal bovine serum (Sigma Aldrich, St Louis, MO), penicillin (100 units/ml) and streptomycin (100 μg/ml) (both Invitrogen), and insulin (5μg/mL) and hydrocortisone (1 μg/ml). MCF-7 and T47D cells were cultured in log-growth phase in Dulbecco's Modified Eagle Medium (DMEM) (Invitrogen, Carlsbad, CA) supplemented with 10% fetal bovine serum, penicillin and streptomycin. All cells were grown in a humidified incubator at 37°C with 5% CO2.

Irradiation

Cells grown as monolayers were irradiated at room temperature using an experimental X-ray irradiator (Gulmay Medical Inc. Atlanta, GA) at a dose rate of 2.789 Gy/min for the time required to apply a prescribed dose. Corresponding controls were sham irradiated. Assessment of cell proliferation, the number of BCSCs, and sphere-forming assays were performed 5 days after radiation.

Flow cytometry

BCSCs were identified based on their low proteasome activity [9, 10] using the ZsGreen-cODC reporter system. Five days after radiation, cells were trypsinized and ZsGreen-cODC expression was assessed by flow cytometry (MACSQuant Analyzer, Miltenyi). Cells were defined as "ZsGreen-cODC positive" if the fluorescence in the FL-1H channel exceeded the fluorescence level of 99.9% of the empty vector-transfected control cells.

Aldefluor assay and separation of the ALDH1-negative population by FACS

Genestier *et al.* previously reported that breast cancer stem cells could be isolated based on their high ALDH1 activity [2]. The ALDEFLUOR kit (StemCell Technologies, Durham, NC, USA) was used to isolate the population with no ALDH1 enzymatic activity. Cells obtained from breast cancer monolayer (SUM159PT and T47D) were suspended in ALDEFLUOR assay buffer containing ALDH1 substrate (BAAA, 1 μmol/l per 1×106 cells) and incubated during 40 minutes at 37°C. As negative control for each sample of cells an aliquot was treated with 50mmol/L diethylaminobenzaldehyde (DEAB), a specific ALDH1 inhibitor. The sorting gates were established using ALDEFLUOR-stained cells treated with DEAB as negative controls.

CD24/CD44 staining and separation of the $CD24^{+/high}/CD44^{-}$ population by FACS

MCF-7 and T47D cells growing as monolayer cultures were stained for CD24 and CD44 expression as described previously [10]. Briefly, cells were incubated with trypsin–EDTA, dissociated and passed through a 40μm sieve. Cells were pelleted by centrifugation at 500 x g for 5 minutes at 4°C, resuspended in 100 μL of monoclonal mouse anti-human CD24–fluorescein isothiocyanate (FITC) antibody (BD Pharmingen, San Jose, CA) and a monoclonal mouse anti-human CD44–phytoerythrin (PE) antibody (BD Pharmingen), and incubated for 20 minutes at 4°C. The sorting gates were established using cells stained with isotype controls (isotype control FITC-conjugated antibodies (BD pharmingen) and isotype control PE-conjugated antibodies (BD pharmingen), respectively).

Sphere forming capacity

After irradiation, cells were trypsinized and plated in mammosphere media (DMEM-F12, 0.4% BSA (Sigma), 10 ml/500ml B27 (Invitrogen) 5 μg/ml bovine insulin (Sigma), 4 μg/ml heparin (Sigma), 20 ng/ml fibroblast growth factor 2 (bFGF, Sigma) and 20 ng/ml epidermal growth factor (EGF, Sigma)) into 96-well ultra-low adhesion plates, ranging from 1 to 256 cells/well. Growth factors, EGF and bFGF, were added every 3 days, and the cells were allowed to form spheres for 20 days. The number of spheres formed per well was then counted and expressed as a percentage of the initial number of cells plated. Cells were also plated in mammosphere media into 100 mm suspension dishes at 10,000 cells/ml, and allowed to form spheres for 15 days, these cells were used for secondary sphere forming experiments. Three independent experiments were performed.

Quantitative Reverse Transcription-PCR

Total RNA was isolated using TRIZOL Reagent (Invitrogen). cDNA synthesis was carried out using the SuperScript Reverse Transcription III (Invitrogen). Quantitative PCR was performed in the My iQ thermal cycler (Bio-Rad, Hercules, CA) using the 2x iQ SYBR Green Supermix (Bio-Rad). C_t for each gene was determined after normalization to GAPDH or RPLP0 and $\Delta\Delta C_t$ was calculated relative to the designated reference sample. Gene expression values were then set equal to $2^{-\Delta\Delta Ct}$ as described by the manufacturer of the kit (Applied Biosystems). All PCR primers were synthesized by Invitrogen and designed for the human sequences of Oct4, Sox2, Nanog, Klf4, c-Myc. Primers for the customized stem cell gene expression array were synthesized by Real Time Primers LLC (Elkins Park, PA).

Two channel flow cytometry for OCT4/Sox2/Nanog/Klf4/c-Myc and DNA content

Cells were harvested at relevant time points, washed in cold TBS, and fixed overnight in cold (–20 °C) 70% ethanol. After two washes in TBS, cells were permeabilized with TBS/4% BSA/0.1% Triton X-100 for 10 min at RT. Samples were incubated with a rabbit polyclonal anti-Oct4 antibody (Cell Signaling), a monoclonal mouse anti-Sox2 (R&D Systems), a rabbit polyclonal anti-Nanog (Abcam), a monoclonal mouse anti-Klf4 (Abgen), monoclonal mouse anti-c-Myc (Abcam), or corresponding isotype control (Biolegend) in TBS/4% BSA/0.1% Triton X100 for 1 h at RT. Following three washes in TBS, cells were incubated with goat anti-rabbit Alexa Fluor 750-APC (Invitrogen) or goat anti-mouse PE-Cy7 (Sigma) antibodies in TBS/4%BSA/0.1% Triton X100, 1:200 for 1 h in the dark. DNA was counterstained with 10 μg/ml propidium iodide (PI) solution in PBS, containing 200 μg/ml RNAse (Sigma) and assessed by flow cytometry using a MACSQuant Analyzer (Miltenyi Biotec) and analyzed using the FlowJo Software (version 9.3.1).

Animals

Nude (nu/nu), 6-8-week-old female mice, originally obtained from The Jackson Laboratories (Bar Harbor, ME) were re-derived, bred and maintained in a pathogen-free environment in the American Association of Laboratory Animal Care-accredited Animal Facilities of Department of Radiation Oncology, University of California (Los Angeles, CA) in accordance to all local and national guidelines for the care of animals.

Tumor xenotransplantation

SUM159PT-ZsGreen-cODC negative cells derived from monolayer cultures and sorted by fluorescence activated cell sorting were plated in F12 media supplemented with 5% fetal bovine serum and penicillin (100 units/ml) and streptomycin (100 μg/ml) cocktail, Insulin (5μg/mL) and hydrocortisone (1 μg/ml). The following day, cells were irradiated with 0, 4, or 8Gy. Five days after irradiation, cells were injected subcutaneously into the thighs and shoulders of 6-week old female Nu/Nu mice (10^6, 10^5, 10^4, 10^3, or 10^2 cells per inoculum, n=8) within Matrigel (BD Biosciences). Tumor growth was assessed on a weekly basis, and the

mice were sacrificed when the tumor size reached tumor diameters requiring euthanasia. The experiment was terminated after 13 weeks. Data was fitted using a sigmoidal regression model (Y=a*X^b/(c+X^b), Graphpad Prism 5.0). The number of cells needed to obtain tumors in 50% of the animals (TD50) was calculated for each radiation dose.

Human breast cancer primary specimens

Primary tumor specimens were obtained under a protocol approved by the University of California, Los Angeles Institutional Review Boards through the Translational Pathology Core Laboratory (TCPL) at UCLA (IRB# 02-02-057-22).

- Patient Sample 1: Invasive mammary carcinoma (90%), Lobular carcinoma in situ (10%), grade 2, TNM Stage: *pT3, N0 (i-), Mx*, ER3+, PR3+, HER/Neu1+, no amplification (FISH).

- Patient Sample 2: Invasive ductal carcinoma, grade 3, TNM Stage: *pT2, N0, Mx*, ER-, PR-, HER/Neu3+. Amplification (FISH).

- Patient Sample 3: Extensive ductal carcinoma in situ (90%), Invasive ductal carcinoma (10%), grade 1, TNM Stage: *pT1b, N0 (i-)(sn), Mx*, ER3+, PR2+, Her/neu1, no amplification (FISH).

The tumors specimen were digested and cells were expanded *ex vivo* for 2-3 weeks. ALDH-negative cells were isolated using fluorescence activated cell sorting.

Notch1-4 and Sox2/Nanog siRNA Transfection

SUM159PT cells were subjected to transfection with Notch1, Notch2, Notch3, Notch4, Sox2, or Nanog-specific siRNA (Sigma Aldrich). MISSION® siRNA universal negative control (Sigma Aldrich) was used as a transfection control. Briefly, siRNA (100ng total) and Lipofectamine (invitrogen) were diluted in OptiMEM I reduced serum media (Invitrogen), mixed and incubated for 20 min as described by the manufactor. Cells were rinsed with PBS 1X, twice, and incubated in 750 µL of OptiMEM I. siRNA/Lipofectamine mix was added on the top of the cells, and incubated at 37°C, 5% CO_2 for 6h. After incubation, media was removed and 2 mL of serum containing F12 Medium were added. Twenty-four hours after transfection, cells were plated for a sphere forming capacity assay, or cells were sorted and treated as previously described.

Noscapine treatment and cell cycle analysis

In order to identify the contribution of polyploidy to CSCs generation, non-tumorigenic MCF-7, T47D, SUM159PT and 2 patient samples (2 and 3) were treated with Noscapine [11]. Non-tumorigenic cells ($CD24^{+/high}/CD44^{-}$, ALDH1-negative, or ZsGreen-cODC-negative) were sorted and plated as monolayer cultures. Each following day, MCF-7 and T47D cells were treated with Noscapine (0, 10, or 25 µM). SUM159PT cells and patient samples 1 and 2 were treated with Noscapine at 0, 25, or 50 µM (Sigma Aldrich). At day 5, the presence of $CD24^{-/low}/CD44^{high}$, ALDH1-positive, or ZsGreen-cODC-positive cells was analyzed by flow cytometry. In parallel, cells were analyzed for polyploidy as described above.

Statistical methods

All results are expressed as mean values. A *p*-value of ≤ 0.05 in a paired two-sided Student's *t*-test was considered to indicate statistically significant differences. The test was applied to normalized data to compensate for the variance of measurements between biologically independent replicates of the same experiments.

RESULTS

Radiation induces a BCSCs phenotype in previously non-tumorigenic cells

Consistent with a radioresistant phenotype for BCSCs, we and others previously reported that ionizing radiation increased the number of BCSCs in the overall breast cancer cell population [5, 6, 10]. This has been ascribed to selective killing of non-tumorigenic cells and/or

a switch from an asymmetric to symmetric type of cell division of BCSCs that gives rise to two identical daughter BCSCs and thus, leading to a relative and absolute increase in BCSCs.

In the present study, we used single cell suspensions from fresh human breast specimen and stained them for ALDH1 activity, a recently described marker for BCSCs [2, 3]. Using fluorescence activated cell sorting (FACS), we isolated non-BCSCs (ALDH1-negative cells) from these specimens after purging BCSCs (ALDH1-positive cells). Purified non-BCSCs (ALDH1-negative cells) were then plated and irradiated the following day with 0, 4, or 8 Gy. Five days after irradiation, we assessed the number of BCSCs arising within the non-BCSC population. We found that radiation led to a dose-dependent increase in the number of ALDH1-positive cells (Figure 1a; patient sample 1: 0Gy, 0.92%, 4Gy, 1.92%, 8Gy, 4.05%; Patient sample 2: 0Gy, 1.46%, 4Gy, 3.56%, 8Gy, 8.59%, Patient sample 3: 0Gy, 1.24%, 4Gy, 2.9%, 8Gy, 3.45%).

From previous experience with FACS-purified cell populations we were aware of the fact that in practice these purified cell population are not 100% pure [9]. Indeed, a closer look at the FACS-purified populations of ALDH1-negative cells revealed that they always contained a very small population of contaminating ALDH1-positive cells. However, calculations based on the number of contaminating cells, the long doubling time of BCSCs (~72hours), which is not affected by irradiation [10], and the surviving fraction of BCSCs for each dose point (Supplementary figure 1), suggested that contaminating BCSCs present at the time of irradiation were unlikely to be the sole source of the absolute increase in BCSC numbers seen 5 days after irradiation. We therefore chose to test an alternative explanation, namely that non-tumorigenic breast cancer cells acquire a BCSC phenotype in response to ionizing radiation, thus contributing to the enrichment in BCSCs seen after radiation treatment.

To test this alternative hypothesis, we employed a panel of three established and widely used breast cancer cell lines (SUM159PT, MCF-7 and T47D). This panel allowed for the necessary number of experimental repeats in a large number of different assays. In addition to the Aldefluor test (Figure 1b) we used CD24 and CD44 to identify BCSCs and made use of a previously described imaging system for CSCs in breast cancer and glioma. This latter system is based on a fusion protein between the green fluorescent protein ZsGreen and the C-terminal degron of murine ornithine decarboxylase (cODC) and reports for 26S proteasome activity (Figure 1d, e), a protease activity that was found to be very low in CSCs [9]. Cells with low proteasome activity accumulate the fluorescent fusion protein while in cells with high proteasome activity the cODC portion of the fusion protein directs ZsGreen to ubiquitin-independent degradation by the 26S proteasome. Importantly, in breast cancer, cells with intrinsically low proteasome activity overlapped with the $CD24^{-/low}/CD44^{high}$ cell population [10] and with cells positive for ALDH1 (Supplementary figure 2a/b).

Next, we confirmed that radiation-induced increases in the number of BCSCs did not only occur in non-BCSCs from patient samples but also in non-BCSCs from established cells lines. Therefore, sorted ALDH1-negative cells from SUM159PT (Figure 1b) and T47D (Supplementary Figure 3a) cell lines were plated as monolayer cultures and irradiated the following day with 0, 4, or 8Gy. Like in patient-derived samples, we observed a significant dose-dependent increase in the number of ALDH1-positive cells, five days after irradiation (Figure 1b, SUM159PT: 0Gy: 0.3%; 4Gy, 1.76%, p = 0.008; 8Gy, 5.74%, p = 0.002; two-sided Student's t-test). To confirm this observation we employed the $CD24^{high}/CD44^{low}$ marker combination to isolate non-tumorigenic MCF-7 and T47D breast cancer cells. Again, five days after irradiation, we observed the induction of $CD24^{-/low}/CD44^{high}$ from previously non-tumorigenic $CD24^{high}/CD44^{low}$ cells (MCF-7:

0Gy: 0.37%: 4Gy: 2.35%, p=0.016; 8Gy: 6.33%, p=0.221. T47D: 0Gy: 0.08%: 4Gy: 0.38%, p=0.025; 8Gy: 1.38%, p=0.006). In parallel experiments we used SUM159PT, MCF-7, and T47D cells transfected with the ZsGreen-cODC reporter construct for proteasome activity. Using this third marker for BCSCs we also observed a dose-dependent, radiation-induced increase of ZsGreen-cODC-positive (low proteasome activity) cell numbers (Figure 1d/e, Figure 2, Supplementary Table 1 and 2). Importantly, cells positive for BCSC markers could not only be generated from differentiated cells in monolayer cultures but also from differentiating cells sorted from mammospheres (Figure 2, Supplementary figure 3b).

Previous studies reported a role for the Notch signaling pathway in maintaining a stem cell phenotype in mammary epithelial cells [12]. We decided to repeat the above radiation experiments in the presence of a γ-secretase inhibitor to block Notch signaling. Inhibition of Notch signaling attenuated the generation of cells positive for the BCSC marker (ZsGreen-cODC-positive) but did not completely abrogate the ability of non-tumorigenic cells (ZsGreen-cODC-negative) to give rise to cells with intrinsically low proteasome activity (Figure 2a-c, Supplementary Table 1 and 2). To further test the involvement of the Notch pathway in the induction of BCSCs, we inhibited the expression of Notch receptors by transfecting cells with targeting siRNA. SUM159PT-ZsGreen-cODC cells were transfected with specific siRNA targeting the Notch1, Notch2, Notch3, or Notch4 receptors using lipofectamine. Twenty-four hours after transfection, SUM159PT-ZsGreen-cODC-negative cells were isolated and plated as monolayer cultures. The following day, cells were irradiated with 0, 4, or 8 Gy. Five days after irradiation we observed a decrease in the number of BCSCs generated if compared to cells transfected with a scrambled siRNA control. Down-regulation of Notch2, 3 and 4 did not prevent induction of BCSCs (Figure 2d, 8Gy: siCTL: 3.04%, siNotch1: 1.54%, p=0.013). This indicated that signaling through the Notch1 receptor was either involved in inducing BCSCs or in maintaining the stem cell phenotype of newly generated BCSCs.

In order to study if non-tumorigenic cells could also generate BCSCs in the presence of pre-existing BCSCs, we reconstituted a mixed population of non-tumorigenic cells and StrawberryRed-labeled BCSCs at different dilutions (0, 2 and 10% BCSCs). After sorting, SUM159PT-ZsGreen-cODC-negative non-tumorigenic cells and SUM159PT-ZsGreen-cODC-positive/StrawberryRed-expressing BCSCs were mixed and plated as monolayer cultures. The following day, cells were irradiated with 0, 4, or 8Gy. When we analyzed the cells five days after irradiation by flow cytometry, we found that radiation-induced generation of BCSCs (ZsGreen-cODC-positive/StrawberryRed-negative) was decreased in the presence of pre-existing BCSCs (Figure 2e.) suggesting a negative feedback loop of existing BCSC in the generation of induced BCSCs (iBCSCs).

Using operational means, we next sought to test if the occurrence of ALDH1-positive cells and ZsGreen-cODC-positive cells with low proteasome activity reflected only an induction of BCSC marker expression or whether it was truly the induction of a BCSC phenotype. In order to assess the self-renewal capacity of iBCSC we employed a sphere-forming assay in which cells depleted from BCSCs with low proteasome activity were seeded at clonal densities into ultra-low adhesion plates in the absence of fetal calf serum to allow formation of mammospheres from single cells. In breast cancer, mammosphere formation is a measure of *in vitro* BCSC self-renewal capacity and correlates closely with tumorigenicity [13]. In order to test if radiation induced a BCSC phenotype on the non-tumorigenic cells, we compared the sphere-forming capacity of irradiated samples and the non-irradiated control. Furthermore, the number of spheres formed for each radiation dose were compared with the hypothetical number of mammospheres

expected. The expected number of mammospheres at each dose were calculated based on 1) the number of contaminating ZsGreen-cODC-positive cells after sorting, 2) a doubling time of 72 hours during the 5 days of culture, and 3) on their clonogenic surviving fraction at each dose point (Supplementary Figure 1).

In primary spheres, the self-renewal capacity of irradiated cells remained either the same or exceeded that of corresponding non-irradiated control cells. With the exception of T47D, this effect was also observed in secondary mammospheres. However, when the observed number of mammospheres was compared to the expected number of mammospheres at each dose point, mammosphere formation of irradiated cells significantly exceeded the numbers of mammospheres expected to be formed (Figure 3a and Supplementary figure 3b).

Next, we sorted SUM159PT cells based on ZsGreen-cODC expression and irradiated non-BCSCs (ZsGreen-cODC-negative) with 0, 4, and 8 Gy. After 5 days, cells were injected into the thighs and shoulders of 6-week old female Nu/Nu mice in a limiting dilution assay (10^6, 10^5, 10^4, 10^3, or 10^2 cells per inoculum, n=8 per injection). 13 weeks after injection, the number of cells required to initiate tumor growth in 50% of the animals (TD_{50}) was calculated. As expected, TD_{50} values of non-irradiated non-BCSCs were high ($1.15x10^5$ cells) consistent with a small number of contaminating BCSCs after FACS-sorting. However, TD_{50} values were reduced 32-fold after a single dose of 4Gy ($3.6x10^3$) and 9-fold ($1.26x10^4$) after a single dose of 8Gy suggesting a radiation-induced relative and absolute increase in BCSC numbers the (Figure 3b and Supplementary Table 3). Taken together, these data indicated that ionizing irradiation not only induced expression of BCSC markers in non-tumorigenic BSCSs but also led to the acquisition of cancer stem cell traits.

Finally, we decided to compare the expression profile of 86 genes associated with stem cell traits between non-irradiated ZsGreen-cODC-negative cells, non-irradiated ZsGreen-cODC-positive BCSCs and ZsGreen-cODC-positive iBCSCs induced by 8Gy. 10 genes were consistently and significantly up-regulated in ZsGreen-cODC-positive BCSCs and iBCSCs generated by 8Gy (Figure 4a and Supplementary Figure 4). Genes included key elements of the Notch, Wnt, Shh, and FGF signaling pathways as well as genes involved cell cycle regulation, cell adhesion, and cell-to-cell contact. The comparable gene expression profiles of ZsGreen-cODC-positive iBCSCs after a single radiation dose of 8Gy given to FACS-sorted ZsGreen-cODC-negative non-BCSC and preexisting ZsGreen-cODC-positive BCSCs, suggested that iBCSCs are driven by the same set of stem cell-related genes. There were however some differences in that expression of SRY (Sex determining region Y)-box 1 (Sox-1), SRY (Sex determining region Y)-box 2 (Sox-2), S100 calcium binding protein B (S100B), Par-6 partitioning defective 6 homolog alpha (PARP6A), Deltex homolog 1 (DTX1), and Delta-like 1 (DLL1) were significantly higher in iBSCSs, while expression of Frizzled homolog 1 (FZD1) and collagen type II alpha 1 (COL2A1) were significantly lower (Figure 6b). Overall, the expression profile of stemness-related genes in iBCSCs reassembled the expression profile found in BCSCs much closer than the expression profile found in the non-irradiated non-BCSC population they originated from.

Radiation induces re-expression of Oct4, Sox-2, Nanog, and Klf4

Acquisition of a stem cell phenotype has been described for non-malignant differentiated cells after overexpression of Oct4, Sox-2, Nanog, Klf4, and c-Myc. These transcription factors are now routinely used to generate induced pluripotent stem (iPS) cells from differentiated somatic cells [14, 15] and have also been shown to maintain the BCSCs phenotype [16]. Interestingly, Oct4, Sox-2, Nanog, and Klf4 are known substrates of the 26S proteasome [17-20] and therefore expected to be stabilized in cells with low proteasome activity. To determine if

these transcription factors were re-activated in non-BCSCs populations after irradiation, we analyzed their expression levels 5 days after 0, 4, or 8 Gy of radiation, the time point at which we observed absolute increases in BCSC numbers. As expected, we found a significant radiation dose-dependent increase of Oct4, Sox-2, Nanog, and Klf4 mRNA expression levels that matched the expression levels for these transcription factors in intrinsically occurring, non-irradiated BCSCs (Figure 5).

To test if re-expression of the above four transcription factors occurred randomly or in a specific subset of cells, we analyzed the expression of Oct4, Sox-2, Nanog, and Klf4 protein levels and correlated it to the DNA content of the cells. In irradiated cells we observed increased numbers of polyploid cells (SUM159PT: 0Gy: 0.74%, 4Gy: 4.63%, $p<0.0001$; 8Gy: 6.33%, $p<0.0001$; Patient sample 2: 0Gy: 12.6%, 4Gy: 14.4%, $p<0.032$; 8Gy: 22.5%, $p<0.0003$; Patient sample 3: 0Gy: 6.41%, 4Gy: 12.6%, $p<0.012$; 8Gy: 15.4%, $p<0.0004$; MCF-7: 0Gy: 3.60%, 4Gy: 6.96%, $p<0.004$; 8Gy: 24.7%, $p<0.0006$; T47D: 0Gy: 12.0%, 4Gy: 17.6%, $p<0.007$; 8Gy: 47.23%, $p<0.003$; Figure 6a and Supplementary figure 5a/b) in which Oct4, Sox-2, Nanog and Klf4 proteins were up-regulated (SUM159PT: Oct4: 0Gy, 2.71%, 4Gy: 17.02%, $p=0.041$; 8Gy: 20.1%, $p=0.003$; Sox2: 0Gy, 4.52%, 4Gy: 14.5%, $p=0.0002$; 8Gy: 48.98%, $p<0.0001$; Nanog: 0Gy, 0.39%, 4Gy: 18.9%, $p=0.223$; 8Gy: 27.58%, $p=0.222$: Klf4: 0Gy, 1.89%, 4Gy: 4.74%, $p=0.031$; 8Gy: 9.86%, $p=0.084$; Figure 6b/c and supplementary figure 5c/d) and which were also highly enriched for ZsGreen-cODC-positive cells with low proteasome activity (Total population: 0Gy, 0.64%, 4Gy: 1.84%, $p<0.0001$; 8Gy: 9.09%, $p<0.0001$; Polyploid: 0Gy, 0.08%, 4Gy: 0.94%, $p=0.01$; 8Gy: 2.69%, $p=0.005$; Polyploid/Oct4$^+$: 0Gy, 0%, 4Gy: 3.97%, $p<0.0001$; 8Gy: 12.14%, $p=0.031$; Polyploid/Sox2$^+$: 0Gy, 0%, 4Gy: 3.84%, $p=0.041$; 8Gy: 10.19%, $p=0.042$; Polyploid/Nanog$^+$: 0Gy, 0.45%, 4Gy: 1.14%, $p=0.107$; 8Gy: 2.79%, $p=0.029$; Figure 6d and Supplementary figure 5b). c-Myc levels were not increased (Figure 6b/d, 5d). Consistent with a previous report [21], inhibition of Notch activation attenuated the induction of polyploidy (4Gy: 4.87%; 4Gy + γ-secretase inhibitor: 2.72, $p=0.03$; 8Gy: 6.32%; 8Gy + γ-secretase inhibitor: 3.42, $p=0.028$; Supplementary figure 5b) and the induction of Oct4, Sox-2, Nanog, and Klf4 expressing polyploid cells (Supplementary Figure 5d). This again supported involvement of Notch signaling in radiation reprograming.

In order to identify the role of these transcription factors in the generation of iBCSCs, we used siRNA to target the expression of Sox2 and Nanog. Non-tumorigenic cells transfected with siRNA-Sox2 and siRNA-Nanog were sorted, plated, and irradiated with 0, 4, and 8Gy the following day. Down-regulation of either Sox2 or Nanog alone had no effect on the induction of iBCSCs. However, generation of iBCSCs was significantly reduced when Sox2 and Nanog were down-regulated simultaneously (0Gy: siRNA control: 0.37%, siRNA-Sox2/Nanog: 0.57%, $p=0.505$; 4Gy: siRNA control: 1.36%, siRNA-Sox2/Nanog: 0.49%, $p=0.008$; 8Gy: siRNA control: 3.04%, siRNA-Sox2/Nanog: 1.63%, $p=0.047$; Figure 6e).

Induction of polyploidy induced generation of iBCSCs

In differentiated cells, Sox2 and Oct4 are epigenetically silenced. The suppression of gene expression for both transcription factors is incomplete but still sufficient to maintain protein levels below a critical threshold. We hypothesized that in polyploid cells found after irradiation multiple copies of partially silenced Oct4 and Sox2 genes might be sufficient to drive gene expression beyond this threshold, thereby inducing a BCSC phenotype. To test this hypothesis we explored if the effect of radiation could be mimicked by pharmacological induction of polyploidy. Treatment of breast cancer cell lines and patient samples with noscapine caused a substantial increase in the number of polyploid cells on day 5 after addition

of the drug. The observed increase was comparable to the amount of polyploidy found after irradiation (Figure 7a and Supplementary figure 7a/b). Next we tested if the number of BCSCs was also increased. In both patient samples noscapine treatment increased the number of ALDH1-positive cells significantly (Figure 7b). Increased numbers of BCSCs with low proteasome activity were also found when MCF-7, T47D or SUM159PT ZsGreen-cODC expressing cells were analyzed for ZsGreen-cODC-positive cells (Figure 7c and Supplementary figure 7c) and when MCF-7 and T47D cells were analyzed for the number of $CD24^{low/-}/CD44^{high}$ cells (Figure 7d). These results suggested that increased gene dose in polyploid cells could indeed be one of the mechanisms leading to acquisition of a CSC phenotype in breast cancer in response to radiation treatment.

Finally, we confirmed that BCSCs rely on Notch signaling using specific siRNAs targeting the Notch1, Notch2, Notch3, or Notch4 receptor. Cells were transfected with Lipofectamine, 24h after transfection cells were plated in sphere media for a sphere forming capacity assay. As expected, down-regulation of Notch receptor expression reduced the ability of the cells to form mammospheres (Figure 7e). Furthermore, in order to demonstrate that BCSCs rely on the transcription factors induced by radiation, we down-regulated Sox2 and Nanog using specific siRNAs. Cells were transfected with Lipofectamine, 24h after transfection cells were plated and tested for sphere formation. As expected, down-regulation of Sox2 and Nanog expression reduced self-renewal capacity of cells from established breast cancer cell lines and primary breast cancer samples and Sox2, which acts upstream of Nanog and has targets in addition to Nanog was more efficient in (Figure 7f).

DISCUSSION

Treatment gaps in radiation therapy have long been known to worsen the outcome for patients suffering from epithelial cancers including cancers of the head and neck region and the breast [22, 23]. The underlying mechanisms are incompletely understood but in general are attributed to accelerated repopulation, a phenomenon that refers to the increased growth rates of cancers during treatment gaps that far exceed their initial growth rates. It is thought that during accelerated repopulation CSCs switch from an asymmetric type of cell division, which leads to one daughter CSC and one differentiating cell, to a symmetric type of cell division which yields two identical daughter CSCs. Our data suggest that in addition to the classical view of accelerated repopulation in which CSCs switch from an asymmetric type of cell division that leads to one daughter CSCs and one differentiating cells to a symmetric type of cell division that yields in two daughter CSCs, differentiated cancer cells may also be able to acquire stem cell traits under certain conditions of tumor micro-environmental stress, including stress induced by ionizing radiation. Acquisition of stem cell traits by CD133-negative, non-tumorigenic glioma cells was previously reported under hypoxic conditions [24] and in response to nitric oxide-induced notch signaling [25], suggesting that cancer stem cell plasticity may be a common response to multiple stimuli including cancer therapies.

Our observation that ionizing radiation reactivated the same transcription factors in differentiated breast cancer cells that reprogram differentiated somatic cells into iPS cells is provoking. However, it is in line with recent reports that baseline levels of Sox2, Oct4, and Nanog expression can be detected in breast cancers [26, 27] and that ectopic overexpression of Oct4 in normal mammary epithelial cells induces a BCSCs phenotype [28]. Our data further indicate that an increase number of gene copies of Oct4 and Sox2 in polyploid cells could be one possible mechanism behind radiation-

induced reprogramming. This was supported by our data showing that down-regulation of Sox2 prevented mammosphere formation. Down-regulation of the Sox2 downstream target Nanog was less efficient, indicating that multiple genes downstream of Sox2 contribute to the acquisition of a cancer stem cells phenotype. Similar observations have been reported for lymphoma cells [29]. Furthermore, this is in accordance with previous reports on Notch-dependent induction of polyploidy [21] and our data showing that inhibition of Notch-signaling partially prevented the occurrence of iBCSCs (Supplementary figure 5b), suggesting that targeting Notch-signaling might enhance local control after radiation therapy.

The CSC hypothesis was formulated more than a century ago [30]. However, until recently prospective identification of CSCs was impossible. The discovery of marker combinations that identify CSCs have resulted in novel insights into the biology of cancer. Still, the CSC hypothesis has been challenged and some experimental data support a model of clonal evolution as an alternative organizational structure of tumors [31] in which every cancer cell may acquire stem cell traits at some point.

Our study unites the competing models of clonal evolution and hierarchical organization of cancers [32] as it suggests that undisturbed growing tumors indeed maintain a low number of CSCs. However, if challenged by various stressors including ionizing radiation, iCSCs are generated, which may together with the surviving CSCs repopulate a tumor. These findings have implications for the design of novel treatment protocols that target CSCs, including radiation therapy. The curability of a cancer may not only be dependent on the intrinsic radiosensitivity of CSCs but also on the radiosensitivity of induced CSCs and the rate at which they are generated. Controlling the radio-resistance of BCSCs and the generation of new iBCSCs during radiation treatment may ultimately improve curability and may allow for de-escalation of the total radiation doses currently given to breast cancer patients thereby reducing acute and long-term adverse effects.

CONCLUSION AND SUMMARY

In summary, our study shows that ionizing radiation reactivated the expression of Oct4 and Sox2 and induced a CSC phenotype in previously non-tumorigenic breast cancer cells. The phenomenon was dependent on the induction of polyploidy and Notch signaling. We conclude that a detailed understanding of the underlying pathways could lead to novel combination therapies that will potentially enhance the efficacy of radiation treatment.

REFERENCES

1. Al-Hajj M, Wicha MS, Benito-Hernandez A, et al. Prospective identification of tumorigenic breast cancer cells. Proc. Natl Acad. Sci. USA. 2003;100:3983-3988.
2. Ginestier C, Hur MH, Charafe-Jauffret E, et al. ALDH1 Is a Marker of Normal and Malignant Human Mammary Stem Cells and a Predictor of Poor Clinical Outcome. Cell Stem Cell. 2007;1:555-567.
3. Charafe-Jauffret E, Ginestier C, Iovino F, et al. Aldehyde dehydrogenase 1-positive cancer stem cells mediate metastasis and poor clinical outcome in inflammatory breast cancer. Clin Cancer Res. 2010;16:45-55.
4. Marcato P, Dean CA, Pan D, et al. Aldehyde Dehydrogenase Activity of Breast Cancer Stem Cells is Primarily Due to Isoform ALDH1A3 and Its Expression is Predictive of Metastasis. Stem Cells. 2010.
5. Phillips TM, McBride WH, Pajonk F. The response of CD24(-/low)/CD44+ breast cancer-initiating cells to radiation. J Natl Cancer Inst. 2006;98:1777-1785.
6. Woodward WA, Chen MS, Behbod F, et al. WNT/beta-catenin mediates radiation resistance of mouse mammary progenitor cells. Proc Natl Acad Sci U S A. 2007;104:618-623.
7. Li HZ, Yi TB, Wu ZY. Suspension culture combined with chemotherapeutic agents for sorting of breast cancer stem cells. BMC Cancer. 2008;8:135.
8. Bao S. Glioma stem cells promote radioresistance by preferential activation of the DNA damage response. Nature. 2006;444:756-760.

9. Vlashi E, Kim K, Lagadec C, et al. In vivo imaging, tracking, and targeting of cancer stem cells. J Natl Cancer Inst. 2009;101:350-359.
10. Lagadec C, Vlashi E, Della Donna L, et al. Survival and self-renewing capacity of breast cancer initiating cells during fractionated radiation treatment. Breast Cancer Res. 2010;12:R13.
11. Mitchell ID, Carlton JB, Chan MY, et al. Noscapine-induced polyploidy in vitro. Mutagenesis. 1991;6:479-486.
12. Dontu G, Jackson KW, McNicholas E, et al. Role of Notch signaling in cell-fate determination of human mammary stem/progenitor cells. Breast Cancer Res. 2004;6:R605-615.
13. Fillmore CM, Kuperwasser C. Human breast cancer cell lines contain stem-like cells that self-renew, give rise to phenotypically diverse progeny and survive chemotherapy. Breast Cancer Res. 2008;10:R25.
14. Patel M, Yang S. Advances in reprogramming somatic cells to induced pluripotent stem cells. Stem Cell Rev. 2010;6:367-380.
15. Zhao R, Daley GQ. From fibroblasts to iPS cells: induced pluripotency by defined factors. J Cell Biochem. 2008;105:949-955.
16. Wu K, Jiao X, Li Z, et al. The cell-fate determination factor dachshund reprograms breast cancer stem cell function. J Biol Chem. 2010.
17. Chen ZY, Wang X, Zhou Y, et al. Destabilization of Kruppel-like factor 4 protein in response to serum stimulation involves the ubiquitin-proteasome pathway. Cancer Res. 2005;65:10394-10400.
18. Baltus GA, Kowalski MP, Zhai H, et al. Acetylation of sox2 induces its nuclear export in embryonic stem cells. Stem Cells. 2009;27:2175-2184.
19. Moretto-Zita M, Jin H, Shen Z, et al. Phosphorylation stabilizes Nanog by promoting its interaction with Pin1. Proc Natl Acad Sci U S A. 2010;107:13312-13317.
20. Xu H, Wang W, Li C, et al. WWP2 promotes degradation of transcription factor OCT4 in human embryonic stem cells. Cell Res. 2009;19:561-573.
21. Baia GS, Stifani S, Kimura ET, et al. Notch activation is associated with tetraploidy and enhanced chromosomal instability in meningiomas. Neoplasia. 2008;10:604-612.
22. Bese NS, Sut PA, Ober A. The effect of treatment interruptions in the postoperative irradiation of breast cancer. Oncology. 2005;69:214-223.
23. Withers HR, Maciejewski B, Taylor JM, et al. Accelerated repopulation in head and neck cancer. Front Radiat Ther Oncol. 1988;22:105-110.
24. Heddleston JM, Li Z, McLendon RE, et al. The hypoxic microenvironment maintains glioblastoma stem cells and promotes reprogramming towards a cancer stem cell phenotype. Cell Cycle. 2009;8:3274-3284.
25. Charles N, Ozawa T, Squatrito M, et al. Perivascular nitric oxide activates notch signaling and promotes stem-like character in PDGF-induced glioma cells. Cell Stem Cell. 2010;6:141-152.
26. Leis O, Eguiara A, Lopez-Arribillaga E, et al. Sox2 expression in breast tumours and activation in breast cancer stem cells. Oncogene. 2011.
27. Ezeh UI, Turek PJ, Reijo RA, et al. Human embryonic stem cell genes OCT4, NANOG, STELLAR, and GDF3 are expressed in both seminoma and breast carcinoma. Cancer. 2005;104:2255-2265.
28. Beltran AS, Rivenbark AG, Richardson BT, et al. Generation of tumor-initiating cells by exogenous delivery of OCT4 transcription factor. Breast Cancer Res. 2011;13:R94.
29. Salmina K, Jankevics E, Huna A, et al. Up-regulation of the embryonic self-renewal network through reversible polyploidy in irradiated p53-mutant tumour cells. Exp Cell Res. 2010;316:2099-2112.
30. Paget S. The distribution of secondary growths in cancer of the breast. Lancet 1889;1:571–573.
31. Quintana E, Shackleton M, Sabel MS, et al. Efficient tumour formation by single human melanoma cells. Nature. 2008;456:593-598.
32. Reya T, Morrison SJ, Clarke MF, et al. Stem cells, cancer, and cancer stem cells. Nature. 2001;414:105-111.

See www.StemCells.com for supporting information available online.

Figure 1. Radiation induces *de novo* generation of CSCs. (**a**) Freshly isolated patient samples and (**b**) SUM159PT cells were stained for ALDH1 activity. ALDH1-negative cells were sorted, plated as monolayer cultures and irradiated with 0, 4, or 8Gy the following day. The presence of ALDH1-positive ($ALDH1^{+}$) cells was analyzed 5 days after irradiation. Percentages of ALDH1-positive cells are show for 3 patient samples. Representative dot blots of SUM159PT and means of ALDH1-positive ($ALDH1^{+}$) SUM159PT are shown (n=3). (**c**) MCF-7 and T47D were stained for CD24 and CD44, and purged by flow cytometry from $CD24^{-/low}/CD44^{high}$ cells. Cells were then plated as monolayers and irradiated the following day with 0, 4, or 8Gy. Five days after treatment, cells were stained for CD24 and CD44, and the presence of $CD24^{-/low}/CD44^{high}$ cells was analyzed by FACS. ZsGreen-cODC-negative cells from SUM159PT were sorted and plated as monolayers or mammospheres. The following day, cells were irradiated. Five days after treatment, the presence of ZsGreen-cODC-positive cells was analyzed by flow cytometry. (**d**) Representative dot blots and (e) pictures (phase contrast and green fluorescence) of SUM159PT-ZsGreen-cODC mammospheres 5 days after irradiation are shown. Means, s.e.m. and p-value for relative increases of ZsGreen-cODC-positive cell numbers are shown in supplementary table 1 and 2.

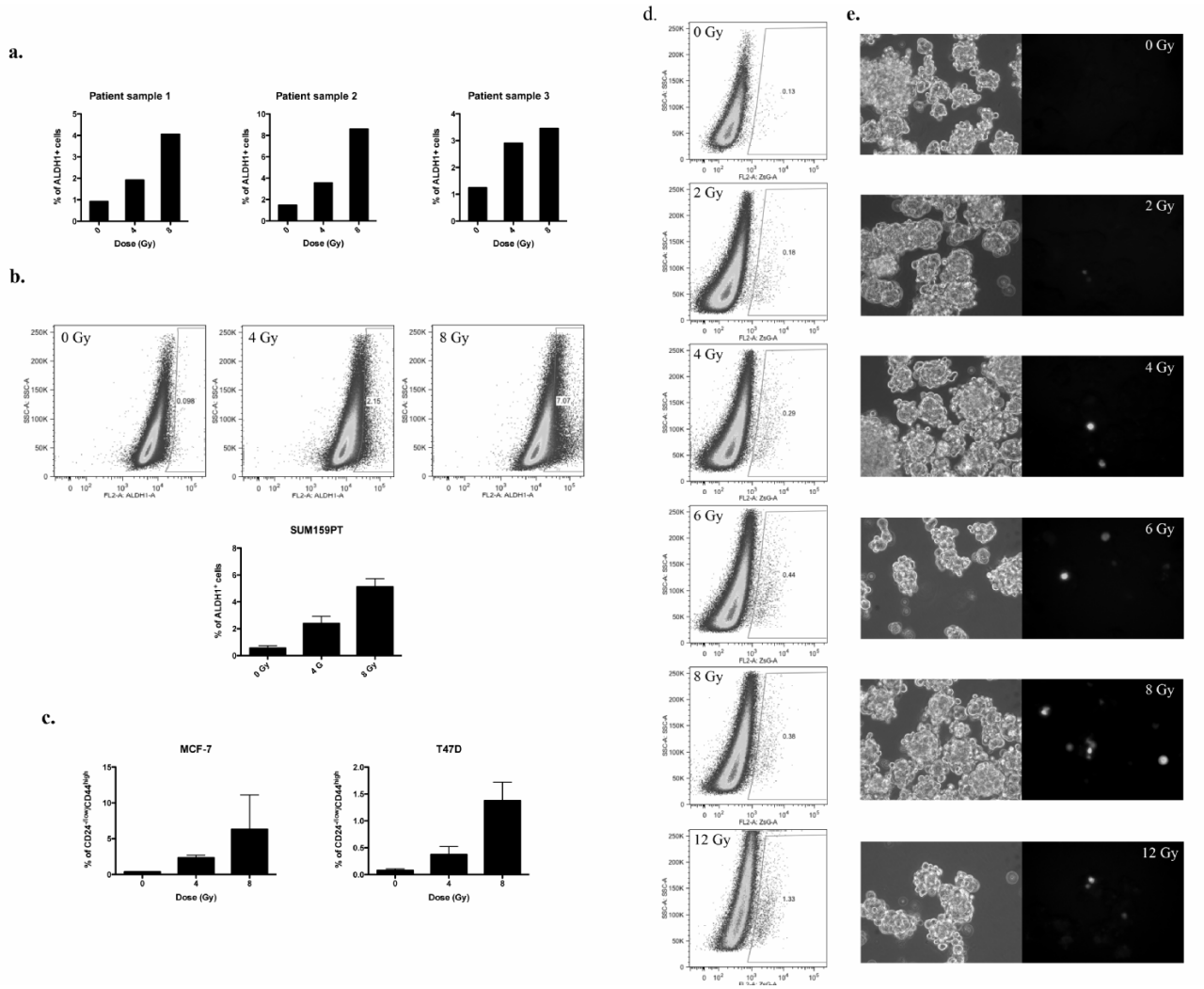

Figure 2. Radiation induces Notch-dependent *de novo* generation of CSCs. (**a**) SUM159PT-, (**b**) MCF-7-, and (**c**) T47D-ZsGreen-cODC-negative cells were sorted and plated as monolayers or mammospheres. The following day, cells were then treated with 0, 2, 4, 6, 8, or 12 Gy (dose rate: 2.789 Gy/min). 1h before irradiation and every day after irradiation, cells were treated with a γ-secretase inhibitor (5μM). Five day after treatment, the presence of ZsG-cODC positive cells was analyzed by FACS. The mean for relative increases in ZsG-cODC positive cell numbers are shown (* and # indicates $p<0.05$, see supplementary table 1 and 2 for means, 95% CI and P value). (**d**) SUM159PT cells were transfected with Notch1, Notch2, Notch3, or Notch4-specific siRNA, and then sorted for ZsGreen-cODC-negative cells. Cells were plated as monolayers and irradiated with 0, 4, or 8 Gy the following day. Presence of ZsGreen-cODC-positive cells was analyzed 5 days after treatment. The mean percentage of ZsGreen-cODC-positive cell numbers are shown (*indicates $p<0.05$, n=4). (**e**) SUM159PT-ZsGreen-cODC cells were transfected with constitutively expressed Strawberry-Red vector. ZsGreen-cODC-positive/StrawberryRed-positive cells were isolated by follow cytometry and mixed with SUM159PT-ZsGreen-cODC-negative (Non-StrawberryRed transfected) cells at different concentration (0, 2, or 10%). Cells were plated and irradiated the following day. Five days after irradiation, the presence of ZsGreen-cODC-positive/StrawberryRed-negative cells was assessed by FACS. The mean percentages of ZsGreen-cODC-positive/StrawberryRed-negative cell numbers are shown (n=3).

a.

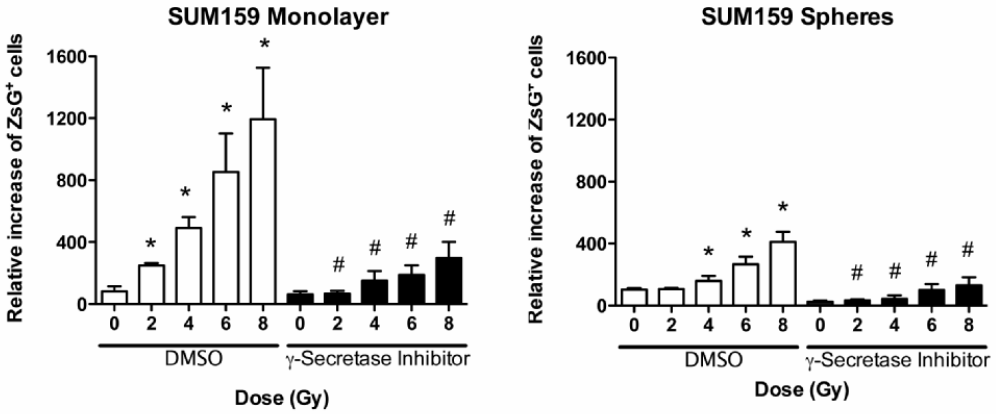
SUM159 Monolayer
SUM159 Spheres
Relative increase of ZsG+ cells
1600
1200
800
400
0
0 2 4 6 8 0 2 4 6 8
DMSO
γ-Secretase Inhibitor
Dose (Gy)

b.

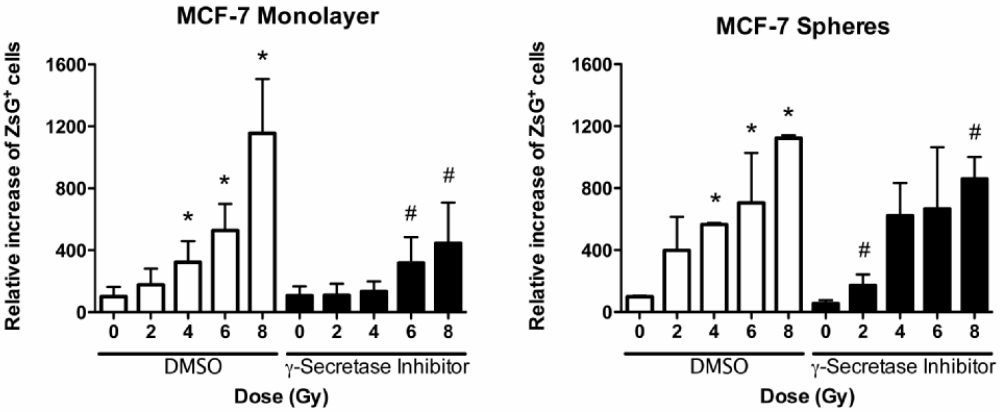
MCF-7 Monolayer
MCF-7 Spheres
Relative increase of ZsG+ cells
1600
1200
800
400
0
0 2 4 6 8 0 2 4 6 8
DMSO
γ-Secretase Inhibitor
Dose (Gy)

c.

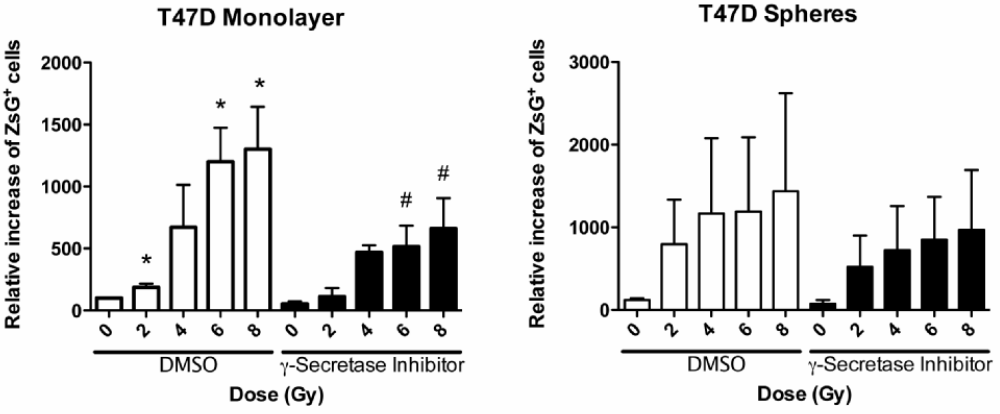
T47D Monolayer
T47D Spheres
Relative increase of ZsG+ cells
2000
1500
1000
500
0
3000
2000
1000
0
0 2 4 6 8 0 2 4 6 8
DMSO
γ-Secretase Inhibitor
Dose (Gy)

d.

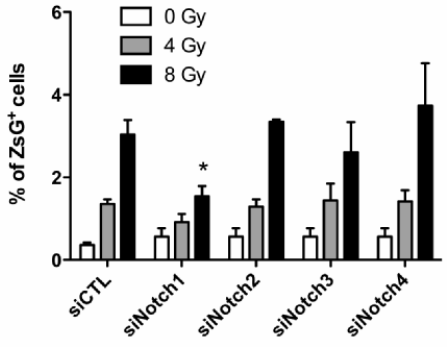
0 Gy
4 Gy
8 Gy
% of ZsG+ cells
6
4
2
0
siCTL
siNotch1
siNotch2
siNotch3
siNotch4

e.

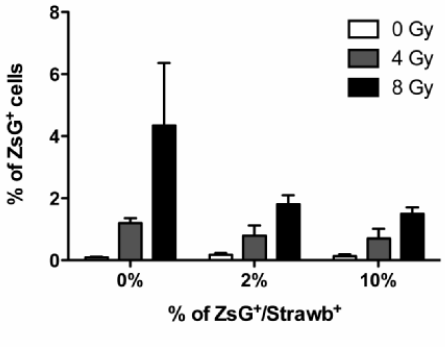
0 Gy
4 Gy
8 Gy
% of ZsG+ cells
8
6
4
2
0
0%
2%
10%
% of ZsG+/Strawb+

Figure 3. Radiation induces *de novo* generation of functional CSCs.
ZsGreen-cODC-negative cells from SUM159PT, MCF-7, and T47D were sorted and plated as monolayers or mammospheres (See Supplementary figure 3b). The following day, cells were irradiated. (**a**) Five days after irradiation, MCF-7, T47D, and SUM159PT cells were seeded at clonal densities to assess sphere-forming capacity. Means and s.e.m. are shown, *indicates $p<0.05$. Dark line graphs represent the mean of number of mammospheres observed (n=3), dashed lines represent the number of mammospheres expected to derive from contaminating BCSCs. Secondary sphere forming capacity was assessed 15 days after irradiation. (**b**) SUM159PT-ZsGreen-cODC-negative cells were sorted and plated as monolayer cultures. The following day, cells were irradiated with 0, 4, or 8 Gy. Five days after irradiation, cells were injected subcutaneously into nude mice. 13 weeks after injection, TC_{50} values were calculated.

a.

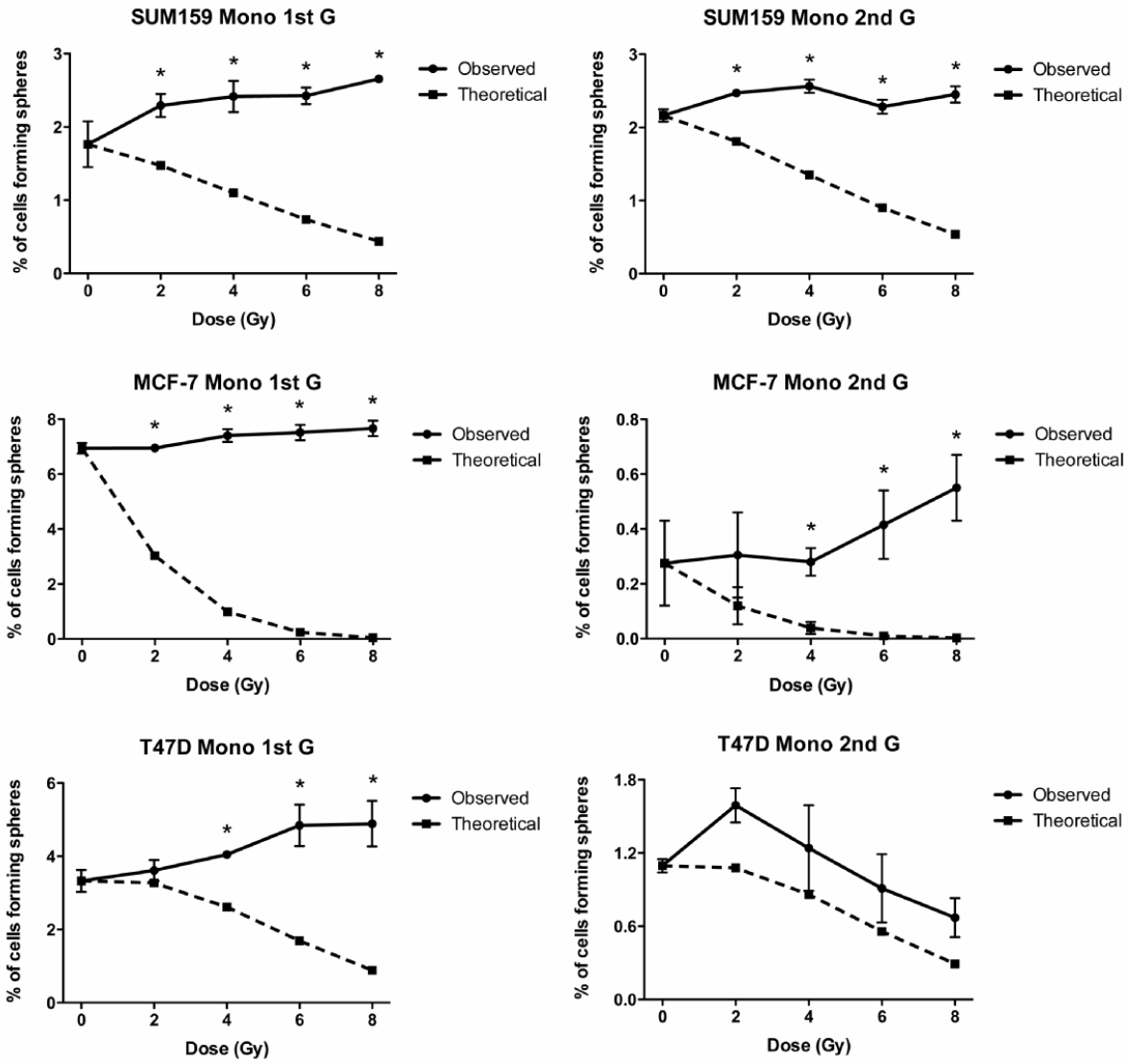
SUM159 Mono 1st G
SUM159 Mono 2nd G
MCF-7 Mono 1st G
MCF-7 Mono 2nd G
T47D Mono 1st G
T47D Mono 2nd G
% of cells forming spheres
Dose (Gy)
Observed
Theoretical

b.

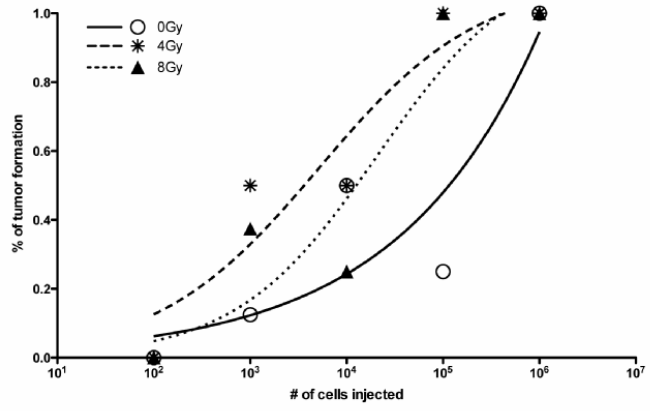
0Gy
4Gy
8Gy
% of tumor formation
# of cells injected

Figure 4. Stem cell gene expression of BCSCs and iBSCS Expression of 86 stem cell related genes and 10 housekeeping genes was analyzed by semi-quantitative RT-PCR in ZsGreen-cODC-negative, -positive cells and iBCSCs (8 Gy). (**a**) Heat map of differentially expressed genes between ZsGreen-cODC-negative, ZsGreen-cODC-positive cells non-irradiated or iBCSCs 8Gy, and the mean expression (Mean of ZsGreen-cODC-negative cells, non-irradiated ZsGreen-cODC-positive cells and iBCSCs 8Gy cells) are shown (see also supplementary Figure 6). (**b**) Significant different expression between ZsGreen-cODC-positive non-irradiated BCSCs and iBCSCs 8Gy are shown (n=3), * indicates $p<0.05$.

a.

	Relative expression to the mean					
	ZsG-	ZsG+	ZsG+ 8Gy	ZsG-	ZsG+	ZsG+ 8Gy
SOX2				0.04	1.11	21.09
SOX1				0.13	1.02	7.85
COL9A1				0.14	1.60	4.59
WNT1				0.15	1.64	4.17
FGF3				0.15	2.92	2.35
BMP2				0.47	0.90	2.35
DLL1				0.49	0.84	2.41
CDC2				0.51	1.24	1.58
FOXA2				0.68	1.04	1.40
NOTCH1				0.82	1.01	1.20

b.

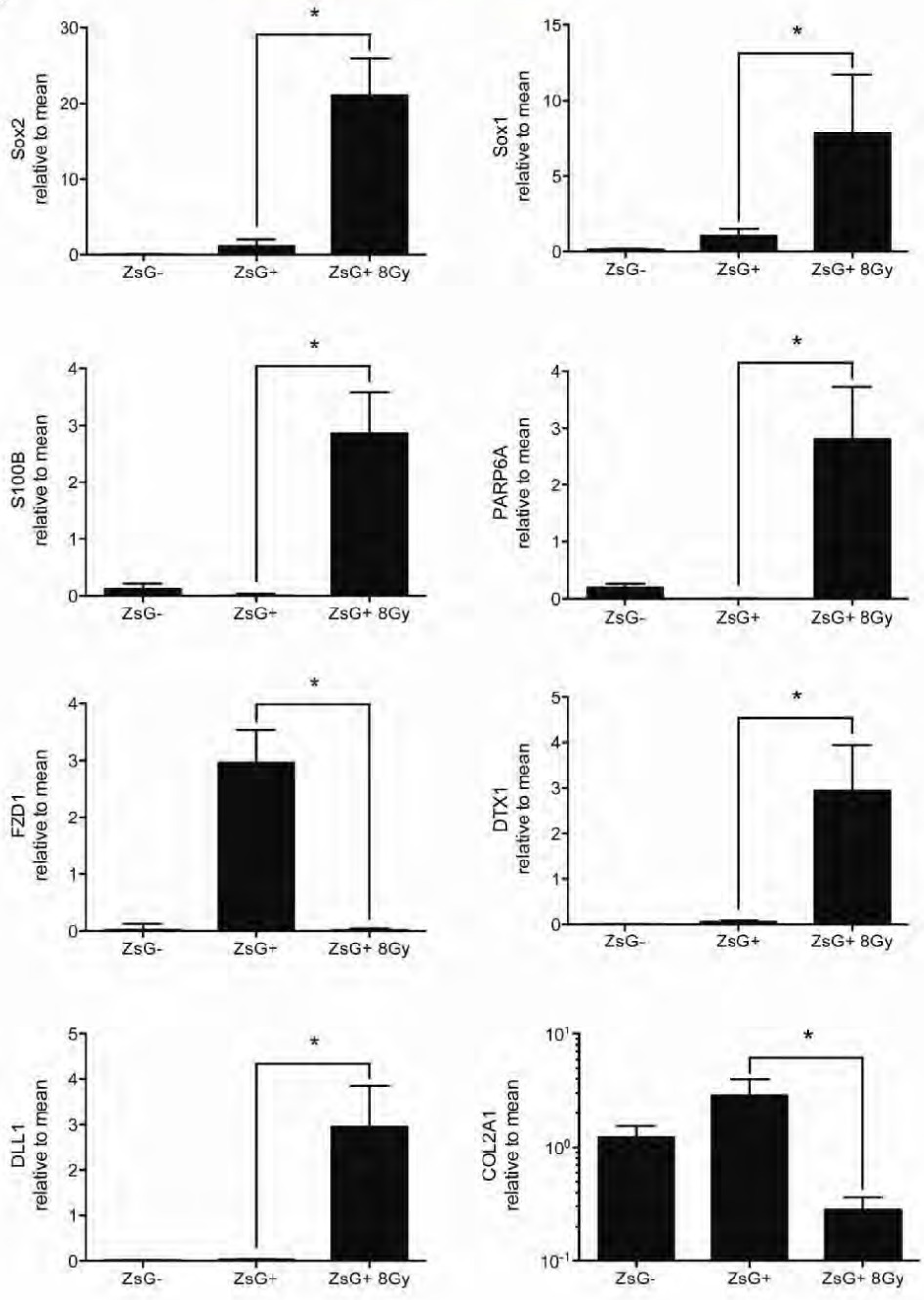

Figure 5. iBCSCs overexpress Oct4, Sox2, Nanog, and Klf4, but not c-Myc SUM159PT-ZsGreen-ODC cells were sorted into ZsGreen-cODC-positive and -negative cells. ZsGreen-cODC-negative cells were plated as monolayers, and irradiated the following day with 4 or 8 Gy. iBCSCs cells were sorted at day 5 post-irradiation. Expression of Oct4, Sox2, Nanog, Klf4, and c-Myc was analyzed by semi-quantitative RT-PCR. The means of transcription factor gene expression levels (n=4) are shown, * indicates $p<0.05$.

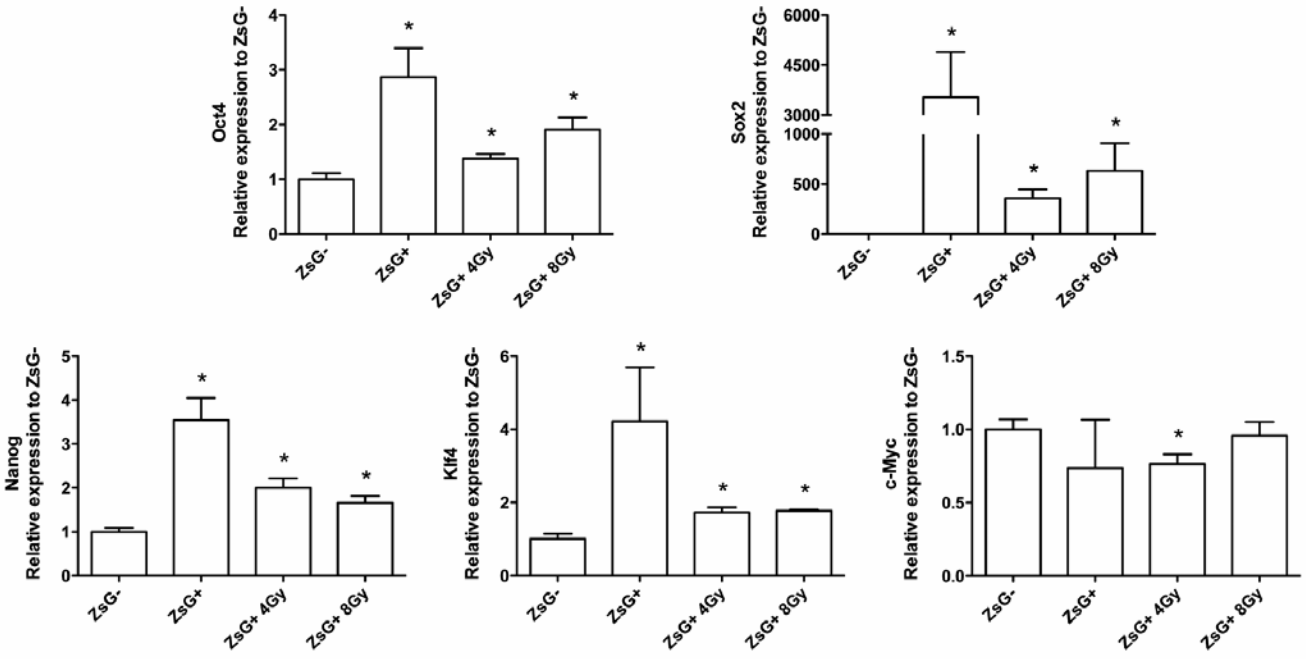

Figure 6. Irradiation-induced polyploid cells express Oct4, Sox2, Nanog, and Klf4 and are enriched for BCSCs. Protein expression levels of ZsGreen-cODC, Oct4, Sox2, Nanog, Klf4 and c-Myc, and DNA content were analyzed by flow cytometry. (**a**) The means and s.e.m. of radiation-induced polyploid cells are shown. (**b**) The means and s.e.m. of the number of polyploid Oct4-, Sox2-, Nanog-, Klf4- and c-Myc-positive cells after irradiation are shown. (**c**) Expression of Oct4, Sox2 and Nanog in polyploid were analyzed in patient derived samples (For MCF-7 and T47D see Supplementary figure 5). (**d**) Distributions of SUM159PT BCSCs in the total population, the non-polyploid population, in polyploid Oct4-, Sox2-, Nanog-, Klf4-, or c-Myc-positive population are shown (see also Supplementary figure 6 for MCF-7 and T47D). Data are expressed as means and s.e.m., * indicates $p<0.05$. (**e**) SUM159PT-ZsGreen-cODC cells were transfected with Sox2 and/or Nanog-targeting siRNA, and ZsGreen-cODC-negative were sorted and irradiated. Means (± s.e.m.) of ZsGreen-cODC-positive cells found 5 days after irradiation are shown. * indicates $p<0.05$.

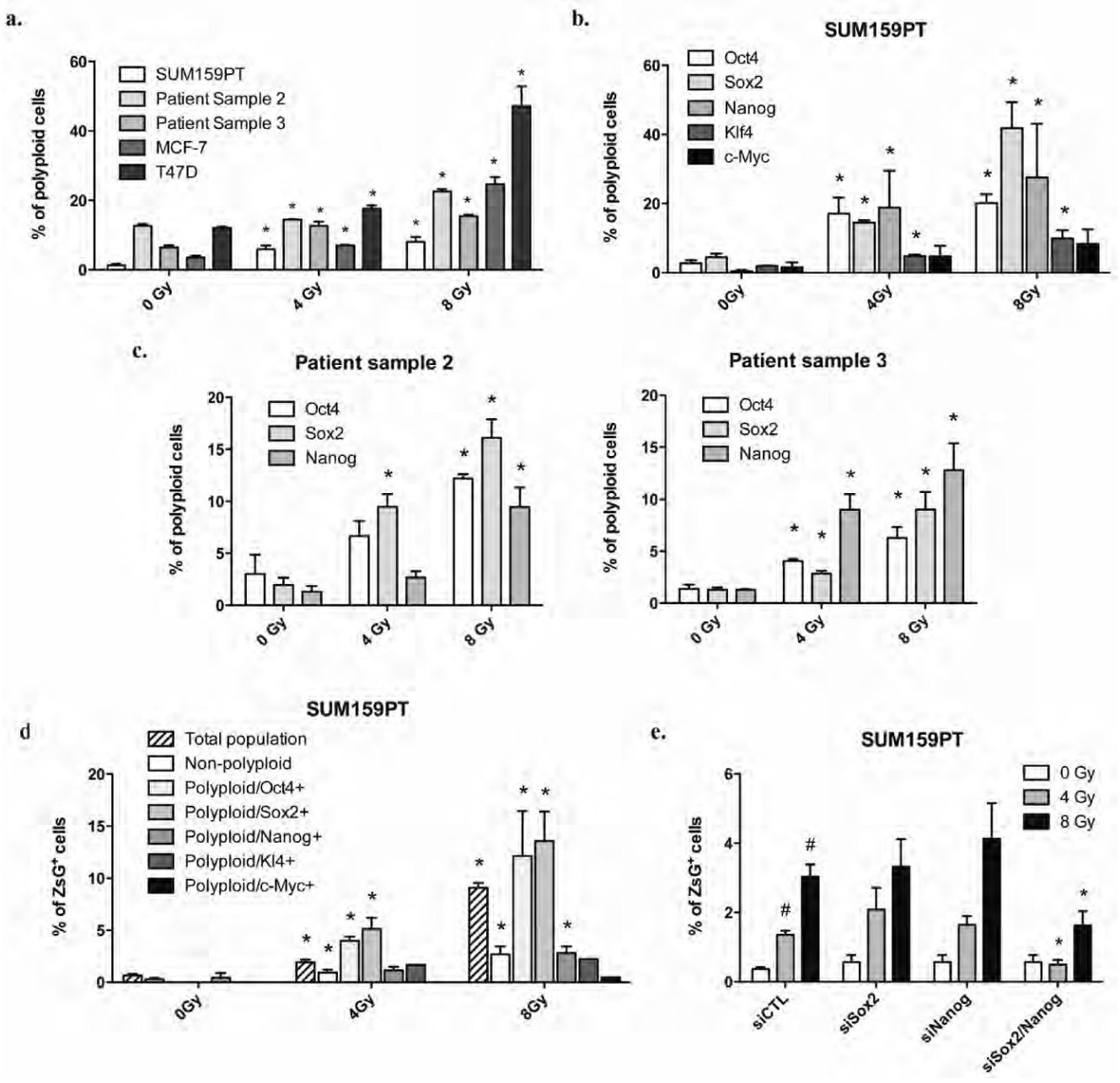

Figure 7. Polyploidy induces *de novo* generation of CSCs.
(**a**) Assessment of noscapine-induced polyploidy in MCF-7, T47D, SUM159PT cell lines and 2 patient derived samples, five days after drug treatment.
Non-tumorigenic cells ALDH1-negative patient-derived cells (**b**), MCF-7-, T47D-, and SUM159PT-ZsGreen-cODC-negative (**c**), and $CD24^{+}/CD44^{-}$ MCF-7 and T47D cells (**d**) were treated with noscapine at 0, 25 or 50µM. The presence of iBCSCs was assessed after 5 days by flow cytometry.
SUM159PTcell and patient samples 2 and 3 were transfected with specific siRNA targeting Notch receptors (**e**), or Sox2 and Nanog (**f**). Scrambled sequences were used as control. Twenty-four hour after transfection, cells were plated for a sphere forming capacity assay. Percentages of cells able to form a sphere are shown for each condition.

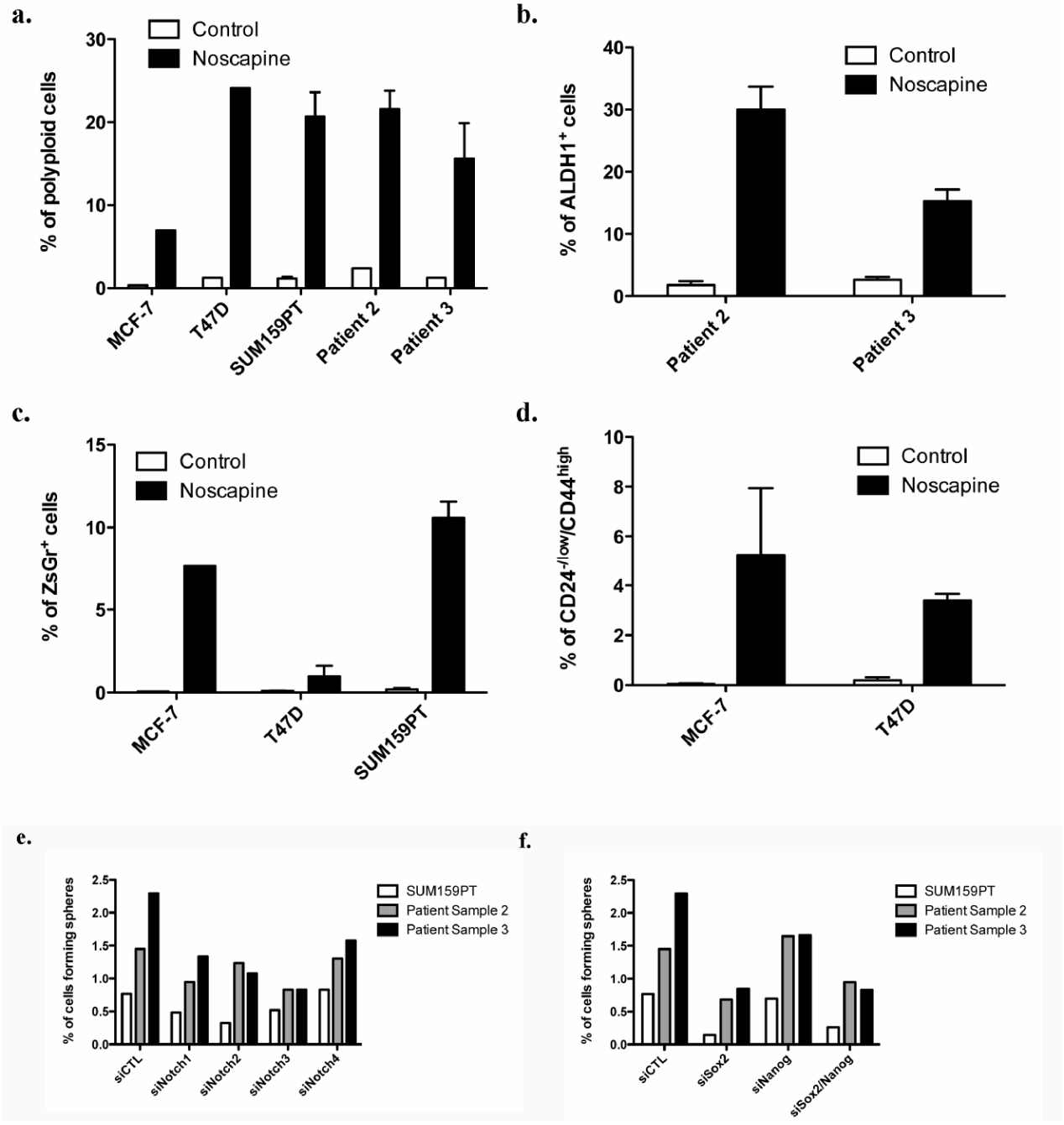

STEM CELLS®

CANCER STEM CELLS

Radiation Resistance of Cancer Stem Cells: The 4 R's of Radiobiology Revisited

FRANK PAJONK,[a,b] ERINA VLASHI,[a] WILLIAM H. MCBRIDE[a,b]

[a]Department of Radiation Oncology, Division of Molecular and Cellular Oncology, David Geffen School of Medicine at UCLA, and [b]Jonsson Comprehensive Cancer Center at UCLA, Los Angeles, California, USA

Key Words. Cancer stem cells • Cancer-initiating cells • Radiation biology

ABSTRACT

There is compelling evidence that many solid cancers are organized hierarchically and contain a small population of cancer stem cells (CSCs). It seems reasonable to suggest that a cancer cure can be achieved only if this population is eliminated. Unfortunately, there is growing evidence that CSCs are inherently resistant to radiation, and perhaps other cancer therapies. In general, success or failure of standard clinical radiation treatment is determined by the 4 R's of radiobiology: repair of DNA damage, redistribution of cells in the cell cycle, repopulation, and reoxygenation of hypoxic tumor areas. We relate recent findings on CSCs to these four phenomena and discuss possible consequences. STEM CELLS *2010;28:639–648*

Disclosure of potential conflicts of interest is found at the end of this article.

INTRODUCTION

It has been postulated for more than 4 decades that most if not all cancers are hierarchically organized and contain a subtle subpopulation of cancer stem cells (CSCs) [1–4] within a tumor that possess the capacity to self-renew and to cause the heterogeneous lineages of cancer cells that comprise the tumor [5]. The CSC concept has its origin in the leukemia literature [6], and although the term CSC does suggest normal tissue stem cells as the cell of origin in leukemia, there is evidence that leukemia stem cells may actually arise from progenitor cells (recently reviewed in [7] and [8]). However, since most radiotherapy is delivered locally to solid tumors, we will focus this review exclusively on CSCs in solid cancers and their response to radiation.

The existence of CSCs in solid tumors has been hotly debated [9–11]. It is an appealing hypothesis that has often been challenged theoretically but its opponents have not yet been able to disprove it experimentally [12]. A recent study by Quintana et al. [13] challenged the existence of CSCs in human melanoma on the basis of the ability of single cells to initiate tumors in severely immune-compromised mice. However, this study did not investigate CSC-defining characteristics of self-renewal and differentiation capacity and unlimited proliferative capacity [5] in serial marker-defined human to mouse xenotransplantation experiments. Although the CSC model may not fit perfectly the behavior of all solid tumors, it describes the way many epithelial and brain tumors respond and recur after radiation treatment more accurately than a stochastic model in which all cancer cells have the same tumorigenic potential [14]. Although no one would argue against the existence of cells with the potential to regrow a tumor, the key questions any model has to address are their frequency, do they possess "stemness", and do they have a distinct response to therapy that might allow them to be responsible for a significant number of tumor recurrences.

It is very likely that the frequency of CSCs will depend on the type of tumor and the model system studied and the actual numbers may vary substantially [15–17], which makes any analysis that is numerically based difficult.

Numerous studies that prospectively identified subpopulations of cells with stem cell phenotypic markers in many solid cancers have been the major source of support for the existence of a hierarchical structure derived from CSCs. These cells can be enriched if grown as spheroids under serum-free conditions, express gene expression programs seen during normal tissue development, such as *Wnt* and *Notch* [18–20], and appear to be highly tumorigenic in transplantation assays [15, 21–26]. Additionally, breast CSCs share with normal mammary gland stem cells-specific molecular gene expression patterns like downregulation of microRNA clusters [27]. Their origin from normal tissue stem cells, or at least very early progenitor cells, is further supported by four recent murine studies demonstrating that oncogene expression or loss of tumor suppressor genes in the stem cell compartment, but not in committed progenitor or differentiated cells, is both required and sufficient for full malignant transformation [28–31]. Although these data are convincing, the exact definition of stemness is elusive and stemness may be more of a continuum or a property that may be regained in cancer, which would suggest that neither the hierarchical model nor the stochastic model are exclusively right.

The CSC concept has been elevated to a higher level of significance in cancer therapy by recent evidence in several

Author contributions: F.P., E.V., and W.H.M.: manuscript writing and final approval of manuscript.

Correspondence: Frank Pajonk, MD, PhD, David Geffen School of Medicine at UCLA, Division of Molecular and Cellular Oncology, Department of Radiation Oncology, 10833 Le Conte Avenue, Los Angeles, California 90095-1714, USA. Telephone: 1-310-206-8733, Fax: 1-310-206-1260; e-mail: fpajonk@mednet.ucla.edu Received December 8, 2009; accepted for publication January 23, 2010; first published online in STEM CELLS *EXPRESS* February 4, 2010 available online without subscription through the open access option. 1066-5099/2009/$30.00/0 doi: 10.1002/stem.318

cancers that they can resist conventional treatments including ionizing radiation [19, 20, 32–39] and chemotherapy [16, 33, 40]. This has been explained by a metabolic status that is associated with high free radical scavenger levels [19, 41], low proteasome activity [42], activated DNA checkpoints [32], and expression of the *ABCB5* multi-drug resistance protein [16]. Their possible relative radioresistance indicates the need for re-evaluation of the mechanisms underlying the response of solid tumors to conventional and newer radiation treatments with a specific emphasis on CSCs. This has recently been discussed with reference to classic radiobiological end points [43] and will therefore not be addressed here. This review will instead summarize current data pertaining to the radiation responsiveness of CSCs within the framework of the "4 R's of Radiobiology" that determine the outcome of a conventional fractionated course of radiation therapy for cancer, as originally described by Withers: repair of sublethal DNA damage, cell repopulation, redistribution of cells in the cell cycle, and reoxygenation of previously hypoxic tumor areas [44] (Fig. 1). It is obvious that tumor responses to radiation treatment are modulated by many additional factors, and in fact, Steel even suggested 2 decades ago that intrinsic radiosensitivity should be considered as the 5th R [45]. However, the intrinsic radiosensitivity of individual CSCs has not yet been investigated and it is not clear if this changes during a fractionated course, and therefore we will focus on the 4 R's originally described by Withers [44] as they represent hubs on which many other mechanisms converge and because they provide a simple model for understanding the efficacy of fractionated radiotherapy for cancer.

It should be noted that the vast majority of experimental studies that were used to originally define the 4 R's were based on clonogen survival in hierarchical normal tissues or tumors, such as in vitro clonogenic cell survival assays, in vivo splenic colony-forming unit (CFU) or colonic/jejunal crypt cell assays, or tumor regrowth assays and evaluated responses in the short term (see Appendix). Recent data indicate that normal and also malignant stem cells, for example, in the normal colon [46], in bone marrow (long-term repopulating hematopoetic stem cells), or in melanoma [13], cycle very slowly and would not be evaluated by most of the standard radiobiological assays, such as those listed above. Although these assays are often described as measuring "stem" cells, in fact, they rather favor progenitor cells. Such progenitor cell responses are highly relevant to preserving normal tissue function because in hierarchical normal tissues they rapidly restore tissue integrity. However, in tumors, complete cell kill is required to prevent a recurrence and this will be determined by a composite of the radioresistance of different subpopulations and the number of cells with that level of radioresistance. The representation of CSCs may be particularly important for clinical consideration of the relative radiation sensitivities of cancers like melanomas in which the frequency of CSCs may vary [13, 16] and epithelial cancers where it may be low [15]. With our growing ability to study CSC populations directly, future studies should be able to take this heterogeneity into account.

Repair of Radiation-Induced DNA Damage

Cell kill by ionizing radiation is based on production of unrepairable lesions involving DNA double-strand breaks (DSBs). Most radiation-induced DNA damage is however sublethal. Although this is repaired at lower doses, at higher doses accumulation of sublethal lesions also contributes to lethality. Repair of sublethal damage between radiation fractions is exploited in radiation therapy because critical normal tissues and tumors often differ in their ability to repair radiation damage.

Highly reactive oxygen species (hROS), which radiation generates by ionization of water molecules, are short-lived and rapidly interact with various biomolecules in cells. Those that are generated within 2 nm of the DNA are more important in causing DNA damage than direct ionization of the DNA strands and, consequently, free radical scavengers, such as glutathione, within this location play a major role in determining the extent of initial radiation-induced DNA damage and cell survival [47].

$CD24^{-/low}/CD44^{+}$ breast cancer cells, which are believed to be a clinically relevant CSC-containing subpopulation, when compared to the whole population were originally found to have increased tumorigenicity and to be relatively resistant to radiation at the DNA and cellular levels, which could be attributed to significantly lower levels of basal and radiation-induced ROS, indicating higher levels of free radical scavengers [19]. The low ROS levels before and after irradiation of murine and human breast CSCs from cell lines was recently confirmed by Diehn and coworkers using primary breast cancer cultures and who further described an anti-oxidant gene expression profile for breast CSCs by single-cell reverse transcription-polymerase chain reaction (RT-PCR) [41]. In this study, depletion of glutathione by buthionine sulfoximine reversed the radioresistant phenotype of breast CSCs. Low constitutive and radiation-inducible ROS levels may therefore be a useful marker for identification of CSCs [48] and perhaps even normal stem cells, and could also be crucial in determining the response of this subpopulation to radiation and other therapies. They may be why breast CSCs were found to be more radiation-resistant in clonogenic assays [19, 20, 41], in particular, in the lower dose range, and why CSCs are enriched by repeated fractions of radiation that preferentially kill the more radiosensitive, less tumorigenic cancer cells [19].

A hallmark of DNA DSB recognition and repair is phosphorylation of the histone *H2AX* by *ATM* or *ATR* (*γ-H2AX*) [49], which is thought to form one immunohistochemically detectable focus per DSB. Radiation induced few [19] or significantly less [50] *γ-H2AX* foci in human breast CSCs, and in murine breast CSCs they resolved faster than in non-CSC populations [20]. Also, in glioma, although CSCs showed a normal initial *γ-H2AX* response to irradiation, here also the DNA DSBs were repaired more efficiently and more rapidly [32]. This response may however depend on the experimental context as the ability of glioma stem cells to repair DNA damage more efficiently than their non-CSC counterparts was recently challenged by Ropolo and coworkers who reported no change in base excision repair, resolution of *γ-H2AX* foci, or single-strand DNA repair in cell lines enriched for $CD133^{+}$ cells in vitro [51]. Additionally, McCord et al. reported [52] that $CD133^{+}$ glioma cells were not always more radiation-resistant than $CD133^{-}$ cells, although this study did not attempt to demonstrate aspects of the CSC phenotype other than CD133 positivity.

Currently, it is prudent to believe that there is no ideal single marker for CSCs in any tumor system [53]. Furthermore, sorting of cancer stem cells and how to report the isolation methods used still need to be standardized to allow comparison of data obtained from different laboratories [54]. For example, CD133 surface expression is commonly used to identify CSCs in glioma, but doubts have been expressed as to whether this marker may define progenitor cells rather than

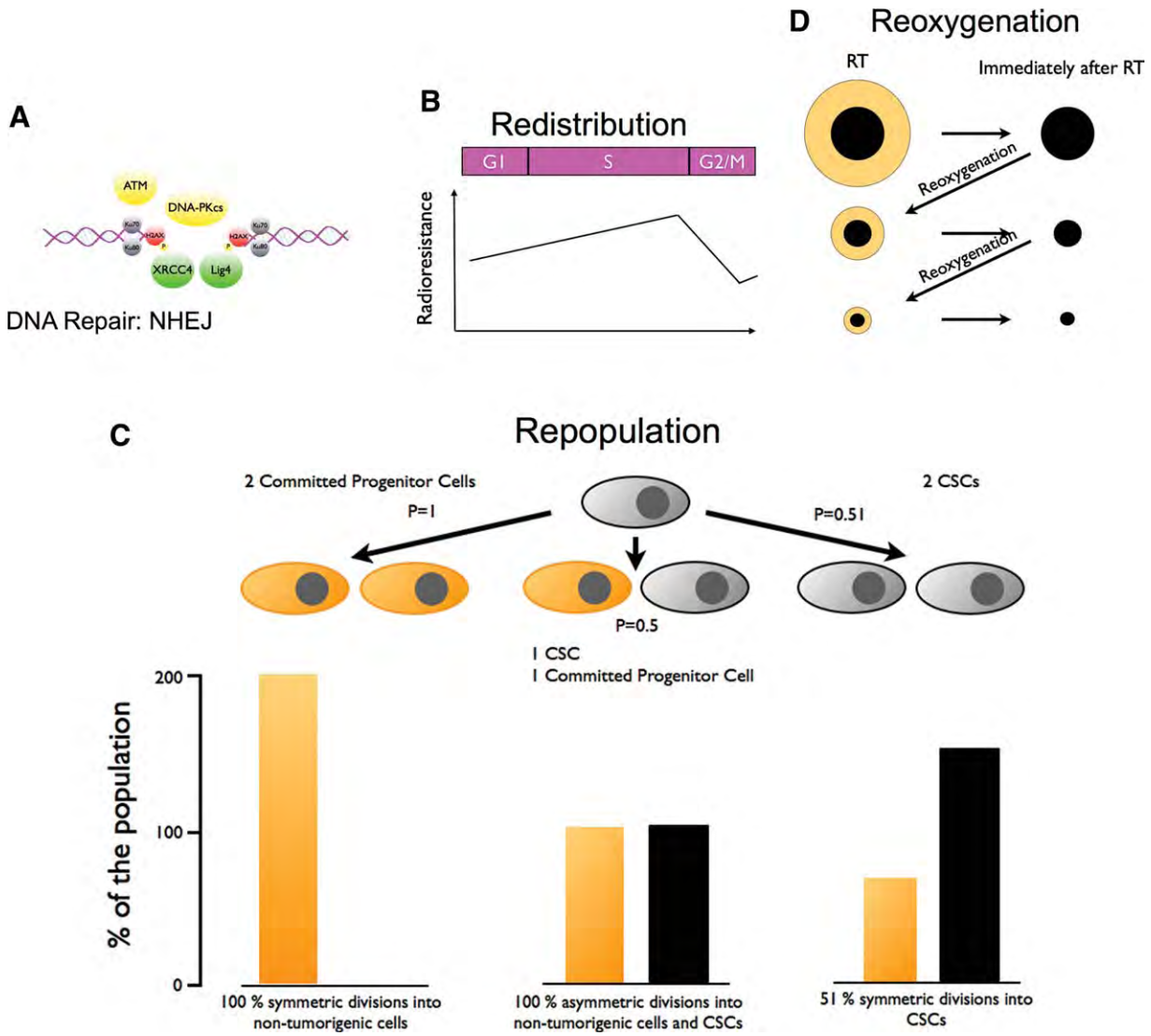

Figure 1. The 4 R's of radiation biology. **(A):** Repair of sublethal DNA damage. DNA double-strand breaks (DSBs) after exposure to ionizing radiation are mainly repaired by NHEJ. NHEJ involves recognition of the DNA DSBs by *Ku70/80*, recruitment of the histone *H2AX* to the DNA leasion, phopshorylation of *H2AX* by *ATM*, *DNA-PKcs*, or *ATR*, and finally rejoining of the strand ends by *XRCC4* and *Ligase 4*. **(B):** Redistribution. Mammalian cells exhibit different levels of radioresistance during the course of the cell cycle. Cells in the late S-phase are especially resistant and cells in the G2/M-phase are most sensitive to ionizing radiation. During fractionated radiation cells in the G2/M-phase are preferentially killed. The time between two fractions allows resistant cells from the S-phase of the cell cycle to redistribute into phases in which cells are more radiosensitive. **(C):** Repopulation. Normal and malignant stem cells have the ability to perform asymmetric cell division, which give rise to a daughter stem cell and a committed progenitor cell. In a symmetric cell division in contrast, stem cells divide into two committed progenitor cells or two daughter stem cells. If the latter happens only in 1% of the stem cell divisions, the number of stem cells after 20 cell doublings will be twice as high as the number of committed progenitor cells. This indicates that small changes in the way stem cells divide have huge impact on the organization of a tissue or tumor and are thought to be the mechanism behind accelerated repopulation. **(D):** Reoxygenation. Tumors contain regions of hypoxia in which cancer cells are thought to be resistant to radiation. During fractionated radiotherapy, these regions are reoxygenated by various mechanisms including reduction of intratumoral pressure and normalization of the vasculature. Reoxygenation between radiation fractions will lead to radiosensitization of previously hypoxic tumor areas and is thought to increase the efficiency of radiation treatment. Abbreviations: CSCs, cancer stem cells; NHEJ, nonhomologous end joining.

CSCs or has any specificity for glioma CSCs, and as to whether it reflects a state of bioenergetic stress rather than stemness [55–57]. Recent data on neural stem cells even suggest the possibility that expression of CD133 depends on the cell cycle and is specifically downregulated in the G_0/G_1 phase [58]. In spite of these caveats, $CD133^+$ glioma cells were used to show increased ability to repair single-strand breaks by the alkaline Comet assay and preferential activation of the DNA damage checkpoint [59] in the response to radiation [32], as assessed by hyperphosphorylation of *Chk1*, and to a lesser extent *Chk2*. Inhibition of this response radiosensitized $CD133^+$ glioma cells [32] (Fig. 2C). This was confirmed in $CD133^+$ atypical teratoid/rhabdoid tumor cells, a rare and aggressive pediatric brain tumor of uncertain origin [34] and in glioma cultures enriched for $CD133^+$ cells [51]. *Chk1* phosphorylation protects cells from radiation cytotoxicity, although not through stimulating repair by nonhomologous end joining [60]. However, *RAD51*, a protein involved in the search for homology and strand pairing during homologous recombination of DNA double-strand breaks [61], is part of

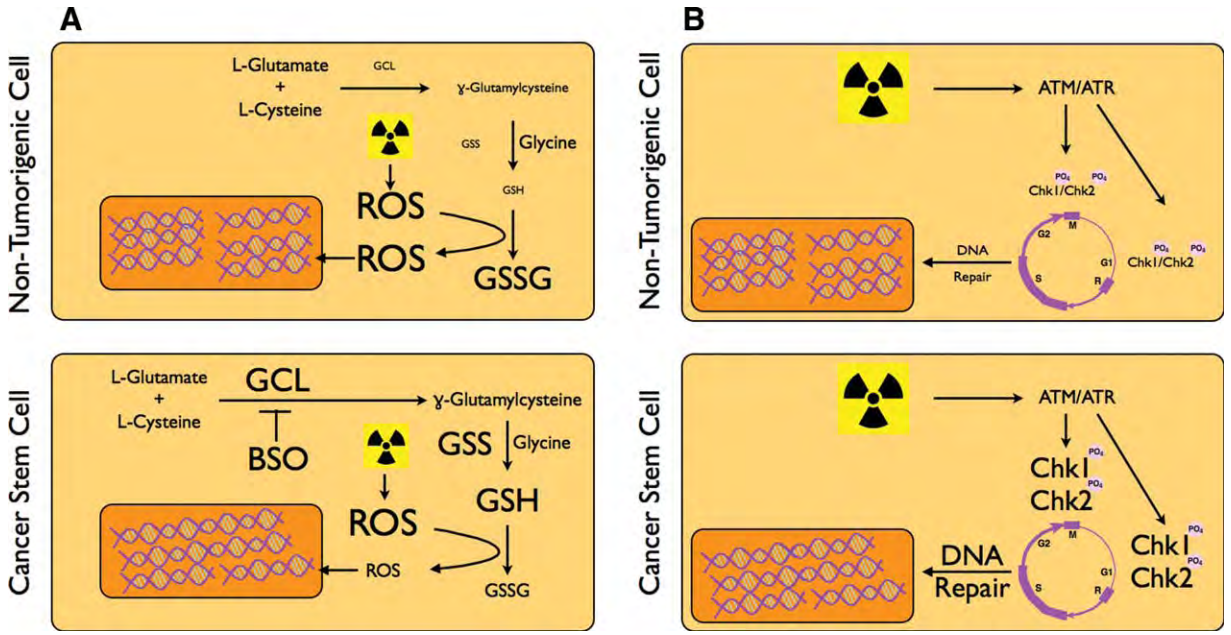

Figure 2. CSCs and DNA repair. **(A):** CSCs exhibit less DNA double-strand breaks (DSBs) after exposure to ionizing radiation than nontumorigenic cells. *GCL* catalyzes the reaction of cysteine and glutamate to form γ-glutamylcysteine in an ATP-dependent step. In a second step, *GSS* condensates γ-glutamylcysteine and glycine to form glutathione. Breast CSCs were found to express high levels of *GCL* and *GSS*. Consequently, most radiation-induced free radicals were scavenged in breast CSCs and ionizing radiation caused only little DNA damage if compared to nontumorigenic cells. Inhibition of glutamate cysteine ligase by buthionine sulfoximine reversed the radioresistant phenotype. **(B):** CSCs repair DNA DSBs more efficiently than nontumorigenic cells. CSCs in breast and brain cancers hyperphosphorylated the DNA checkpoint kinases *Chk1* and *Chk2* constitutively and in response to ionizing radiation, thereby removing DNA DSBs more rapidly and more efficiently. Abbreviations: BSO, Buthionine Sulfoximine; CSCs, cancer stem cells; GCL, glutamate cysteine ligase; GSS, glutathione synthetase; GSSG, glutathione disulfide; ROS, reactive oxygen species.

the CSCs signature in breast cancer [62], suggesting that *Chk1*-dependent homologous recombination may be more important in DNA repair in CSCs.

It is sometimes difficult to dissociate DNA repair, or lack thereof, from induced cell death following radiation exposure. Indeed, induction of the apoptosis inhibitor survivin was proposed by Woodward et al. [20] as an additional cytoprotective mechanism of breast CSC following irradiation based on their observation that *ß-catenin* and *survivin* expression was induced in normal murine *Sca-1*$^{+}$ *(stem cell antigen 1)* but not *Sca-1*$^{-}$ mammary epithelial cells. Survivin expression has been linked to radioresistance in other studies [63]. The mechanisms by which *survivin* affects DNA repair are incompletely understood but seem to involve changes in cell cycle distribution and direct effects on DNA DSB repair [64–66]. *Survivin* may be targeted by small-molecule inhibitors [63], but since radiation-induced *survivin* expression may be a conserved response of normal and malignant stem cells, the existence of a therapeutic window for these agents in combination with radiation therapy needs to be shown before these drugs can be considered as having potential radiotherapeutic benefit in targeting CSC.

An alternative radioprotective mechanism for CD133^{+} glioma stem cells was recently suggested by Lomonaco et al. to be induced autophagy. In their study, CD133^{+} cells expressed higher levels of the autophagy-related proteins *LC3, ATG5*, and *ATG12* than CD133^{-} cells after irradiation and inhibition of autophagy preferentially sensitized CD133^{+} cells to radiation and decreased sphere-forming capacity [39].

Fractionation is believed to allow repair of slowly proliferating, late-responding tissue like the central nervous system at the expense of tumors that seem less able to repair sublethal damage. In fact, cells vary greatly in their intrinsic cellular radioresistance and many tumors seem quite adept at repair. Variation both within a tumor and between tumors of the same entity is therefore to be expected and it is difficult to draw hard and fast conclusions that apply in all circumstances. In part, the outcome of radiation exposure will depend upon the extent of DNA damage and repair, but the downstream DNA damage response that determines cell death and cell cycle arrest, in coordination with the signaling pathways that are active and activated, will play roles. It is important to remember that cancer-associated mutations influence DNA repair, cell cycle, and cell arrest and their influence on radiation response should be taken into account when comparing tumors from different individuals. The therapeutic resistance of tumors is therefore multifactorial and complex but the fact that CSCs may differ in the way they handle radiation-induced DNA damage should be considered as a potential parameter determining the outcome of fractionated radiotherapy. In essence, if the dose per fraction of radiation is insufficient to cause sufficient cell death in the CSC population, the frequency of CSCs in a tumor may even increase during treatment, although clinically the tumor may regress macroscopically. However, parameters other than DNA damage and repair must be considered as contributing to this equation.

Redistribution

Redistribution acknowledges the fact that cells exhibit differential radiation sensitivity while in the different phases of the cell cycle, with cells in mitosis being most sensitive to DNA damaging agents and cells in late S-phase being most resistant [67]. Because of cell cycle progression of surviving cells between radiation fractions, dose fractionation allows redistribution of radioresistant S-phase tumor cells into a more

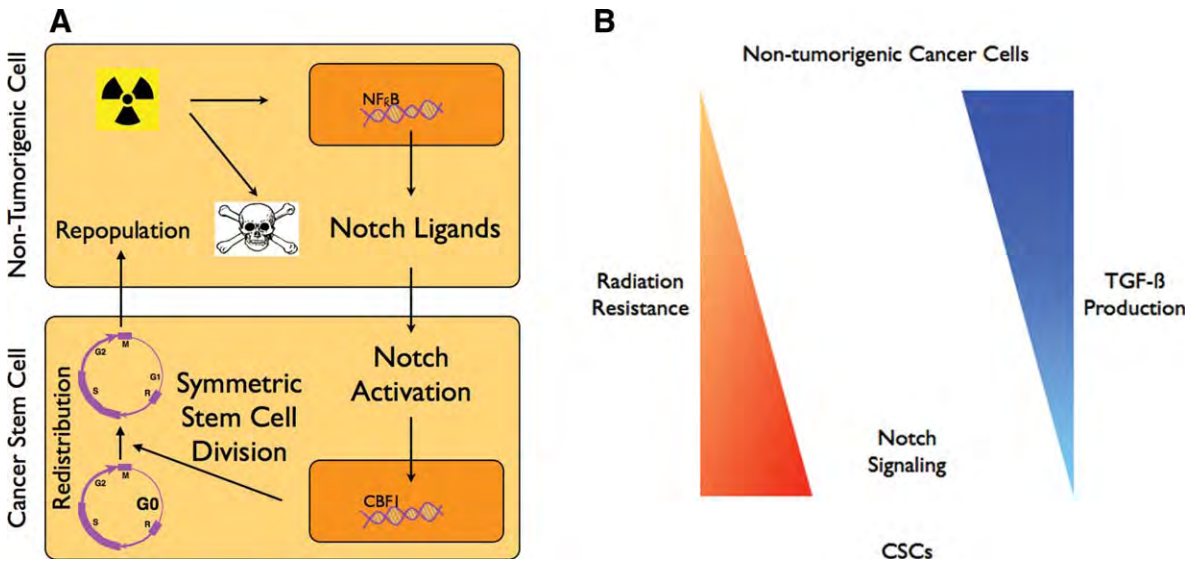

Figure 3. Radiation-induced redistribution and accelerated repopulation employs the developmental *Notch* pathway. **(A):** In breast cancer, ionizing radiation induces the expression of *Notch* receptor ligands on the surface of nontumorigenic cells and possibly other nonmalignant stem cells niche cells like, for example, endothelial cells, which are finally depleted by radiation. Activation of *Notch* signaling in CSCs may than redistribute quiescent CSCs into the cell cycle in a symmetric type of stem cell division and finally cause repopulation of the tumor. **(B):** In this model system, *TGF-β* is produced by the mass of the nontumorigenic, radiosensitive cancer cells and activated by radiation. It antagonizes the proliferative effects of *Notch*, which is activated in CSCs through interaction with their niche. During the course of fractionated irradiation, most of the nontumorigenic cancer cells are killed. This causes *TGF-β* levels to drop while *Notch* is still being activated, resulting in increased regrowth rates and thus accelerated repopulation. Abbreviation: CSCs, cancer stem cells.

sensitive phase of the cell cycle, and a resultant therapeutic benefit for slowly cycling normal cells (Fig. 3A) [68]. Normal tissue stem cells and CSCs are believed to exist in the G0-phase of the cell cycle and to cycle slowly. They are thought to be maintained in this state by intrinsic genetic programs and extrinsic influences from the niche in which they reside. Although there is good experimental evidence for the quiescent state of hematopoetic stem cells [69, 70], evidence for the quiescent state of cancer stem cells comes currently rather from theoretical considerations and mathematical modeling than from experimental data. Several molecules like, for example, Notch ligands, have been implicated in the transition of stem cells into cycle and their emergence from the niche [71], which potentially offers novel opportunities for therapeutic intervention [72, 73]. Niches for most CSCs have yet to be convincingly demonstrated but glioma CSCs appear to reside in a perivascular location [42, 74]. Most putative CSCs in this site are negative for the proliferation marker Ki67 [42]. Multiple fractions of radiation promotes recruitment of CSCs from the niche and increases the proportion of cycling cells [42], with a concomitant increase in radiosensitivity. For normal tissue stem cells and CSCs, therefore, redistribution following irradiation may be tied to their mobilization and entry into the cell cycle, and thus regeneration. This raises the interesting possibility that mobilization of CSCs may be strategy for increasing their radiosensitivity. The effect of radiation on expression of developmental gene expression profiles is still in its infancy, but it is interesting to note that the effects of fractionated irradiation on Notch/Jagged expression by breast CSCs were far greater than those for single doses [19], suggesting that fractionated irradiation may specifically alter the kinetics of CSCs and perhaps normal stem cell regenerative behavior through specific activation of developmental pathways.

Redistribution of cells during fractionated irradiation has been interpreted as sparing dose-limiting tissues with a small content of rapidly cycling cells such as the central nervous system in comparison with normal tissues such as the bone marrow and intestine and tumors that are considered to have a high content of cells with rapid turnover. If, in fact, tumors have a high percent of slowly cycling CSCs, this logic may not apply.

Repopulation

Repopulation of tumors may be one of the most common reasons for the failure of conventional fractionated courses of radiation therapy [75, 76], as judged by the dramatic effects of treatment prolongation over the conventional 6 weeks on local control rates [75, 77, 78]. For decades, radiation oncologists hypothesized that depopulation of certain hierarchical normal tissues, such as the jejunum, by ionizing radiation caused "stem" cells to switch from an asymmetric type of cell division, which gives rise to a daughter stem cell and a lineage-committed progenitor cell, to a symmetric form of cell division that results in two proliferative daughter stem cells. Cell loss from the proliferative compartment in normal tissues seems to be decreased until regeneration is complete. A similar process was postulated for tumors, giving rise to accelerated repopulation, which describes the situation where the regrowth rate of a tumor after treatment with a sublethal radiation dose exceeds the growth rate of the untreated tumor.

Importantly, like normal tissue stem cells, CSCs employ developmental signaling pathways like the *Notch, Wnt*, and *Sonic hedgehog* pathways [18–20, 79, 80] that are able to perform the switch from an asymmetric to a symmetric type of cell division. Our initial report of activation of the *Notch* pathway by radiation [19] has now been confirmed by others in endothelial cells [81], indicating that this pathway might be part of the acute response to ionizing radiation. Activation of the *Notch* receptor relies on cell-cell contacts and binding of *Notch* receptors to ligands of the *Delta* or *Jagged* family.

Upon ligand binding, the extracellular part of the *Notch* receptor is shed and internalized into the ligand-expressing cell, whereas the remaining part of the *Notch* receptor undergoes intramembranous cleavage by *γ-secretase*, which finally releases the intracellular domain of the receptor (*Notch-ICD*) for nuclear translocation. In the nucleus, *Notch-ICD* binds to *CBF-1*, which turns it from a transcriptional repressor into a transcriptional activator, thereby initiating the transcription of gene products that promote progression into the S-phase of the cell cycle [82]. Activation of *Notch* signaling can recruit quiescent stem cells into the cell cycle [83] and a sustained *Notch* signal maintains the stem cell phenotype whereas termination of this signal leads to differentiation [71]. An important issue here is the extent to which this takes place within and is dependent on cell-cell contact within the "niche" and the relative radiosensitivity of cells as they go through activation.

Another developmental pathway activated in response to radiation is the *TGF-β* pathway [84–86], which is thought to be an antiproliferative pathway that controls tissue homeostasis [87]. It mediates its effects through proteins of the *smad* family, which can compete with *Notch-ICD* for binding to CBF-1 [88, 89]. This draws an interesting model of tumor tissue homeostasis and accelerated repopulation during fractionated radiation therapy for epithelial cancers in which the bulk of the tumor is characterized by relative radiosensitivity but produces most of the *TGF-β*. If CSCs can respond to *TGF-β*, it could antagonize their division until most of the non-CSCs are eliminated and *TGF-β* levels drop, whereupon the *Notch* pathway would be activated, driving CSC self-renewal and leading to a rapid relapse (Fig. 3B) [90]. This mechanism could also apply in normal hierarchical tissues that are also dependent on developmental pathways like *Notch*, which supports the proposal that the normal stem cell/early progenitor compartment is the origin of CSCs [28–31], and at the same time offers novel targets for therapeutic intervention [73, 91–93] in combination with radiation therapy.

Accelerated repopulation is very difficult to demonstrate in vitro, and in vivo results can be influenced by many factors other than altered proliferative status. However, with marker profiles for CSCs available for a variety of different solid cancers, several groups have recently reported an increase in such phenotypes after repeated, clinically relevant doses of radiation in vitro and in vivo [19, 20, 32]. However, it is possible that if radiation recruits CSCs into the proliferating pool, their intrinsic radiosensitivity may alter, which would give a therapeutic advantage to fractionated as opposed to single-dose radiotherapy.

Clearly, repopulation of tumors and regeneration of normal tissue are critical elements in the success of fractionated radiotherapy. Again, drawing broad conclusions is difficult but the CSC concept provides markers for studying this process in vivo and targets for possible intervention.

Reoxygenation

Since the initial experiments of Schwarz in 1909, Holthusen in 1921, and Thomlinson and Gray in 1955, oxygen has been known as one of the most potent modifiers of radiation sensitivity and hypoxic cells have been repeatedly shown to be 2-3 times more resistant to radiation [94–96]. In addition, human tumors contain regions of acute and chronic hypoxia that have often been shown to be associated with poor prognosis because of local recurrence or systemic disease [97–101]. The tumor microenvironment is dynamic with ever-changing oxygen and pH gradients [102, 103]. Transient areas of acute hypoxia due to intermittent vessel closure may reoxygenate rapidly, whereas chronic hypoxia due to the limitation of oxygen diffusion may take longer. A major concept in clinical radiobiology is that tumor subpopulations in hypoxic areas are critical to target for increased therapeutic benefit but there is still discussion as to whether acute or chronic hypoxic cells are most important [103].

Reoxygenation between dose fractions is generally believed to improve the efficacy of radiation treatment by increasing tumor radiosensitivity. It should however be noted that many of these experiments were performed under conditions where oxygen levels were rapidly decreased and tumors were then reoxygenated after irradiation. This drastic and stressful change in the tumor microenvironment could affect CSCs, for example, by triggering rapid differentiation [48]. Such studies should be interpreted with caution as they may fail to recapitulate tumor microenvironmental conditions in vivo.

As discussed above, it seems that brain CSCs reside in a perivascular niche [42, 74]. Although one might consider such cells as being in the most perfectly oxygenated region in a tumor, it is also likely that these would be exposed to rapidly changing bouts of hypoxia-reperfusion. This can generate damaging free radicals. It seems likely that the low hROS metabolic profile [19, 41] and slow cycling of CSCs may selectively protect them from some of these free radical effects and, indeed, survival pathways may be induced that encourage radioresistancy at the expense of non-CSC cells (Fig. 4).

There is increasing evidence that the length of time that cells are under hypoxic conditions and the extent of the hypoxia are critical factors in terms of the biological and radiation response of these cells. Indeed, cells irradiated shortly after reoxygenation or after exposure to long-term chronic hypoxia are radiosensitive [104] compared to those irradiated after 4-24 hours of hypoxia. The underlying mechanisms are incompletely understood but the suggestion is that the radioprotective effect of hypoxia does not exclusively rely on the radiochemistry of oxygen but rather involves complex signaling events, which adjust the homeostatic rheostat if the hypoxia persists long enough, thereby losing its protective effects. Indeed, chronic hypoxia may make cells radiosensitive by decreasing DNA repair, in particular, RAD51-mediated homologous recombination [105]. In light of these observations, cells undergoing intermittent hypoxia might be the most relevant for therapy resistance, and because of their presence in a perivascular niche, it would be of great interest to know more about the response of CSCs to irradiation under varying hypoxic conditions. Indeed, if as seems likely intermittent hypoxia were to have an effect similar to that of irradiation in selecting for CSCs, recruiting them into cycle, and mobilizing them [19, 42], CSCs could be responsible for the relationship that has been found between hypoxia and metastasis [98, 106].

There are other possible consequences of the presence of CSCs in the perivascular niche. They may be more accessible to drugs delivered systemically and also more dependent on endothelial cell viability and function than cells more distant from the vasculature. It is of interest in this regard that an earlier report showed that the effect of ionizing radiation on tumor cells in vivo may be preceded by radiation-induced death of endothelial cells [107]. Furthermore, synergy between anti-angiogenic therapies and radiation has been observed [108], which is counterintuitive from a classic view of tumor hypoxia as one could argue that anti-angiogenesis should increase tumor hypoxia and thus radiation resistance. Normalization of blood flow [109–111] may partly explain this synergy but the proximity of CSCs to endothelial changes offers an alternative explanation for this synergy. It should

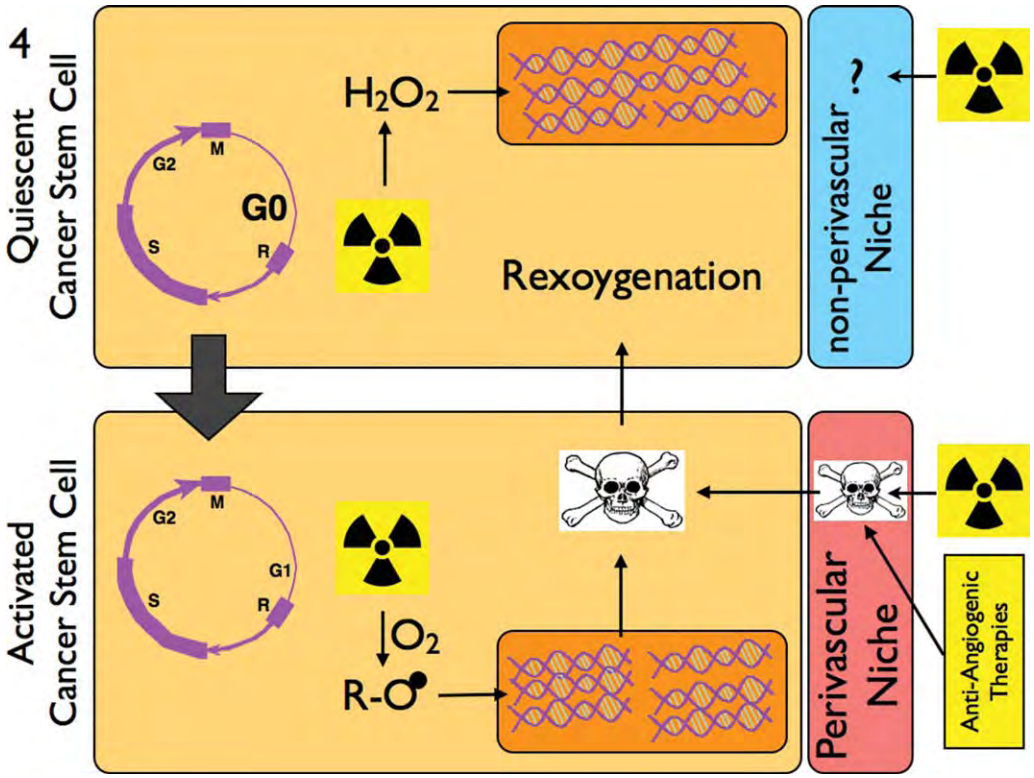

Figure 4. CSCs and tumor hypoxia. Like long-term repopulating hematopoetic stem cells, quiescent CSCs may exist in a nonperivascular hypoxic niche, relatively protected from ionizing radiation. Activated, and thus cycling, CSCs are found in a perivascular niche with confers increased radiation sensitivity and the dependence of CSCs on that niche makes them vulnerable to anti-angiogenic strategies, which target endothelial cells, thereby destroying the CSC niche. Reoxygenation of the hypoxic CSC niche during radiation fractionation redistributes quiescent CSCs as increasing oxygen levels will modify the niche conditions to render those found in pervascular regions and may cause the transition from a quiescent into an activated, proliferative CSC state. Abbreviation: CSCs, cancer stem cells.

also be noted that single and fractionated radiation regimens can "prune" tumor and normal tissue vasculature, converting acute hypoxia to chronic hypoxia [112], and it will be important to determine the fate of CSCs as the microenvironment changes with time after exposure.

The observation of a perivascular CSC niche may explain the variable results [113] of clinical trials aimed at improving tumor oxygenation. One other possible conclusion would be that, like long-term repopulating bone marrow cells [48], CSCs exist in two different stem cell niches, one hypoxic for quiescent CSCs and one adjacent to endothelial cells for more activated CSCs. Transition between both states could be bidirectional, as it is in bone marrow [48]. Better marker profiles for quiescent CSCs will be needed to elucidate whether or not this is the case.

Another example of the potential relevance of CSCs to clinical practice is the use of erythropoiesis-stimulating agents (ESAs) in anemic cancer patients. These aim to decrease hypoxia and increase therapeutic benefit, but have been found to cause an unexpected decrease in local control rates after radiation treatment of epithelial cancers [114–116]. Although preclinical models investigating the effects of ESAs on unselected cell populations led to conflicting results [117–122], breast CSCs were clearly stimulated by ESAs, explaining the unexpected clinical findings [18].

Related to the question of how relevant hypoxia is for clinical radiation responses of tumors is the metabolic state of CSCs. Rapidly proliferating cancer cells, which form the bulk of the tumor, rely mainly on glycolysis [123], a less efficient way of energy production that requires drastically increased glucose uptake, a phenomenon utilized in ^{18}FDG-PET imaging of tumors. It is a general assumption that CSCs, in contrast, are mostly quiescent and as such metabolize glucose by oxidative phosphorylation rather than by glycolysis [124]. Consequently, areas with high numbers of quiescent CSCs with moderate or low glucose uptake will not be detectable by ^{18}FDG-PET and should therefore not be excluded from the defined clinical radiation target volume.

Concluding Remarks

Despite enormous research efforts, systemic therapies still fail to cure most solid cancers, irrespective of the stage and spread of the disease. Even so-called targeted therapies are mainly cytostatic and as such aim to turn cancer into a chronic and eventually controllable rather than curable disease. Surgery and radiation therapy are currently the only treatment options leading to cancer cure for patients suffering from localized cancers, but fail against systemic disease. More importantly, most current strategies do not target CSCs but rather more differentiated tumor cells [125]. Existing paradigms for cancer treatment need to be re-evaluated for relevance based upon recent insights into the response of CSCs to conventional treatments, such as radiation therapy. Conventional fractionated radiation therapy has evolved in over a century as a means of delivering radiation dose over a period of time and is a compromise between sparing normal tissues at the expense of tumors while avoiding loss of tumor control. The principles involved are enshrined in the 4 R's of radiobiology. At this point in time, these are not tailored for individual treatment and predictive markers are needed to

allow this to be part of the treatment planning strategy. Obviously, CSC markers should be part of this effort as they may change the way radiation is delivered.

CSCs also offer novel targets to enhance the efficacy of radiation therapy [32, 36, 50] and future targeted therapies should have this aim. Also, because their metabolic status may differ from the majority of cells in a tumor, the effect of this heterogeneity on functional imaging of tumors should be taken into account. With the advent of novel imaging technologies for CSCs [42], biology-guided radiation treatment planning may offer ways for specifically delivering high radiation doses to areas with high CSCs numbers. Finally, it should be noted that partial tumor responses to therapy mean little if CSCs are the major cells determining outcome. Radiation therapy will kill CSCs and their number and relative radioresistance will determine if they survive a fractionated course of radiation, or whether another delivery strategy or even therapy would be superior.

Appendix

Classic Radiobiology Assays

Clonogenic Survival Assay: The In Vitro Gold Standard Assay To Assess the Effect of Radiation on Tumor Cells. A defined low number of cells is plated into culture dishes and exposed to increasing doses of radiation. The low number of cells treated allows outgrowth of colonies from single surviving cells (clonogens). In general, colonies of more than 50 cells are considered survivors. This is equivalent to 5-6 cell divisions if none of the cells are lost. The surviving fraction of cells for each radiation dose is normalized to the surviving fraction of the corresponding control to compensate for acute toxicity of the assay itself. Results are presented on a log-linear scale and measure the number of clonogens, which reflects the survival of committed progenitor cells and cancer stem cells.

Splenic CFU Assay: In Vivo Assay To Assess the Number of Clonogens of Normal Hematopoetic Cells, Leukemia, and Lymphoma Cells. A defined number of cells is injected into immunodeficient animals. The number of macroscopic colonies on the spleen surface is counted and CFU numbers after radiation treatment are normalized to numbers obtained from nontreated controls. The radiation can be applied in vivo or ex vivo to the cells injected. The assay suffers from the same problems described for in vitro clonogenic survival assays and results may also depend on the ability of the injected cells to home to the microenvironment in the spleen.

Colonic/Jejunal Crypt Assay. The jejunum is one of the most radiosensitive organ systems and loss of its integrity defines the gastrointestinal syndrome in the response of mammalian organisms to radiation. Radiation causes denudation of the jejunum of its crypts and recovery of the crypts can be measured to estimate the fraction of surviving stem cells/progenitor cells.

Tumor Assays. In limiting dilution assays, a decreasing number of cells are injected into immunodeficient animals, either subcutaneously or orthotopically into the corresponding organ site. True cancer stem cell populations can be serially transplanted from one animal to the next.

Acknowledgments

This work was supported in part by a grant from the California Breast Cancer Research Program (BC060077), the Department of Defense (PC060599), and the National Cancer Institute (1R01CA137110-01) to F.P. and by a grant from the Biomedical Advance Research and Development Authority (1RC1A1081287) to W.H.M.

Disclosure of Potential Conflicts of Interest

The authors indicate no potential conflicts of interest.

References

1 Hewitt HB. Studies of the dissemination and quantitative transplantation of a lymphocytic leukaemia of CBA mice. Br J Cancer 1958; 12(3):378–401.
2 Southam C, Brunschwig A. Quantitative studies of autotransplantation of human cancer. *Preliminary report*. Cancer 1961;14(5): 971–978.
3 Reya T, Morrison SJ, Clarke MF et al. Stem cells, cancer, and cancer stem cells. Nature 2001;414(6859):105–111.
4 Hill RP, Milas L. The proportion of stem cells in murine tumors. Int J Radiat Oncol Biol Phys 1989;16(2):513–518.
5 Clarke MF, Dick JE, Dirks PB et al. Cancer Stem Cells---Perspectives on Current Status and Future Directions: AACR Workshop on Cancer Stem Cells. Cancer Res 2006;66(19):9339–9344.
6 Lapidot T, Sirard C, Vormoor J et al. A cell initiating human acute myeloid leukaemia after transplantation into SCID mice. Nature 1994;367(6464):645–648.
7 Lane SW, Gilliland DG. Leukemia stem cells. Semin Cancer Biol 2009 [Epub ahead of print].
8 Chao MP, Seita J, Weissman IL. Establishment of a normal hematopoietic and leukemia stem cell hierarchy. Cold Spring Harb Symp Quant Biol 2008;73:439–449.
9 Trott KR. Tumour stem cells: the biological concept and its application in cancer treatment. Radiother Oncol 1994;30(1):1–5.
10 Hill RP. Identifying cancer stem cells in solid tumors: case not proven. Cancer Res 2006;66(4):1891–1895, discussion 1890.
11 Hill RP, Perris R. "Destemming" cancer stem cells. J Natl Cancer Inst 2007;99(19):1435–1440.
12 Park CY, Tseng D, Weissman IL. Cancer stem cell-directed therapies: recent data from the laboratory and clinic. Mol Ther 2009; 17(2):219–230.
13 Quintana E, Shackleton M, Sabel MS et al. Efficient tumour formation by single human melanoma cells. Nature 2008;456(7222):593–598.
14 Kummermehr JC. Tumour stem cells---the evidence and the ambiguity. Acta Oncol 2001;40(8):981–988.
15 Al-Hajj M, Wicha MS, Benito-Hernandez A et al. Prospective identification of tumorigenic breast cancer cells. Proc Natl Acad Sci U S A 2003;100:3983–3988.
16 Schatton T, Murphy GF, Frank NY et al. Identification of cells initiating human melanomas. Nature 2008;451(7176):345–349.
17 Hemmati HD, Nakano I, Lazareff JA et al. Cancerous stem cells can arise from pediatric brain tumors. Proc Natl Acad Sci U S A 2003; 100(25):15178–15183.
18 Phillips TM, Kim K, Vlashi E et al. Effects of recombinant erythropoietin on breast cancer-initiating cells. Neoplasia 2007;9(12): 1122–1129.
19 Phillips TM, McBride WH, Pajonk F. The response of CD24(-/low)/CD44+ breast cancer-initiating cells to radiation. J Natl Cancer Inst 2006;98(24):1777–1785.
20 Woodward WA, Chen MS, Behbod F et al. WNT/beta-catenin mediates radiation resistance of mouse mammary progenitor cells. Proc Natl Acad Sci U S A 2007;104(2):618–623.
21 Singh SK, Clarke ID, Terasaki M et al. Identification of a cancer stem cell in human brain tumors. Cancer Res 2003;63(18): 5821–5828.
22 Singh SK, Hawkins C, Clarke ID et al. Identification of human brain tumour initiating cells. Nature 2004;432(7015):396–401.

23 Collins AT, Berry PA, Hyde C et al. Prospective identification of tumorigenic prostate cancer stem cells. Cancer Res 2005;65(23): 10946–10951.
24 Li C, Heidt DG, Dalerba P et al. Identification of pancreatic cancer stem cells. Cancer Res 2007;67(3):1030–1037.
25 Fang D, Nguyen TK, Leishear K et al. A tumorigenic subpopulation with stem cell properties in melanomas. Cancer Res 2005;65(20): 9328–9337.
26 Prince ME. Identification of a subpopulation of cells with cancer stem cell properties in head and neck squamous cell carcinoma. Proc Natl Acad Sci U S A 2007;104:973–978.
27 Shimono Y, Zabala M, Cho RW et al. Downregulation of miRNA-200c links breast cancer stem cells with normal stem cells. Cell 2009;138(3):592–603.
28 Zhu L, Gibson P, Currle DS et al. Prominin 1 marks intestinal stem cells that are susceptible to neoplastic transformation. Nature 2009; 457(7229):603–607.
29 Barker N, Ridgway RA, van Es JH et al. Crypt stem cells as the cells-of-origin of intestinal cancer. Nature 2009;457(7229):608–611.
30 Pérez-Caro M, Cobaleda C, Gonzalez-Herrero I et al. Cancer induction by restriction of oncogene expression to the stem cell compartment. Embo J 2009;28(1):8–20.
31 Llaguno SA, Chen J, Kwon CH et al. Neural and cancer stem cells in tumor suppressor mouse models of malignant astrocytoma. Cold Spring Harb Symp Quant Biol 2008;73:421–426.
32 Bao S. Glioma stem cells promote radioresistance by preferential activation of the DNA damage response. Nature 2006;444:756–760.
33 Eramo A, Ricci-Vitiani L, Zeuner A et al. Chemotherapy resistance of glioblastoma stem cells. Cell Death Differ 2006;13(7):1238–1241.
34 Chiou SH, Kao CL, Chen YW et al. Identification of CD133-positive radioresistant cells in atypical teratoid/rhabdoid tumor. PLoS One 2008;3(5):e2090.
35 Blazek ER, Foutch JL, Maki G. Daoy medulloblastoma cells that express CD133 are radioresistant relative to CD133- cells, and the CD133+ sector is enlarged by hypoxia. Int J Radiat Oncol Biol Phys 2007;67(1):1–5.
36 Chang CJ, Hsu CC, Yung MC et al. Enhanced radiosensitivity and radiation-induced apoptosis in glioma CD133-positive cells by knockdown of SirT1 expression. Biochem Biophys Res Commun 2009;380(2):236–242.
37 Holtz MS, Forman SJ, Bhatia R. Nonproliferating CML CD34+ progenitors are resistant to apoptosis induced by a wide range of proapoptotic stimuli. Leukemia 2005;19(6):1034–1041.
38 Lu KH, Chen YW, Tsai PH et al. Evaluation of radiotherapy effect in resveratrol-treated medulloblastoma cancer stem-like cells. Childs Nerv Syst 2009;25(5):543–550.
39 Lomonaco SL, Finniss S, Xiang C et al. The induction of autophagy by gamma-radiation contributes to the radioresistance of glioma stem cells. Int J Cancer 2009;125(3):717–722.
40 Fillmore CM, Kuperwasser C. Human breast cancer cell lines contain stem-like cells that self-renew, give rise to phenotypically diverse progeny and survive chemotherapy. Breast Cancer Res 2008;10(2): R25.
41 Diehn M, Cho RW, Lobo NA et al. Association of reactive oxygen species levels and radioresistance in cancer stem cells. Nature 2009; 458(7239):780–783.
42 Vlashi E, Kim K, Dealla DL et al. In-vivo imaging, tracking, and targeting of cancer stem cells. J Natl Cancer Inst 2009;101(5): 350–359.
43 Baumann M, Krause M, Hill R. Exploring the role of cancer stem cells in radioresistance. Nat Rev Cancer 2008;8(7):545–554.
44 Withers HR, ed. The four R's of radiotherapy. New York: Academic Press, 1975. Lett JT AH, ed. Advances in radiation biology; No. 5.
45 Steel GG, McMillan TJ, Peacock JH. The 5Rs of radiobiology. Int J Radiat Biol 1989;56(6):1045–1048.
46 Barker N, van Es JH, Kuipers J et al. Identification of stem cells in small intestine and colon by marker gene Lgr5. Nature 2007; 449(7165):1003–1007.
47 Mitchell JB, Russo A. The role of glutathione in radiation and drug induced cytotoxicity. Br J Cancer 1987;8:96–104.
48 Jang YY, Sharkis SJ. A low level of reactive oxygen species selects for primitive hematopoietic stem cells that may reside in the low-oxygenic niche. Blood 2007;110(8):3056–3063.
49 Olive PL. Detection of DNA damage in individual cells by analysis of histone H2AX phosphorylation. Methods Cell Biol 2004;75: 355–373.
50 Diehn M, Clarke MF. Cancer stem cells and radiotherapy: new insights into tumor radioresistance. J Natl Cancer Inst 2006;98(24): 1755–1757.
51 Ropolo M, Daga A, Griffero F et al. Comparative analysis of DNA repair in stem and nonstem glioma cell cultures. Mol Cancer Res 2009;7(3):383–392.
52 McCord AM, Jamal M, Williams ES et al. CD133+ glioblastoma stem-like cells are radiosensitive with a defective DNA damage response compared with established cell lines. Clin Cancer Res 2009;15(16):5145–5153.
53 Al-Assar O, Muschel RJ, Mantoni TS et al. Radiation response of cancer stem-like cells from established human cell lines after sorting for surface markers. Int J Radiat Oncol Biol Phys 2009;75(4): 1216–1225.
54 Alexander CM, Puchalski J, Klos KS et al. Separating stem cells by flow cytometry: reducing variability for solid tissues. Cell Stem Cell 2009;5(6):579–583.
55 Griguer CE, Oliva CR, Gobin E et al. CD133 is a marker of bioenergetic stress in human glioma. PLoS One 2008;3(11):e3655.
56 Clément V, Dutoit V, Marino D et al. Limits of CD133 as a marker of glioma self-renewing cells. Int J Cancer 2009;125(1):244–248.
57 Wang J, Sakariassen PO, Tsinkalovsky O et al. CD133 negative glioma cells form tumors in nude rats and give rise to CD133 positive cells. Int J Cancer 2008;122(4):761–768.
58 Sun Y, Kong W, Falk A et al. CD133 (Prominin) negative human neural stem cells are clonogenic and tripotent. PLoS One 2009;4(5): e5498.
59 Heideker J, Lis ET, Romesberg FE. Phosphatases, DNA damage checkpoints and checkpoint deactivation. Cell Cycle 2007;6(24): 3058–3064.
60 Wang H, Hu B, Liu R et al. CHK1 affecting cell radiosensitivity is independent of non-homologous end joining. Cell Cycle 2005;4(2): 300–303.
61 Wu Y, Kantake N, Sugiyama T et al. Rad51 protein controls Rad52-mediated DNA annealing. J Biol Chem 2008;283(21):14883–14892.
62 Charafe-Jauffret E, Ginestier C, Iovino F et al. Breast cancer cell lines contain functional cancer stem cells with metastatic capacity and a distinct molecular signature. Cancer Res 2009;69(4): 1302–1313.
63 Iwasa T, Okamoto I, Suzuki M et al. Radiosensitizing effect of YM155, a novel small-molecule survivin suppressant, in non-small cell lung cancer cell lines. Clin Cancer Res 2008;14(20):6496–6504.
64 Chakravarti A, Zhai GG, Zhang M et al. Survivin enhances radiation resistance in primary human glioblastoma cells via caspase-independent mechanisms. Oncogene 2004;23(45):7494–7506.
65 Rödel F, Hoffmann J, Distel L et al. Survivin as a radioresistance factor, and prognostic and therapeutic target for radiotherapy in rectal cancer. Cancer Res 2005;65(11):4881–4887.
66 Rödel F, Frey B, Leitmann W et al. Survivin antisense oligonucleotides effectively radiosensitize colorectal cancer cells in both tissue culture and murine xenograft models. Int J Radiat Oncol Biol Phys 2008;71(1):247–255.
67 Pawlik TM, Keyomarsi K. Role of cell cycle in mediating sensitivity to radiotherapy. Int J Radiat Oncol Biol Phys 2004;59(4):928–942.
68 Withers HR. Cell cycle redistribution as a factor in multifraction irradiation. Radiology 1975;114(1):199–202.
69 Arai F, Hirao A, Ohmura M et al. Tie2/angiopoietin-1 signaling regulates hematopoietic stem cell quiescence in the bone marrow niche. Cell 2004;118(2):149–161.
70 Wilson A, Laurenti E, Oser G et al. Hematopoietic stem cells reversibly switch from dormancy to self-renewal during homeostasis and repair. Cell 2008;135(6):1118–1129.
71 Wu M, Kwon HY, Rattis F et al. Imaging hematopoietic precursor division in real time. Cell Stem Cell 2007;1(5):541–554.
72 Korkaya H, Wicha MS. HER-2, notch, and breast cancer stem cells: targeting an axis of evil. Clin Cancer Res 2009;15(6):1845–1847.
73 Hoey T, Yen WC, Axelrod F et al. DLL4 blockade inhibits tumor growth and reduces tumor-initiating cell frequency. Cell Stem Cell 2009;5(2):168–177.
74 Calabrese C, Poppleton H, Kocak M et al. A perivascular niche for brain tumor stem cells. Cancer Cell 2007;11(1):69–82.
75 Withers HR, Maciejewski B, Taylor JM et al. Accelerated repopulation in head and neck cancer. Front Radiat Ther Oncol 1988;22: 105–110.
76 Bese NS, Sut PA, Ober A. The effect of treatment interruptions in the postoperative irradiation of breast cancer. Oncology 2005;69(3): 214–223.
77 Suwinski R, Sowa A, Rutkowski T et al. Time factor in postoperative radiotherapy: a multivariate locoregional control analysis in 868 patients. Int J Radiat Oncol Biol Phys 2003;56(2):399–412.
78 Maciejewski BA, Skates S, Zajusz A et al. Importance of tumor size and repopulation for radiocurability of skin cancer. Neoplasma 1993; 40(1):51–54.
79 Bisson I, Prowse DM. WNT signaling regulates self-renewal and differentiation of prostate cancer cells with stem cell characteristics. Cell Res 2009;19(6):683–697.
80 Xu Q, Yuan X, Liu G et al. Hedgehog signalingregulates brain tumor-initiating cell proliferation and portends shorter survival for

patients with PTEN-coexpressing glioblastomas. Stem Cells 2008; 26(12):3018–3026.
81 Scharpfenecker M, Kruse JJ, Sprong D et al. Ionizing radiation shifts the PAI-1/ID-1 balance and activates notch signaling in endothelial cells. Int J Radiat Oncol Biol Phys 2009;73(2):506–513.
82 Weinmaster G, Kopan R. A garden of Notch-ly delights. Development 2006;133(17):3277–3282.
83 Campa VM, Gutierrez-Lanza R, Cerignoli F et al. Notch activates cell cycle reentry and progression in quiescent cardiomyocytes. J Cell Biol 2008;183(1):129–141.
84 Ehrhart EJ, Segarini P, Tsang ML et al. Latent transforming growth factor beta1 activation in situ: quantitative and functional evidence after low-dose gamma-irradiation. FASEB J 1997;11(12):991–1002.
85 Barcellos-Hoff MH, Derynck R, Tsang ML et al. Transforming growth factor-beta activation in irradiated murine mammary gland. J Clin Invest 1994;93(2):892–899.
86 Barcellos-Hoff MH, Dix TA. Redox-mediated activation of latent transforming growth factor-beta 1. Mol Endocrinol 1996;10(9): 1077–1083.
87 Tian M, Schiemann WP. The TGF-beta paradox in human cancer: an update. Future Oncol 2009;5(2):259–271.
88 Itoh F, Itoh S, Goumans MJ et al. Synergy and antagonism between Notch and BMP receptor signaling pathways in endothelial cells. EMBO J 2004;23(3):541–551.
89 Masuda S, Kumano K, Shimizu K et al. Notch1 oncoprotein antagonizes TGF-beta/Smad-mediated cell growth suppression via sequestration of coactivator p300. Cancer Sci 2005;96(5):274–282.
90 Withers HR, Peters LJ, Taylor JM et al. Local control of carcinoma of the tonsil by radiation therapy: an analysis of patterns of fractionation in nine institutions. Int J Radiat Oncol Biol Phys 1995;33(3): 549–562.
91 Rizzo P, Osipo C, Foreman K et al. Rational targeting of Notch signaling in cancer. Oncogene 2008;27(38):5124–5131.
92 van Es JH, van Gijn ME, Riccio O et al. Notch/gamma-secretase inhibition turns proliferative cells in intestinal crypts and adenomas into goblet cells. Nature 2005;435(7044):959–963.
93 Farnie G, Clarke RB. Mammary stem cells and breast cancer–role of Notch signalling. Stem Cell Rev 2007;3(2):169–175.
94 Schwarz G. Ueber Desensibilisierung gegen Roentgen und Radium Strahlen. Muenchner Medizinische Wochenschrift 1909(24):1–2.
95 Holthusen H. Beiträge zur Biologie der Strahlenwirkung. Pflüger's Arch Ges Physiol 1921;187:1–24.
96 Thomlinson RH, Gray LH. The histological structure of some human lung cancers and the possible implications for radiotherapy. Br J Cancer 1955;9:539–549.
97 Hockel M, Schlenger K, Aral B et al. Association between tumor hypoxia and malignant progression in advanced cancer of the uterine cervix. Cancer Res 1996;56(19):4509–4515.
98 Brizel DM, Scully SP, Harrelson JM et al. Tumor oxygenation predicts for the likelihood of distant metastases in human soft tissue sarcoma. Cancer Res 1996;56(5):941–943.
99 Brizel DM, Sibley GS, Prosnitz LR et al. Tumor hypoxia adversely affects the prognosis of carcinoma of the head and neck. Int J Radiat Oncol Biol Phys 1997;38(2):285–289.
100 Fyles A, Milosevic M, Hedley D et al. Tumor hypoxia has independent predictor impact only in patients with node-negative cervix cancer. J Clin Oncol 2002;20(3):680–687.
101 Nordsmark M, Bentzen SM, Rudat V et al. Prognostic value of tumor oxygenation in 397 head and neck tumors after primary radiation therapy. An international multi-center study. Radiother Oncol 2005;77(1):18–24.
102 Bertout JA, Patel SA, Simon MC. The impact of O2 availability on human cancer. Nat Rev Cancer 2008;8(12):967–975.
103 Bristow RG, Hill RP. Hypoxia and metabolism. Hypoxia, DNA repair and genetic instability. Nat Rev Cancer 2008;8(3):180–192.
104 Zölzer F, Streffer C. Increased radiosensitivity with chronic hypoxia in four human tumor cell lines. Int J Radiat Oncol Biol Phys 2002; 54(3):910–920.
105 Chan N, Koritzinsky M, Zhao H et al. Chronic hypoxia decreases synthesis of homologous recombination proteins to offset chemoresistance and radioresistance. Cancer Res 2008;68(2):605–614.
106 Sundfor K, Lyng H, Rofstad EK. Tumour hypoxia and vascular density as predictors of metastasis in squamous cell carcinoma of the uterine cervix. Br J Cancer 1998;78(6):822–827.
107 Garcia-Barros M, Paris F, Cordon-Cardo C et al. Tumor response to radiotherapy regulated by endothelial cell apoptosis. Science 2003; 300(5622):1155–1159.
108 Seiwert TY, Cohen EE. Targeting angiogenesis in head and neck cancer. Semin Oncol 2008;35(3):274–285.
109 Fukumura D, Jain RK. Tumor microenvironment abnormalities: causes, consequences, and strategies to normalize. J Cell Biochem 2007;101(4):937–949.
110 Wu J, Long Q, Xu S et al. Study of tumor blood perfusion and its variation due to vascular normalization by anti-angiogenic therapy based on 3D angiogenic microvasculature. J Biomech 2009;42(6):712–721.
111 Batchelor TT, Sorensen AG, di Tomaso E et al. AZD2171, a pan-VEGF receptor tyrosine kinase inhibitor, normalizes tumor vasculature and alleviates edema in glioblastoma patients. Cancer Cell 2007; 11(1):83–95.
112 Chen FH, Chiang CS, Wang CC et al. Radiotherapy decreases vascular density and causes hypoxia with macrophage aggregation in TRAMP-C1 prostate tumors. Clin Cancer Res 2009;15(5):1721–1729.
113 Eriksen JG, Overgaard J. Lack of prognostic and predictive value of CA IX in radiotherapy of squamous cell carcinoma of the head and neck with known modifiable hypoxia: an evaluation of the DAHANCA 5 study. Radiother Oncol 2007;83(3):383–388.
114 Henke M, Mattern D, Pepe M et al. Do erythropoietin receptors on cancer cells explain unexpected clinical findings? J Clin Oncol 2006; 24(29):4708–4713.
115 Henke M, Laszig R, Rübe C et al. Erythropoeitin to treat head and neck cancer patients with anaemia undergoing radiotherapy: randomised, double-blind, placebo-controlled trial. The Lancet 2003;262: 1255–1260.
116 Wright JR, Ung YC, Julian JA et al. Randomized, double-blind, placebo-controlled trial of erythropoietin in non-small-cell lung cancer with disease-related anemia. J Clin Oncol 2007;25(9):1027–1032.
117 Belenkov AI, Shenouda G, Rizhevskaya E et al. Erythropoietin induces cancer cell resistance to ionizing radiation and to cisplatin. Mol Cancer Ther 2004;3(12):1525–1532.
118 Pajonk F, Weil A, Sommer A et al. The erythropoietin-receptor pathway modulates survival of cancer cells. Oncogene 2004;23(55): 8987–8991.
119 Stüben G, Pottgen C, Knuhmann K et al. Erythropoietin restores the anemia-induced reduction in radiosensitivity of experimental human tumors in nude mice. Int J Radiat Oncol Biol Phys 2003;55(5): 1358–1362.
120 Thews O, Koenig R, Kelleher DK et al. Enhanced radiosensitivity in experimental tumours following erythropoietin treatment of chemotherapy-induced anaemia. Br J Cancer 1998;78(6):752–756.
121 Santucci MA, Pierce JH, Zannini S et al. Erythropoietin increases the radioresistance of a clonal hematopoietic progenitor cell line expressing a transgene for the erythropoietin receptor. Stem Cells 1994;12(5):506–513.
122 Joiner B, Hirst VK, McKeown SR et al. The effect of recombinant human erythropoietin treatment on tumour radiosensitivity and cancer-associated anaemia in the mouse. Br J Cancer 1993;68(4): 720–726.
123 Warburg O, Posener K, Negelein E. Ueber den Stoffwechsel der Tumoren. Biochem Z 1924;152:319–344.
124 DeBerardinis RJ, Lum JJ, Hatzivassiliou G et al. The biology of cancer: metabolic reprogramming fuels cell growth and proliferation. Cell Metab 2008;7(1):11–20.
125 Li S, Li D. Stem cell and kinase activity-independent pathway in resistance of leukaemia to BCR-ABL kinase inhibitors. J Cell Mol Med 2007;11(6):1251–1262.

PROSPECT
Journal of Cellular Biochemistry 108:339–342 (2009)

Journal of Cellular Biochemistry

Radiation Responses of Cancer Stem Cells

Erina Vlashi,[1] William H. McBride,[1,2] and Frank Pajonk[1,2]*

[1] *Division of Molecular and Cellular Oncology, Department of Radiation Oncology, David Geffen School of Medicine at UCLA, Los Angeles, California*

[2] *Jonsson Comprehensive Cancer Center at UCLA, Los Angeles, California*

ABSTRACT

Recent experimental evidence indicates that many solid cancers have a hierarchical organization structure with a subpopulation of cancer stem cells (CSCs). The ability to identify CSCs prospectively now allows for testing the responses of CSCs to treatment modalities like radiation therapy. Initial studies have found CSCs in glioma and breast cancer relatively resistant to ionizing radiation and possible mechanisms behind this resistance have been explored. This review summarizes the landmark publications in this young field with an emphasis on the radiation responses of CSCs. The existence of CSCs in solid cancers place restrictions on the interpretation of many radiobiological observations, while explaining others. The fact that these cells may be a relatively quiescent subpopulation that are metabolically distinct from the other cells in the tumor has implications for both imaging and therapy of cancer. This is particularly true for biological targeting of cancer for enhanced radiotherapeutic benefit, which must consider whether the unique properties of this subpopulation allow it to avoid such therapies. J. Cell. Biochem. 108: 339–342, 2009.

KEY WORDS: CANCER STEM CELLS; CANCER INITIATING CELLS; RADIATION BIOLOGY

INTRODUCTION

Cancer cells in solid carcinomas display considerable heterogeneity in many aspects of their malignant phenotype and a single tumor can harbor cells with a wide range of radiosensitivity [Suwinski et al., 1999] and tumorgenicity [Hill and Milas, 1989]. One possible interpretation of this observation is that, like normal tissues, malignant tumors are organized hierarchically and contain a relatively rare and radioresistant subpopulation of cells that have an increased ability to initiate tumor growth and display accelerated regrowth after a sublethal treatment [Reya et al., 2001]. In a consensus publication that prospectively identified cells with increased tumorgenicity, this subpopulation was termed "Cancer Stem Cells" (CSCs) [Clarke et al., 2006].

This concept of CSCs has been and still is being rejected by some radiobiologists [Hill, 2006; Hill and Perris, 2007] because for some time the existence of such a CSC subpopulation could only be demonstrated retrospectively using a functional test, which left room for the interpretation that every cell in a tumor could gain a CSC phenotype if it had enough time. However, recent technical progress supports the presence of a hierarchical organization for breast cancer [Al-Hajj et al., 2003], brain tumors [Hemmati et al., 2003; Singh et al., 2003], prostate cancer [Collins et al., 2005], colon cancer [Ricci-Vitiani et al., 2007], head and neck cancer [Prince, 2007], lung cancer [Eramo et al., 2007], and melanoma [Schatton et al., 2008], which seems to replicate the hierarchical organization of the corresponding normal tissue of origin.

This review will summarize current data describing the radiation response of CSCs.

THE ORIGIN OF CANCER STEM CELLS

Normal tissue stem cells are defined by their ability to self-renew and their multi-lineage potency. Together with increased tumorgenicity the same features define CSCs [Clarke et al., 2006]. This definition led to considerable confusion as it was inferred that normal stem cells were the origin of CSCs. Even without data on the origin of CSCs, this controversy over semantics is despite the point. The reality is that a subpopulation of cancer cells exist that can be identified prospectively, that have characteristics of "stemness," and

Grant sponsor: California Breast Cancer Research Program; Grant number: BC060077; Grant sponsor: Department of Defense; Grant number: PC060599; Grant sponsor: Biomedical Advance Research and Development Authority; Grant number: 1 RC1A1081287.

*Correspondence to: Frank Pajonk, Division of Molecular and Cellular Oncology, Department of Radiation Oncology, David Geffen School of Medicine at UCLA, 10833 Le Conte Ave., Los Angeles, CA 90095-1714.
E-mail: fpajonk@mednet.ucla.edu

Received 9 June 2009; Accepted 11 June 2009 • DOI 10.1002/jcb.22275 • © 2009 Wiley-Liss, Inc.
Published online 21 July 2009 in Wiley InterScience (www.interscience.wiley.com).

that are important if we want to improve cancer treatment. The field should acknowledge their importance and study them rather than fighting over terminology [Jordan, 2009].

Four recent publications addressed the origin of CSCs using elegant mouse models. Reports from two independent groups reported that oncogene expression in intestinal stem cells but not in committed progenitor or differentiated cells led to the formation of intestinal tumors [Barker et al., 2009; Zhu et al., 2009]. Comparable results were reported for neuronal stem cells. Only oncogene expression in cells of the subventricular zone caused astrocytomas to form [Alcantara Llaguno et al., 2009]. Additionally, Perez-Caro et al. [2009] demonstrated that bcr-abl oncogene expression in sca-1-positive bone marrow cells was sufficient to induce leukemia and that elimination of CSCs cured the disease while STI571 application did not alter its course. These reports indicated that at least in murine tumor models CSCs arise from normal tissue stem cells. It remains to be shown if this is also the case for human cancers.

IDENTIFICATION AND PROPAGATION OF CANCER STEM CELL

Assays to propagate stem cells and precursor cells developed in the neural stem cell field [Smukler et al., 2006] and were essential for the development of ways to propagate CSCs and identify them phenotypically. If performed accurately [Singec et al., 2006], when tumor cells are seeded at clonal densities of $<$1,000 cells/ml in serum-free conditions only CSCs and early progenitor cells survive and form non-adherent spheres cultures, consisting of up to a few hundred cells. Addition of a limited number of growth factors, mainly bFGF and EGF, stimulates growth and helps maintaining the stem cell phenotype. These conditions are clearly distinct from spheroids that had previously been commonly grown. These were cultured in the presence of serum, usually consisted of thousands of cells, and with no effort to make them clonal. Interestingly, spheroids were often appeared to be a better model of tumors than were monolayer cultures, which could be because of enrichment for CSCs in the spheroid central region. Reinvestigation of spheroids with an emphasis on CSC content might give a better understanding of radiobiological data obtained with these systems in the past.

Initially, CSCs were prospectively identified using combinations of antibodies against cell surface proteins. In a landmark publication, Al-Hajj et al. [2003] identified a subset of $CD24^{-/low}/CD44^{high}/ESA^{+}$ cells from hormone receptor-positive breast cancer specimens that exhibited increased tumorgenicity and multi-lineage potency. These cells were enriched if cells were cultured as mammospheres. A breast CSC population was also found in murine breast cancer models. However, in this case the cells were defined by a CD29+/CD49+ expression profile, which was also later used to identify normal mammary stem cells in mice. Interestingly, $CD24^{-/low}/CD44^{high}/ESA^{+}$ cells seem to be the earliest cells found in breast cancer metastases suggesting that these cells initiate metastatic disease, although the number of $CD24^{-/low}/CD44^{high}/ESA^{+}$ cells in the primary tumor section did not predict for outcome in another study. However, using the gene expression profile of $CD24^{-/low}/CD44^{high}/ESA^{+}$ cells, Michael Clarke's group defined a gene expression signature that was highly predictive for clinical outcome indicating the clinical significance of breast CSCs [Cho et al., 2008].

More recently Gabriela Dontu's laboratory reported expression and activity of aldehyde dehydroxygenase 1 (ALDH1), an enzyme already known to be overexpressed in hematopoietic stem cells, as an even better marker for breast CSCs. In this study, $ALDH1^{+}$ breast CSCs partially overlapped with $CD24^{-/low}/CD44^{high}/ESA^{+}$ cells in human breast cancers, indicating heterogeneity of $CD24^{-/low}/CD44^{high}/ESA^{+}$ cells [Ginestier et al., 2007].

Two publications, one from the laboratory of Harley Kornblum [Hemmati et al., 2003] and a second by Singh et al. [2003] reported comparable data for a subset of $CD133^{+}$ cells in brain tumors. In both cases, this subpopulation not only exhibited increased tumorgenicity but the xenografts also reassembled the histopathological phenotype of the original tumor. In an additional study, the presence of high numbers of CD133+ cells in gliomas was shown to be a valuable predictor of clinical outcome [Pallini et al., 2008].

Since 2003, several groups have identified CSCs in a variety of solid carcinomas (Table I). However, all require dissociation of the tumor to identify CSCs by marker expression and were thus not suitable for in vivo investigations. The first study addressing this problem expressed GFP under the control of the regulatory elements of BMI-1 [Hosen et al., 2007]. BMI-1 is a E3-ubiquitin ligase, which is upregulated in some normal tissue stem cells and CSCs. BMI-1 itself is degraded by the 26S proteasome [Cao et al., 2005]. More recently, we reported that CSCs in breast cancers and gliomas have low proteasome activity and we utilized this feature to identify, track, and target CSCs in vivo [Vlashi et al., 2009]. Using this system we were able to show that, as in leukemia [Perez-Caro et al., 2009], elimination of CSCs was sufficient to cause regression of solid cancers [Vlashi et al., 2009]. This system provides a unique opportunity to investigate the effect of cancer therapies on CSCs in vitro and in vivo.

TABLE I. Surface Markers of Solid Cancer Stem Cells

Tumor type	Stem cell marker	Refs.
Breast cancer	$CD44^{high}/CD24^{-/low}/lineage^{-}$	Al-Hajj et al. [2003]
Brain tumors	$CD133^{+}$	Hemmati et al. [2003], Singh et al. [2003]
Prostate cancer	$CD44^{+}/\alpha_2\beta_1^{high}/CD133^{+}$	Collins et al. [2005]
HNSCC	$CD44^{+}$	Prince et al. [2007]
Colon cancer	$CD133^{+}$	Ricci-Vitiani et al. [2007]
Lung cancer	$CD133^{+}$	Eramo et al. [2007]
Pancreatic cancer	$CD44^{+}/CD24^{+}/ESA^{+}$	Li et al. [2007]
Melanoma	$ABCB5^{+}$	Schatton et al. [2008]

RADIATION RESPONSES OF CANCER STEM CELLS

Currently, localized solid cancers can only be cured by surgery or radiation treatment and solid tumors that have metastasized are by definition incurable. If tumor growth and regrowth after therapy is a property of CSCs, the response of these cells to radiation is a critical parameter for curability. Again, the first studies addressing the radiation response of CSCs were performed in glioma and breast cancer. Bao and coworkers reported radiation resistance of CD133+ cells in glioma. This resistance was attributed to constitutive activation of the DNA repair checkpoint and inhibition of the corresponding kinase radiosensitized CD133+ cells [Bao, 2006]. We reported radioresistance of breast CSCs but, contrary to glioma, CSCs breast CSCs produced less reactive oxygen species in response to radiation indicating a high level of expression of free-radical scavengers [Phillips et al., 2006].

Since then, radiation resistance of CSCs has been confirmed by several independent groups [Woodward et al., 2007; Chiou et al., 2008; Hambardzumyan et al., 2008; Diehn et al., 2009; Lu et al., 2009; Chang et al., 2009]. Interestingly, survival curves of CSCs isolated from the MCF-7 breast cancer lines showed a clear shoulder. While this could be interpreted as enhanced DNA repair, they failed to phosphorylate H2AX in response radiation suggesting diminished damage or alternative mechanisms might operate [Phillips et al., 2006]. Our data on breast CSCS was confirmed by Diehn et al. [2009] who were able to show a strong radical scavenger gene expression signature using single cell RT-PCR. Interestingly, radiation activated the Notch signaling pathways in breast CSCs in a PI3K-dependent fashion through upregulation of Notch receptor ligands. This pathway is involved in stem cell maintenance in breast cancer and its activation by radiation increased the number of CSCs [Phillips et al., 2006]. Activation of the Notch pathway by radiation was recently confirmed in endothelial cells [Scharpfenecker et al., 2009] indicating that this pathway may contribute to the radiation response of normal and malignant tissues.

Oxygen has long been known to be one of the most potent radiosensitizing agents. Tumors contain areas of low oxygen tension and cells residing in these areas were considered to be relatively protected from radiation. Consequently, considerable effort has been made to overcome tumor hypoxia to improve radiation treatment results. Surprisingly, CSCs were reported to reside in a perivascular niche [Calabrese et al., 2007; Vlashi et al., 2009] and are therefore unlikely to be protected from radiation by hypoxia. However, this observation offers an attractive explanation for the efficiency of anti-angiogenic therapies combined with radiation as they may target the CSC niche rather than tumor cells in general. Anti-angiogenesis combined with radiation, as a concept, is counterintuitive because one would expect the proportion of hypoxic cells and hence radioresistance to increase under such a treatment. However, it supports the importance killing CSCs over the bulk of the tumor because the effects of anti-angiogenic therapies on the CSC niche seem to render therapy-induced tumor hypoxia irrelevant. Those in the radiation field have of course always known that partial responses to therapy are relatively meaningless in terms of patient outcome and that what is most important is killing the last surviving tumor clonogen, which may now be termed a CSC.

CONCLUDING REMARKS

Over the last 114 years, radiation therapy techniques have evolved to a degree of precision that far exceeds the need in most daily standard cancer treatments. At the same time, progress in cancer cure has advanced at a much slower pace and for many cancers like glioma, pancreatic cancer, and lung cancer the success rate of state-of-the-art treatments is still unacceptable and has remained unchanged for decades. This indicates that the cost of future improvements in the technical aspects of radiation delivery is unlikely to be justified by improved treatment outcomes and that cure, for example, of a glioma patient will only occur if we radically change the way we approach the disease.

The existence of CSCs in solid cancer has been advocated by radiobiologists for decades [Withers et al., 1988; Trott, 1994]. However, until recently this concept was only hypothetical. Novel marker signatures and culture systems now allow the unique features of CSCs to be studied and novel therapies tested for their efficiency in killing these cells. The fact that radiation cures cancer patients already implies that this therapy modality is effective against CSCs. Unlike many chemotherapeutic treatments for which anti-cancer efficacy is judged only by temporary partial tumor responses that may not involve CSCs, radiation therapy can undergo biological refinement by combination with agents that increase its efficacy against this critically important CSC subpopulation. Thus, targeting CSCs with radiation holds enormous potential for eventual cure for many of our cancer patients and it should encourage opponents of the CSC concept to stop fighting over terminology and to return to the bedsides and benches.

ACKNOWLEDGMENTS

This work was supported in part by a grant from the California Breast Cancer Research Program (BC060077) and the Department of Defense (PC060599) to F.P. and a by a grant from the Biomedical Advance Research and Development Authority (1 RC1A1081287) to W.H.M.

REFERENCES

Alcantara Llaguno S, Chen J, Kwon CH, Jackson EL, Li Y, Burns DK, Alvarez-Buylla A, Parada LF. 2009. Malignant astrocytomas originate from neural stem/progenitor cells in a somatic tumor suppressor mouse model. Cancer Cell 15:45–56.

Al-Hajj M, Wicha MS, Benito-Hernandez A, Morrison SJ, Clarke MF. 2003. Prospective identification of tumorigenic breast cancer cells. Proc Natl Acad Sci USA 100:3983–3988.

Bao S. 2006. Glioma stem cells promote radioresistance by preferential activation of the DNA damage response. Nature 444:756–760.

Barker N, Ridgway RA, van Es JH, van de Wetering M, Begthel H, van den Born M, Danenberg E, Clarke AR, Sansom OJ, Clevers H. 2009. Crypt stem cells as the cells-of-origin of intestinal cancer. Nature 457:608–611.

Calabrese C, Poppleton H, Kocak M, Hogg TL, Fuller C, Hamner B, Oh EY, Gaber MW, Finklestein D, Allen M, Frank A, Bayazitov IT, Zakharenko SS, Gajjar A, Davidoff A, Gilbertson RJ. 2007. A perivascular niche for brain tumor stem cells. Cancer Cell 11:69–82.

Cao R, Tsukada Y, Zhang Y. 2005. Role of Bmi-1 and Ring1A in H2A ubiquitylation and Hox gene silencing. Mol Cell 20:845–854.

Chang CJ, Hsu CC, Yung MC, Chen KY, Tzao C, Wu WF, Chou HY, Lee YY, Lu KH, Chiou SH, Ma HI. 2009. Enhanced radiosensitivity and radiation-induced apoptosis in glioma CD133-positive cells by knockdown of SirT1 expression. Biochem Biophys Res Commun 380:236–242.

Chiou SH, Kao CL, Chen YW, Chien CS, Hung SC, Lo JF, Chen YJ, Ku HH, Hsu MT, Wong TT. 2008. Identification of CD133-positive radioresistant cells in atypical teratoid/rhabdoid tumor. PLoS ONE 3:2090.

Cho RW, Wang X, Diehn M, Shedden K, Chen GY, Sherlock G, Gurney A, Lewicki J, Clarke MF. 2008. Isolation and molecular characterization of cancer stem cells in MMTV-Wnt-1 murine breast tumors. Stem Cells 26:364–371.

Clarke MF, Dick JE, Dirks PB, Eaves CJ, Jamieson CH, Jones DL, Visvader J, Weissman IL, Wahl GM. 2006. Cancer stem cells—Perspectives on current status and future directions: AACR Workshop on Cancer Stem Cells. Cancer Res 66:9339–44.

Collins AT, Berry PA, Hyde C, Stower MJ, Maitland NJ. 2005. Prospective identification of tumorigenic prostate cancer stem cells. Cancer Res 65:10946–10951.

Diehn M, Cho RW, Lobo NA, Kalisky T, Dorie MJ, Kulp AN, Qian D, Lam JS, Ailles LE, Wong M, Joshua B, Kaplan MJ, Wapnir I, Dirbas F, Somlo G, Garberoglio C, Paz B, Shen J, Lau SK, Quake SR, Brown JM, Weissman IL, Clarke MF. 2009. Association of reactive oxygen species levels and radioresistance in cancer stem cells. Nature 458:780–783.

Eramo A, Lotti F, Sette G, Pilozzi E, Biffoni M, Di Virgilio A, Conticello C, Ruco L, Peschle C, De Maria R. 2007. Identification and expansion of the tumorigenic lung cancer stem cell population. Cell Death Differ 15:504–514.

Ginestier C, Hur MH, Charafe-Jauffret E, Monville F, Dutcher J, Brown M, Jacquemier J, Viens P, Kleer CG, Liu S, Schott A, Hayes D, Birnbaum D, Wicha MS, Dontu G. 2007. ALDH1 is a marker of normal and malignant human mammary stem cells and a predictor of poor clinical outcome. Cell Stem Cell 1:555–567.

Hambardzumyan D, Becher OJ, Rosenblum MK, Pandolfi PP, Manova-Todorova K, Holland EC. 2008. PI3K pathway regulates survival of cancer stem cells residing in the perivascular niche following radiation in medulloblastoma in vivo. Genes Dev 22:436–448.

Hemmati HD, Nakano I, Lazareff JA, Masterman-Smith M, Geschwind DH, Bronner-Fraser M, Kornblum HI. 2003. Cancerous stem cells can arise from pediatric brain tumors. Proc Natl Acad Sci USA 100:15178–15183.

Hill RP. 2006. Identifying cancer stem cells in solid tumors: Case not proven. Cancer Res 66:1891–1895; discussion 1890.

Hill RP, Milas L. 1989. The proportion of stem cells in murine tumors. Int J Radiat Oncol Biol Phys 16:513–5138.

Hill RP, Perris R. 2007. ''Destemming'' cancer stem cells. J Natl Cancer Inst 99:1435–1440.

Hosen N, Yamane T, Muijtjens M, Pham K, Clarke MF, Weissman IL. 2007. Bmi-1-green fluorescent protein-knock-in mice reveal the dynamic regulation of bmi-1 expression in normal and leukemic hematopoietic cells. Stem Cells 25:1635–1644.

Jordan CT. 2009. Cancer stem cells: Controversial or just misunderstood? Cell Stem Cell 4:203–205.

Li C, Heidt DG, Dalerba P, Burant CF, Zhang L, Adsay V, Wicha M, Clarke MF, Simeone DM. 2007. Identification of pancreatic cancer stem cells. Cancer Res 67:1030–1037.

Lu KH, Chen YW, Tsai PH, Tsai ML, Lee YY, Chiang CY, Kao CL, Chiou SH, Ku HH, Lin CH, Chen YJ. 2009. Evaluation of radiotherapy effect in resveratrol-treated medulloblastoma cancer stem-like cells. Childs Nerv Syst 25:543–550.

Pallini R, Ricci-Vitiani L, Banna GL, Signore M, Lombardi D, Todaro M, Stassi G, Martini M, Maira G, Larocca LM, De Maria R. 2008. Cancer stem cell analysis and clinical outcome in patients with glioblastoma multiforme. Clin Cancer Res 14:8205–8212.

Perez-Caro M, Cobaleda C, Gonzalez-Herrero I, Vicente-Duenas C, Bermejo-Rodriguez C, Sanchez-Beato M, Orfao A, Pintado B, Flores T, Sanchez-Martin M, Jimenez R, Piris MA, Sanchez-Garcia I. 2009. Cancer induction by restriction of oncogene expression to the stem cell compartment. EMBO J 28:8–20.

Phillips TM, McBride WH, Pajonk F. 2006. The response of CD24(−/low)/CD44+ breast cancer-initiating cells to radiation. J Natl Cancer Inst 98:1777–1785.

Prince ME. 2007. Identification of a subpopulation of cells with cancer stem cell properties in head and neck squamous cell carcinoma. Proc Natl Acad Sci USA 104:973–978.

Prince ME, Sivanandan R, Kaczorowski A, Wolf GT, Kaplan MJ, Dalerba P, Weissman IL, Clarke MF, Ailles LE. 2007. Identification of a subpopulation of cells with cancer stem cell properties in head and neck squamous cell carcinoma. Proc Natl Acad Sci USA 104:973–978.

Reya T, Morrison SJ, Clarke MF, Weissman IL. 2001. Stem cells, cancer, and cancer stem cells. Nature 414:105–111.

Ricci-Vitiani L, Lombardi DG, Pilozzi E, Biffoni M, Todaro M, Peschle C, De Maria R. 2007. Identification and expansion of human colon-cancer-initiating cells. Nature 445:111–115.

Scharpfenecker M, Kruse JJ, Sprong D, Russell NS, Ten Dijke P, Stewart FA. 2009. Ionizing radiation shifts the PAI-1/ID-1 balance and activates notch signaling in endothelial cells. Int J Radiat Oncol Biol Phys 73:506–513.

Schatton T, Murphy GF, Frank NY, Yamaura K, Waaga-Gasser AM, Gasser M, Zhan Q, Jordan S, Duncan LM, Weishaupt C, Fuhlbrigge RC, Kupper TS, Sayegh MH, Frank MH. 2008. Identification of cells initiating human melanomas. Nature 451:345–349.

Singec I, Knoth R, Meyer RP, Maciaczyk J, Volk B, Nikkhah G, Frotscher M, Snyder EY. 2006. Defining the actual sensitivity and specificity of the neurosphere assay in stem cell biology. Nat Methods 3:801–806.

Singh SK, Clarke ID, Terasaki M, Bonn VE, Hawkins C, Squire J, Dirks PB. 2003. Identification of a cancer stem cell in human brain tumors. Cancer Res 63:5821–5828.

Smukler SR, Runciman SB, Xu S, van der Kooy D. 2006. Embryonic stem cells assume a primitive neural stem cell fate in the absence of extrinsic influences. J Cell Biol 172:79–90.

Suwinski R, Taylor JM, Withers HR. 1999. The effect of heterogeneity in tumor cell kinetics on radiation dose-response. An exploratory investigation of a plateau effect. Radiother Oncol 50:57–66.

Trott KR. 1994. Tumour stem cells: The biological concept and its application in cancer treatment. Radiother Oncol 30:1–5.

Vlashi E, Kim K, Dealla Donna L, Lagadec C, McDonald T, Eghbali M, Sayre J, Stefani E, McBride W, Pajonk F. 2009. In-vivo imaging, tracking, and targeting of cancer stem cells. J Natl Cancer Inst 101:350–359.

Withers HR, Maciejewski B, Taylor JM, Hliniak A. 1988. Accelerated repopulation in head and neck cancer. Front Radiat Ther Oncol 22:105–110.

Woodward WA, Chen MS, Behbod F, Alfaro MP, Buchholz TA, Rosen JM. 2007. WNT/beta-catenin mediates radiation resistance of mouse mammary progenitor cells. Proc Natl Acad Sci USA 104:618–623.

Zhu L, Gibson P, Currle DS, Tong Y, Richardson RJ, Bayazitov IT, Poppleton H, Zakharenko S, Ellison DW, Gilbertson RJ. 2009. Prominin 1 marks intestinal stem cells that are susceptible to neoplastic transformation. Nature 457:603–607.